



**Cortical gene expression profiling in spinal cord repair:
insight into the complexity of the neural regeneration
program**

Inaugural-Dissertation

zur

Erlangung des Doktorgrades der
Mathematisch-Naturwissenschaftlichen Fakultät
der Heinrich-Heine-Universität Düsseldorf

vorgelegt von

Fabian Kruse

aus Düsseldorf

Juni 2009

Aus dem Labor für Molekulare Neurobiologie der neurologischen Klinik
der Heinrich-Heine-Universität Düsseldorf

Gedruckt mit der Genehmigung der
Mathematisch-Naturwissenschaftlichen Fakultät der
Heinrich-Heine-Universität Düsseldorf

Referent: Prof. Dr. Hans Werner Müller
Korreferent: Prof. Dr. Dieter Willbold

Tag der mündlichen Prüfung: 7. Juli 2009

To my family

TABLE OF CONTENTS

Table of contents	1
1. Abstract	1
1. Zusammenfassung.....	3
2. Introduction	6
2.1 Axonal regeneration strategies in the adult mammalian CNS.	6
2.1.1 Axon regeneration research.....	7
2.1.2 Therapeutic cell and tissue transplantations.....	9
2.1.3 Application of neurotrophic substances	10
2.1.4 Neuroprotective and -replacement treatments.....	11
2.1.5 Neutralization of inhibitory molecules at the lesion site.....	12
2.1.6 Possible causes for the absence of any spontaneous CNS regeneration	15
2.1.7 Other strategies for functional recovery.....	17
2.2 Axon outgrowth and regeneration failure	17
2.2.1 Second messenger cascades activated during growth cone turning, collapse, and after axotomy.....	17
2.2.2 Major guidance molecules	17
2.2.3 Known molecular reactions to nervous system injury	17
2.3 Lesion model and treatment	17
2.3.1 The lesion model of the axotomized corticospinal tract (CST)	17
2.3.2 Experimental strategies to suppress the collagen IV containing fibrous scar..	17
2.3.3 The Anti Scarring Treatment (AST)	17
2.3.4 Functional recovery.....	17

2.4	Concluding remarks	17
3.	Materials and Methods	17
3.1	Treatment paradigms and animal groups	17
3.2	Animals	17
3.3	Retrograde labelling of primary motoneurons which project into the CST.....	17
3.4	Corticospinal tract transection and Anti Scarring Treatment.....	17
3.5	Tissue preparation	17
3.5.1	Preparation of brain tissue.....	17
3.5.2	Cortical tissue localization via retrograde labeling with Fluoro-Gold.....	17
3.5.3	Preparation layer V sensorimotor cortex and total RNA isolation.....	17
3.6	Utilized microarray platforms	17
3.7	Probe labeling and array hybridization	17
3.8	Quantitative polymerase chain reaction (qPCR) procedures	17
3.9	Immunohistochemistry.....	17
3.10	Microarray data analysis	17
3.10.1	Affymetrix gene chip technology.....	17
3.10.2	Variations	17
3.10.3	Impact of the experimental setup	17
3.10.4	Low-level analyses.....	17
3.10.5	Statistical analysis	17
3.10.6	Biological pathways and ontology information	17
4.	Results.....	17
4.1	Lesion model and tissue preparation.....	17

4.2	Difficulties and solutions in microarray experiments	17
4.2.1	From raw data to biological meaning.....	17
4.2.2	Data processing	17
4.2.3	Combination of pre-processing methods.....	17
4.2.4	Resulting guidelines for microarray data low-level and statistical analysis	17
4.3	Cortical gene expression profiles following spinal cord injury	17
4.4	Modulation of the cortical lesion-triggered gene expression profile by AST	17
4.4.1	Principle time- and treatment-specific changes in gene expression patterns ...	17
4.4.2	Identification of time- and treatment-specific clusters of regulated genes	17
4.5	Functional groups of regulated genes.....	17
4.6	Identification of regulated genes associated with AST-dependent responses.....	17
4.6.1	Axon outgrowth and guidance	17
4.6.2	Apoptosis, Protection and Stress response.....	17
4.6.3	Myelin associated genes.....	17
4.7	qPCR validation	17
4.8	Cellular localisation.....	17
5.	Discussion	17
5.1	Lesion model and tissue preparation.....	17
5.2	Data analysis and data verification.....	17
5.3	Comparison to optic nerve regeneration	17
5.4	Cortical molecular response after CST axotomy and AST-treatment.....	17
5.5	Important timepoint and treatment-specific regulation pattern.....	17
5.6	Over- and underrepresentation of functional groups of regulated genes	17

5.7	Regulated genes with known roles in regeneration.....	17
5.8	Summary and outlook	17
6.	References	17
7.	Abbreviations	17
8.	Acknowledgments.....	17

1. ABSTRACT

Traumatic injury of the spinal cord results in formation of a collagenous fibrous scar acting as a growth barrier for regenerating axons in the lesion centre. Recently, an anti-scarring treatment (AST) to suppress fibrous scarring by local application of an iron chelator and cyclic adenosin monophosphat (cAMP) was developed in this lab. AST led to long distance axon regeneration and functional recovery in adult rat (Klapka et al., 2005).

In this thesis, gene expression profiles of layer V of sensorimotor cortex following thoracic corticospinal tract (CST) transection from day 1 up to 60 days post-operation (dpo) were investigated by the means of microarray hybridization (Affymetrix). Using this genomic approach, cortical gene regulations triggered by CST-transection as well as by AST-induced axonal regeneration were identified.

Interestingly, more than 900 significantly regulated genes were detected as early as 1 dpo in the lesion-affected sensorimotor cortex. Subsequently, the number of significant regulations further increased to a maximum of approx. 2.000 genes at 21 dpo.

By means of Gene Ontology (GO)-categories (Ashburner et al., 2000) the genes were linked to functional information. GO clustering was then used to reveal processes that were of particular importance and were affected by spinal cord injury. As expected, ontologies representing “wound response”, “growth-associated cytoskeletal reorganization”, and “cell survival” were injury-affected at the early time points, whereas “protein biosynthesis”, “synaptic reorganization” and “apoptosis” were enriched at 21 dpo and/or 60 dpo.

Direct comparison of the temporal expression profiles of lesioned control rats and AST-treated animals documented strong AST-mediated modulation of the lesion-triggered cortical expression profiles, reflecting regeneration-associated molecular responses. Indeed, these data revealed substantial proportions of AST-counter-regulated and AST-boosted genes as well as

discrete AST-specific gene regulations. Interestingly, numerous AST-regulated genes affect crucial biological processes associated with “cell survival“, “stress response“, “cellular protection” as well as “axon guidance” and “axonal outgrowth”.

For the first time, this work presents a comprehensive temporal comparison of gene expression profiles reflecting both the lesion-induced cortical response after traumatic CST lesion, and responses during successful AST-mediated axonal regeneration. Moreover, the results allow to define both distinct phase- and treatment-dependent associated regulation patterns.

Given the complex task of assessing genetic profiles at multiple conditions and stages from such a heterogeneous tissue, like the cerebral cortex, the experimental setup as well as the subsequent data processing and statistical analysis procedures had to be adjusted to cope with the expected variations. An *Excel VBA*-based analysis tool and *Python*-based scripts for automated low-level analysis were developed. Using these tools, based on thresholds for fold-changes and p-values the combined expression patterns calculated from five different analysis algorithms can be visualized and linked with functional information. Especially in the case of expression patterns comprised of multiple timepoints and treatments this method helps in generating a full picture of genetic profiles. The procedures for data analysis and statistical evaluations developed in this thesis have contributed to several publications (Kruse et al., 2008; Barbaria et al., 2009; Heinen et al., 2008; Kury et al., 2004; Kruse et al., 2009; Bosse et al., in preparation).

1. ZUSAMMENFASSUNG

Spezifische Veränderungen der kortikalen Genexpression nach einer Rückenmark-Verletzung wurden untersucht. Die nach traumatischen Verletzungen des Rückenmarks sich bildende kollagenhaltige fibröse Narbe stellt ein Hindernis für regenerierende Axone an der Läsionsstelle dar. Eine jüngst in diesem Labor entwickelte Therapie zur Unterdrückung dieser Narbenbildung (anti-scarring treatment, AST) durch lokale Applikation eines Eisen-Chelators und cyclisches Adenosinmonophosphat (cAMP) führt zu axonaler Regeneration über große Distanzen und funktioneller Erholung.

In dieser Arbeit wurden die Genexpressionsprofile der Schicht V des sensorimotorischen Cortex nach Transsektion des thorakalen Kortikospinaltrakts (cortico spinal tract, CST) zwischen 1 und 60 Tagen nach Operation (days post operation, dpo) mit Hilfe von Microarray-Analysen (Affymetrix) untersucht. Anhand dieses genetischen Ansatzes konnten kortikale Genregulationen identifiziert werden, welche durch die CST-Transsektion sowie die AST-induzierte axonale Regeneration hervorgerufen wurden.

Interessanterweise wurden in der Gruppe der Läsions-Kontrolltiere bereits am 1. Tag nach Operation mehr als 900 Gene signifikant reguliert gefunden. Zu späteren Zeitpunkten stieg die Anzahl der signifikant regulierten Gene noch bis zu einem Maximum von ca. 2.000 am 21. Tag an.

Basierend auf der Gene Ontology (GO, Ashburner et al., 2000) wurden regulierte Gene mit funktionellen Daten verknüpft und geclustert um besonders wichtige und durch die Rückenmarks-Verletzung beeinflusste Prozesse zu identifizieren. Wie erwartet waren zu den frühen Zeitpunkten besonders Gruppen wie „Verletzungs-Antwort“, „Wachstums-assoziierte zytoskeletale Reorganisation“ und „Zellüberleben“ betroffen, zu den späteren Zeitpunkten Gruppen wie „Proteinbiosynthese“, „Synaptische Reorganisation“ und „Apoptose“.

Ein direkter Vergleich der zeitspezifischen Expression von Läsions-Kontrolltieren und AST-behandelten Ratten dokumentierte eine starke AST-vermittelte Änderung der durch Läsion ausgelösten kortikalen Expressionsprofile. Diese Veränderungen spiegeln regenerations-assoziierte molekulare Reaktionen wieder. Tatsächlich zeigten die Microarray-Daten einen großen Anteil an Genen, die in AST-Tieren gegenläufig oder verstärkt sowie ausschließlich in behandelten Tieren reguliert waren. Viele durch AST regulierte Gene beeinflussen wichtige biologische Prozesse, die mit „Zellüberleben“, „Stress-Antwort“, „Zellschutz“ sowie „Axonaler Wegfindung“ und „Axonwachstum“ assoziiert sind.

Diese Arbeit zeigt zum ersten Mal einen umfassenden zeitlichen Vergleich der Genexpressionsprofile, welche die läsions-induzierten kortikalen Reaktionen nach traumatischer CST-Läsion sowie die Veränderungen durch erfolgreiche AST-vermittelte axonale Regeneration widerspiegeln. Zusätzlich erlauben die Ergebnisse phasen- und behandlungsabhängige Regulationsmuster zu definieren.

Das experimentelle Setup sowie die anschließende Datenauswertung und statistische Analyse wurden entsprechend ausgelegt um von heterogenem kortikalem Gewebe in solch komplexem Rahmen Genexpressionsprofile von multiplen Konditionen und Zeitpunkten zu ermöglichen. Ein auf *Excel-VBA* basierendes Programm und *Python*-basierte Skripte wurden zur Datenauswertung sowie Interaktion mit online frei zugänglichen Dataming-Tools programmiert. Basierend auf Schwellenwerten für Regulationsstärke und p-Werte können die gemeinsamen Expressionsprofile von fünf verschiedenen Analyse-Algorithmen visualisiert und mit funktionellen Informationen verknüpft werden. Besonders bei komplexen Expressionsmustern welche aus mehreren Zeitpunkten und Konditionen bestehen, lässt sich so ein komplettes Bild der Expressionsprofile erstellen. Die in dieser Arbeit vorgestellten Konzepte und Methoden zur Analyse und statistischen Auswertung von Microarray-Daten

haben bereits zu mehreren Publikationen beigetragen (Kruse et al., 2008; Barbaria et al., 2009; Heinen et al., 2008; Kury et al., 2004; Kruse et al., 2009; Bosse et al., in preparation).

2. INTRODUCTION

The goal of this study is to partly unravel the complex molecular responses to axotomy in a non-regenerative and a treatment-triggered regenerative CNS environment. To provide profound information for the reader about the regulatory reactions, which could be expected in response to axotomy, as well as current clinical and experimental methods for the treatment of axons injuries, this introduction tries to cover these broad scientific fields.

2.1 Axonal regeneration strategies in the adult mammalian CNS.

Axonal and neurite lesions occur in many neurological diseases, like for example Alzheimer's disease (AD), if neuritic plaques and neurofibrillary tangles are formed or during inflammatory processes in multiple sclerosis (MS, Selkoe, 1999; Trapp et al., 1999; Jeffery et al., 2000). In both AD and MS associated axonal transections could be correlated with increasing mental and physical disabilities. These chronic diseases show manifestation of the full pathology over a longer period of time and it is remarkable that axonal injury was identified as a major cause of the accompanying affections.

In contrast, traumatic axonal lesions that occur in the brain or the spinal cord show an immediate dramatic effect on nervous system functions. Damage to the spinal cord, the major nervous connection from the brain to the body, leads to permanent paralysis. Within a split second all major sensory and motor functions below the site of injury are irreversibly affected.

This is a very dramatic fate, especially as there is at present no cure for spinal cord injury (SCI), which would restore all or at least some of its previous functions. Standard clinical

procedures comprise surgical decompression and stabilization of the severed spine. However, early start of rehabilitation is considered to be the most important step to regain as many functions as possible (DeVivo et al., 1990). A pharmacological promising attempt was believed to be done in 1990 when the FDA (Food and Drug Administration in the USA) approved methylprednisolone for acute treatment of SCI. This corticosteroid was beneficial if given within the first eight hours of injury (Green et al., 1980; Seidl, 2000). Subsequent studies, however, have reported extensive complications with minimal neurological benefit (Fehlings, 2001) and the use of methylprednisolone might also result in steroid myopathy (Qian et al., 2000; Qian et al., 2005). The concurrent use of methylprednisolone, however, might jeopardize the establishment of other neuroprotective regimens in clinical trials. For example the more potent beneficial effects on neurological recovery of Erythropoietin (Boran et al., 2005) were neutralized by methylprednisolone administration in animal trials.

2.1.1 Axon regeneration research

To achieve the goal of restitution of all functions after SCI, a complex set of requirements has to be fulfilled. These requirements could be recognized as the ultimate goal in axonal regeneration research, as complete restoration of functions would demand recapitulation of early developmental events in an adult organism. Despite this apparently insurmountable challenge, limited regeneration success has been achieved in a number of experimental cases, which aimed at resolving one or more of the following general requirements for complete regeneration:

1. survival of axotomized neurons
2. stimulation of axonal outgrowth
3. tissue repair at the lesion site

4. correct pathfinding of outgrowing axons

5. functional reinnervation

In addition to these neuronal and axonal repair steps, mechanical stabilization, rehabilitation and muscle stimulation will probably be necessary. The diversity of the formerly mentioned approaches in the clinical phase originated from a growing number of experimental strategies, which aim at understanding and alleviating the ailments arising after SCI. Since the early regeneration research of Ramon y Cajal (Ramon y Cajal, 1928), lesions to central axons in mammalia were considered to lead to a permanent loss of function. But pioneer work by Aguayo and colleagues (Richardson et al., 1980) revived this increasingly popular field in neuroscience. The demonstrated potency for regeneration was nurtured by the notion that regeneration capabilities in adult mammals were not lost, but needed to be stimulated. The hope that CNS axons could regenerate even in the adult animal was furthermore supported by the regeneration properties found in other animals. It appeared that there was a hierarchical loss of regeneration capabilities,

- phylogenetically:

Lower vertebrates like the zebrafish regenerated most of their spinal axons, and traversal of the lesion site was seen at six weeks after axotomy (Becker et al., 1997). But characteristic reexpression of regeneration associated genes depended on the cell type and the distance of the lesion in the spinal cord (Becker et al., 1998).

- ontogenetically among mammals:

In neonate opossum spinal tissue neurites regenerate until myelination at postnatal day thirteen (Varga et al., 1995). However, this case could be arguable with respect to postnatal regeneration capabilities, as the apparent long lasting ability for regeneration could be attributed to the early birth of marsupialia. The reported developmental stage could better

correlated with embryonic stages in placentalia. Nevertheless, developmental changes relate with a gradual loss of the CNS regeneration capability.

- systemically:

While peripheral nerves do regenerate (Ide, 1996; Fu and Gordon, 1997), only regeneration tendencies are recognized in the CNS. Serotonergic and noradrenergic fibres often display marked regeneration efforts, while corticospinal fibres do not under normal conditions (Ramon-Cueto et al., 2000). On the other hand, transfected corticospinal motor neurons in layer V overexpressing the BDNF receptor trkB showed corticospinal axon regeneration into subcortical lesion sites expressing BDNF after subcortical axotomy (Hollis et al., 2009).

2.1.2 Therapeutic cell and tissue transplantations

The concept to transplant a permissive PNS-derived substrate into a non-permissive CNS-environment, which was introduced by Aguayo and colleagues (Benfey and Aguayo, 1982) stimulated the development of a series of tissue and cell implantation strategies. Transplanted peripheral nerves were developed further for axonal regeneration, for example by combining them with methylprednisolone application (Chen et al., 1996). The apparently better efficacy of predegenerated peripheral nerves (Dahlin, 1995; Decherchi and Gauthier, 1996) lead to the discovery that activated macrophages alone had an unrecognized potential to create a permissive environment and support lesion repair processes, thus allowing extensive axonal regeneration (Rapalino et al., 1998). The importance of macrophage infiltration after axotomy is further supported by data from a *Xenopus* tadpole optic nerve crush paradigm, where regeneration is found after massive invasion of macrophages in the lesion site (Wilson et al., 1992).

Another variant of these cell transplantation approaches was the implantation of olfactory ensheathing cells, which were recognized as a cell type with features of both, peripheral Schwann cells and central oligodendrocytes (Li et al., 1998; Ramon-Cueto et al., 2000). It has been shown, that olfactory ensheathing cell implantation enhances hindlimb-stepping ability in adult spinal transected rats (Kubasak et al., 2008). Primate olfactory ensheathing cells are suitable for culture conditions and transplantation (Rubio et al., 2008). Grafting of embryonic tissue (Reier et al., 1983; Schnell and Schwab, 1993; Itoh et al., 1999) and the embryonic stem cell implantations (McDonald et al., 1999) resulted in a certain degree of functional recovery accompanied by some axonal elongation. There have been several approaches to utilize different types of stem cells in the recent years. Transplantation of predifferentiated embryonic stem cells restores sensory function following spinal cord injury in mice (Hendricks et al., 2006). A autogenous undifferentiated stem cell infusion on human patients showed recovery of somatosensory evoked potentials (SSEPs) to peripheral stimuli after 2.5 years of follow-up (Cristante et al., 2009). Transplantation of bone marrow stromal cells promotes regeneration and improves motor function in SCI (Chiba et al., 2009). The transplantation of fetal brain tissue into the spinal cord lesions of hundreds of patients in china has to be seen problematic. No scientifically supportable data of these human studies has been published so far (Dobkin et al., 2006).

2.1.3 Application of neurotrophic substances

Cellular implants have the advantage to respond in multiple ways to the complex environment that they are placed in. They can migrate into the host tissue, thereby often forming traces which could be followed by regrowing axons. As a response to their environment many of the above mentioned cell types are also able to secrete neurotrophins . Neurotrophins were known

to have neurite promoting and guidance effects in vitro (Campenot, 1994), as well as effects on neuronal survival. Therefore, it was not long until neurotrophins alone were applied to treat experimental spinal cord lesions in vivo (Schnell et al., 1994). But the effects on recovery are still not completely understood. Treatment of adult rat spinal cords with brain-derived neurotrophic factor (BDNF) stimulated hindlimb activity, with sprouting of cholinergic fibres only at the lesion site without long distance regeneration (Jakeman et al., 1998). In similarity to these results, neurotrophin-3 (NT-3) containing collagen gels attracted proximal axons, but did not result in elongation caudally to the lesion (Houweling et al., 1998a), while others were able to demonstrate a correlation of neurotrophin stimulated axonal outgrowth at the dorsal root entry zone with functional recovery (Ramer et al., 2000).

Unfortunately, clinical trials have also revealed side effects of neurotrophin treatment, such as pain and weight loss (Olson, 1993). Thus strategies were developed, such as the implantation of genetically manipulated fibroblasts (Grill et al., 1997), Schwann cells (Tuszynski et al.) and neural stem cells (McDonald et al., 1999), which created experimental cellular tools for long lasting, low dose application of neurotrophins.

2.1.4 Neuroprotective and -replacement treatments

Besides loss of projecting motor neurons in the cerebral cortex after SCI (Hains et al., 2003), motor neuron loss at the lesion site within the spinal cord could be observed after chronic cervical cord compression and decompression (Harkey et al., 1995). Moreover, secondary tissue damage is known to further complicate injuries (Lu et al., 2000). Neuroprotection is the primary prerequisite after lesion to the optic nerve. Apoptotic loss of retinal ganglion cells upon axotomy was treated with a number of anti apoptotic interventions, such as expression of the anti apoptotic protein p35 (Kugler et al., 1999), injection of aurointricarboxylic acid into

the eye (Heiduschka and Thanos, 2000) or cataractogenic lens injury (Fischer et al., 2000). Expression of the proto-oncogene bcl-2 was shown to be anti apoptotic, by protecting red nucleus neurons after cervical axotomy (Zhou et al., 1999) and regeneration stimulatory for axotomized retinal ganglion cells (Chen et al., 1997). Additional knowledge on the preservation of neurons was gathered by studying neurodegenerative diseases, where neurotrophins or synthetic analogues were successful in preventing neuronal loss (Skaper and Walsh, 1998).

In conclusion, many different experimental strategies for neuroreplacement, neuroprotection and stimulation of axonal outgrowth have contributed to the understanding of nervous system functions in the axotomy disease state. Although limited functional recovery was often described, not all examples conclusively demonstrated that the improvements completely rely on the treatment and its postulated effects. This could in part be attributed to the difficulty to dissociate beneficial effects of the therapeutic intervention from accompanying spontaneous plastic changes. Likewise, improved sensoric and motoric abilities could not always be strictly correlated to the length of regenerated axons. Only a few studies demonstrated loss of functions, which were gained by the therapy, after relesioning. Nevertheless, the existing array of therapeutic approaches will hopefully be valuable in the development of new therapies for a variety of lesions to central nervous system axons.

2.1.5 Neutralization of inhibitory molecules at the lesion site

Another mainstream of regeneration research followed the early work of Ramón y Cajal and initial transplantation results, which demonstrated the inhibitory nature of the lesion site and the white matter in the mammalian CNS. Neutralization of the inhibitory effect of CNS white matter was demonstrated for the first time by the administration of the M-type

immunoglobulin IN1 (Caroni and Schwab, 1989), which lead to axonal regeneration and functional recovery (reviewed by Tatagiba et al., 1997). This concept to neutralize myelin resident inhibitors stimulated new experimental therapeutic approaches. Disruption of myelin by x-ray irradiation (Savio and Schwab, 1990; Kalderon and Fuks, 1996) and by immunological means (Keirstead et al., 1995) both proved that myelin removal could enhance regeneration.

Reports on cloning of the IN1 antigen, Nogo-A, promised to provide more insight into the axon inhibitory mechanisms associated with this myelin resident protein (GrandPré et al., 2000; Chen et al., 2000; Prinjha et al., 2000). Surprisingly, these reports revealed that the inhibitory aminoterminal domain of the membrane anchored Nogo-A was localized to the cytoplasmic face of the oligodendrocyte plasma membrane. However, an additional small extracellular fragment of the protein was also shown to possess growth cone collapse activity. Nogo was identified to belong to the family of reticulon proteins, which are associated with the endoplasmic reticulum (GrandPré et al., 2000). None of the extracellular fragments of the other reticulon family members displayed a collapsing activity, like it was recognized for Nogo isoforms. Investigations by Fournier et al. (Fournier et al., 2001), led to the isolation of the corresponding glycosylphosphatidylinositol-linked receptor for this extracellular fragment, which presents a target for the development of agents, which promote axonal outgrowth.

Although the inhibitory nature of CNS white matter is widely accepted, some reports demonstrated surprising results, showing a permissiveness of this apparently hostile substrate. Neuroblasts grafted into the striatum (Victorin et al., 1990) or adult dorsal root ganglia (DRG) neurons microimplanted directly into the corpus callosum or fimbria (Davies et al., 1997) extended their axons for considerable distances along or within the white matter. This apparent contradiction to the approaches mentioned afore could be explained by myelin

geometry, upon which its permissive or inhibitory nature could rely on (Pettigrew and Crutcher, 1999). Neurons cultured on native cryostat-sections of mature rat CNS tissue, were found to extend their neurons preferentially on grey matter. However, interestingly, white matter appeared to support neurite outgrowth, if neurites elongated parallel to existing myelinated tracts, but not nonparallel outgrowth.

On the other hand, it could be shown that elongating axons stop or turn at presumptive barriers consisting of chondroitinsulphate proteoglycans (CSPGs, Davies et al., 1997). These extracellular matrix (ECM) proteins were found to be expressed at axon lesion sites (Stichel et al., 1995) and were shown to inhibit neurite outgrowth in vitro (Fawcett and Asher, 1999b). CSPGs are produced or induced by fibroblasts, astrocytes and macrophages (Fitch and Silver, 1997), interestingly, with the latter cells being also axon regeneration stimulating in other experimental paradigms (Rapalino et al., 1998). Targeting of CSPG inhibition with CSPG degrading matrix metalloprotease, MMP-2, was successful in vitro (Zuo et al., 1998), while in vivo the transected fornix did not regenerate after chondroitinase treatment. The composition of the ECM at the lesion site is influenced by a complex array of inflammatory cytokines, which are known to stimulate reactive gliosis (Logan et al., 1994) or induce ECM formation, like TGF- β 1, which up-regulates tenascin synergistically with basic fibroblast growth factor (bFGF, Smith and Hale, 1997). Other effectors like interferon- γ acted against scarring, but did not increase axonal outgrowth (DiProspero et al., 1997).

As axons grow out along axonal guidance cues during development, either by attractive or inhibitory means, the expression of such molecules at CNS lesion sites was analysed. Indeed, the repulsion mediating proteins semaphorin 3A (Giger et al., 1998) and EphB3 (Miranda et al., 1999) were found to be expressed at several CNS lesion sites, either within fibroblasts or white matter resident astrocytes and grey matter motor neurons, respectively, and might therefore be involved in axonal outgrowth inhibition. In addition to this potential role in

barrier formation, correct expression of guidance cues along the former pathways is a prerequisite for successful target reinnervation. In some cases existing guidance cues were followed by grafted cells. Transplanted into adult rat striatum, human telencephalic neuroblasts followed major myelinated axon tracts up to their putative target regions in the substantia nigra, the pontine nuclei and the cervical spinal cord (Wictorin et al., 1990). Similar results were obtained with human dopaminergic neurons, which were also grafted into the rat brain and specifically extended tyrosine-hydroxylase positive fibres into the nigro-striatal pathway up to the deafferented striatum (Stromberg et al., 1992). Expression of attractive guidance cues, such as L1 and PSA-NCAM along regenerated tracts (Aubert et al., 1998; Weidner et al., 1999) also served as a template for artificial bridges. Bridges are especially important to traverse a gap in the severed spinal cord. There were several synthetic sheaths tested, filled with viable Schwann cells (Steuer et al., 1999) or consist solely of modified polymers (Woerly et al., 1999; Holmes et al., 2000), which could also be enriched with neurotrophic growth factors, like NT-3 (Houweling et al., 1998c). The combination of a Schwann cell bridge, olfactory ensheathing glia, and chondroitinase ABC provided significant benefit in functional recovery (Fouad et al., 2005).

2.1.6 Possible causes for the absence of any spontaneous CNS regeneration

It has been shown that injury to CNS axons leads to limited growth (Li and Raisman, 1994) but the growth stops at the lesion site (Stichel and Müller, 1994). Reasons for this regeneration failure could be:

- a) Missing neurotrophic factor in the CNS tissue (Houweling et al., 1998b)
- b) The presents of inhibitory molecules in the CNS tissue (Fawcett and Asher, 1999a)
- c) The formation of a physical barrier at the lesion site (Reier et al., 1983)

The growth stop in the lesion site implies that this area is of particular interest for research on regeneration failure and regeneration supporting therapy.

The lesion scar

The formation of a wound healing scar at the lesion site in the CNS was first observed by Ramon y Cajal at the beginning of the last century. In this lesion scar two different zones can be distinguished, the glial scar in the peri-lesion area and the fibrous scar in the lesion centre (Fawcett and Asher, 1999a).

The glial scar consists mostly of reactive astrocytes, which are marked by an over-expression of the glial fibrillary acidic protein (GFAP). These astrocytes have been shown to express putative inhibitory molecules like tenascin (Faissner, 1997), CD44 (Mansour et al., 1990), brevican and neurocan (Fawcett and Asher, 1999a). Oligodendrocytes and meningeal cells are also present in the glial scar which synthesize inhibitory molecules like Nogo (Chen et al., 2000), myelin associated glycoprotein (MAG), ephrines and semaphorins (de Winter et al., 2002).

The fibrous scar in the lesion centre consists for the most part of collagen IV (Coll IV). This collagen is an element of basal membranes (BM), which can also be found in blood vessels (Stichel et al., 1999b).

The fibrous scar as a regeneration barrier

Numerous molecules can associate to the BM (Timpl, 1994). Some of these molecules were identified as inhibitor of axonal growth: e.g. chondroitine sulphate proteoglycans (CSPG,

(Morgenstern et al., 2002), semaphorins (de Winter et al., 2002) and ephrins (Bundesen et al., 2003) and thereby prevents axonal regeneration across the lesion site.

2.1.7 Other strategies for functional recovery

Other strategies for functional recovery include the growing field of neuroprostheses. Ten years ago, improvements in muscle mass, general fitness and spasticity have been shown for FES-propelled cycle training (Scremin et al., 1999). It has been shown that a brain-computer interface (BCI) can be used to control a functional electrical stimulation (FES) device by reading bursts of beta oscillations in the electroencephalogram (EEG) of a patient and by that enable the patient to move his paralyzed hand (Pfurtscheller et al., 2003). Numerous new systems of neuroprostheses interfacing with either CNS or PNS both above and below the lesion are under development and at different stages of translation to the clinic (Giszter, 2008).

Due to the fast growing options of technically feasible neuroprostheses this field will surely have the biggest impact on the lives of SCI patients in the next five to ten years.

2.2 Axon outgrowth and regeneration failure

Axon outgrowth in the developing organism is a highly complex task. The complexity of synaptic connections in the brain easily outnumber the quantity of possible instructions directly encoded in an organism's genome. Therefore, this complex network must be realized in a molecular structure and interaction-based code. This chapter intends to provide an overview over general aspects of signal transduction from the growth cone membrane down

to the cytoskeleton. Special emphasis will be put on signalling mechanisms during growth cone turning, the collapse response and axotomy induced molecular responses. In addition, important families of guidance proteins will be briefly introduced.

2.2.1 Second messenger cascades activated during growth cone turning, collapse, and after axotomy

Cyclic nucleotides

Growth cone navigation becomes even more complex, if cAMP associated effects are considered. Decreasing extracellular (and concomitantly intracellular) calcium, increases the advance of elongating neurites, but renders them insensitive to attractive molecules, such as brain derived neurotrophic factor (BDNF), which is signalling through a cAMP/protein kinase A (PKA) dependent pathway. Under standard calcium conditions, addition of a cAMP competitor, PKA inhibitor or an overall decrease in the cAMP level resulted in a switch of the turning response induced by certain attractive guidance molecules, such as netrin-1, from attraction to repulsion. On the other hand, PKA activation or cAMP increase enhanced attractive turning (Ming et al., 1997; Song et al., 1998). Netrin-1 interaction with adenosine receptor A2b was shown to be required for netrin-dependent axonal outgrowth. This G protein coupled receptor was identified as a DCC (deleted in colorectal cancer) interacting receptor, thus implicating DCC only indirectly into netrin-mediated axonal outgrowth. Activation of A2b to stimulate cAMP accumulation could provide a missing link for guidance molecule induced changes in cAMP levels (Corset et al., 2000). However, these data were compromised by a report, showing that netrin-1 binding to DCC derepresses cytoplasmic domain multimerization of the receptor. Furthermore, the cytoplasmic P3 domain was shown

to be required for this self-association of the cytoplasmic DCC domain and sufficient for function of DCC as a chemoattractant (Stein et al., 2001). In similarity to the cAMP associated switch response, attractive or repulsive guidance molecules displayed dependence on cyclic guanosinemonophosphate (cGMP) levels. But this pathway was shown to be independent of extracellular calcium levels and activation of cGMP signalling resulted in a switch from repulsion to attraction (Song et al., 1998). In conclusion, these results demonstrated that growth cone navigation is critically regulated by intracellular calcium and cyclic nucleotide levels. These levels may depend on neuron type, neuron age and also the path an axon has already travelled. Whether levels of intracellular calcium or cyclic nucleotides vary to the same extent in vivo, as it has been demonstrated in vitro remains to be shown.

Growth cone collapse

Another well-known neurite response, the growth cone collapse, was correlated with a rise in intracellular calcium in some cases (Loschinger et al., 1997), while others clearly demonstrated independence from calcium levels within the growth cone (Ivins et al., 1991). This apparent contradiction may depend on the developmental stage of the studied neurites, as only adult rat DRG or chick RGC neurons were found to display a long lasting collapse response with concomitant calcium rise, while their embryonic counterparts collapsed transiently with only small calcium elevations (Bandtlow and Loschinger, 1997). Like during guidance events, different signalling pathways, involving small GTPases or phospholipase A2 and lipoxygenase, could be responsible for the collapse response (Kuhn et al., 1999; de La Houssaye et al., 1999). In the end, the collapse signalling cascades were shown to converge on cytoskeletal rearrangements. Filamentous actin depolymerisation was found to be a

characteristic molecular result of the collapse response, with the microtubule network only being rearranged (Fan et al., 1993; Kuhn et al., 1999).

The relatedness of guidance mechanisms and growth cone collapse became apparent for cultured retinal ganglion cells. Outgrowing pioneering axons extended lateral extensions hundreds of micrometers away from their tip, after ephrin or mechanically induced collapse, and likewise accompanying axons were induced to defasciculate at the same distance (Davenport et al., 1999).

Calcium induced molecular cascades after axotomy

Reinduction of growth cones a few hundred micrometers away from the collapsing axon tip, strikingly resembles the observed morphological changes upon axotomy of *Aplysia* neurons. If these neurons were axotomized, a brief, sharp rise of intracellular calcium to about 1000 μM (resting level is around 0.1 μM) was observed at the severed axon tip. But within minutes the membrane resealed and no further calcium influx was observed. Subsequently a new growth cone was formed within ten minutes at about 100 μm from the transection site. This region colocalized with an area, where calcium concentrations were raised to 300- 500 μM . Elevation of calcium up to this level anywhere along the severed or unsevered axons was sufficient to induce growth cone formation (Ziv and Spira, 1997). Moreover this calcium rise was sufficient to trigger a localized proteolytic activity, which was already known for its ability to induce growth cones. Within about an hour, proteolytic activity reached its maximum and cytoskeletal alterations were manifested.

Submembraneous, heterotetrameric spectrin/fodrin was shown to be one of the targets of proteolytic cleavage (Gitler and Spira, 1998). Spectrin is especially important for membrane associated cytoskeleton organization and signalling. This is already suggested by its multiple binding domains, which interact with many important cytoskeletal components, such as actin

or ankyrin and possibly signalling molecules via its Src-homology-3 (SH3) domain. Spectrin, actin and calmodulin were also directly associated with calcium dependent membrane transport during axonal regeneration (Koenig et al., 1985).

The mentioned axotomy induced events are further supported by data, which also emphasize the necessity of calcium influx and proteolytic activity for membrane resealing and subsequent axon dedifferentiation in cultured rat septal neurons (Xie and Barrett, 1991). Moreover, it was pointed out that microtubule disassembly was also necessary for membrane resealing. In all of these studies, proteolytic activity was associated with the calcium/calmodulin activated, heterodimeric cysteine endopeptidase calpain.

This family of proteases is known to cleave spectrin and microtubule associated protein 2 (MAP2) isoforms. The crucial role for calpains in mediating also cytotoxic effects was demonstrated. Physiological activation of cyclin-dependent kinase 5 (CDK5) by its neuron specific activator p35 is required for neurite outgrowth. But upon calcium or amyloid β -peptide stimulation p35 is cleaved to p25, which in turn up-regulates CDK5 activity and mislocalization. As a result, tau becomes hyperphosphorylated, the cytoskeleton disrupted and apoptosis is initiated. Cleavage of p35 to p25 depends upon calpain activity, placing this protease in the center of calcium induced cytoskeletal alterations in acutely axotomized neurons and during chronic Alzheimer's disease (Lee et al., 2000).

Therefore, the mechanisms leading to calpain induced neurotoxicity in AD could possibly also affect axotomized neurons and may contribute to the distance related effects of axotomy induced cell death in some neuronal populations.

2.2.2 Major guidance molecules

The pivotal role and general importance of second messengers in transducing molecular information to the cytoskeleton has been described above. Alterations in second messenger levels are thought to be initiated by interactions of guidance molecules at the growth cone membrane. These membrane associated proteins belong to the best studied proteins, which are involved during axonal outgrowth and have more comprehensively been reviewed by Tessier-Lavigne and Goodman (Tessier-Lavigne and Goodman, 1996).

Pioneers of neurite growth associated proteins

Cell adhesion molecules (CAMs) belonging to the immunoglobulin superfamily were among the first transmembrane proteins to be implicated in axonal outgrowth. Three major members of that family, NCAM, N-cadherin and L1, were shown to signal via their homo- and heterophilic trans interaction (between membranes of different cells) induced cis clustering (within the same membrane) with fibroblast growth factor (FGF) receptors. Stimulation of the CAM/FGF pathway results in calcium influx via N- and L-type calcium channels and production of inositol phosphate. Furthermore G_i - and G_o -type G proteins participate in the activation of second messenger production, probably by interaction of the $\beta\gamma$ subunit with the pleckstrin homology (PH) domain of phospholipase C γ (PLC γ , Viollet and Doherty, 1997). Whether CAM mediated growth responses are attractive or inhibitory may depend on their extracellular binding partners. Heterophilic interaction of L1 with laminin initially lead to growth cone collapse, but then supported neurite outgrowth, while interaction with a chondroitinsulphate proteoglycan (CSPG) was inhibitory. The presence of an RGD-motif in L1 was shown to specifically recognize several integrin heterodimers.

In addition to the mentioned participation in signalling events, L1 could directly influence cytoskeletal changes. The highly conserved cytoplasmic binding site for ankyrin, indirectly links L1 to the spectrin-actin cytoskeleton, and appears to be crucial for L1 function. The importance of the cytoplasmic tail is further supported by mutation data within this region, which lead to severe brain malformations (Brummendorf et al., 1998). L1 activity could furthermore be modulated by phosphorylation of serine 1181 and 1152 by casein kinase II and p90 rsk, an S6 kinase, respectively. Possible tyrosine phosphorylation of L1 may also be regulated by the intracellular domain of the phosphacan CSPG, RPTP ζ/β , a receptor type protein tyrosine phosphatase (Burden-Gulley et al., 1997), illustrating the multiple interactions which have to be considered in mechanistic guidance models. Castellani et al. (Castellani et al., 2002) showed that L1 and neuropilin-1 are responsible for the axonal responses to semaphoring 3A. Among various other pioneering growth associated proteins, such as NCAM, integrins, low affinity NGF receptor, c-src (a non receptor tyrosine kinase, Skene, 1989), actin and tubulin (McKerracher et al., 1993; Bisby and Tetzlaff, 1992) and c-jun (Herdegen et al., 1993; Herdegen et al., 1997), GAP-43 is one of the best known and studied.

GAP-43 was identified as a protein, which is highly up-regulated and axonally transported upon sciatic nerve transection (Skene and Willard, 1981), its role during axonal outgrowth has been intensively studied. GAP-43 alone is neither sufficient, nor necessary for axonal outgrowth, but its supportive effect for axonal sprouting has been demonstrated. Also other proteins could be equally important, like CAP-23, which has similar biochemical characteristics.

Although GAP-43 up-regulation is often associated with a potential for regeneration, a strict correlation between axotomy and neuronal GAP-43 induction cannot be found. Transection of the central branch of dorsal root ganglia (DRG) does not increase GAP-43 levels, if lesions

are made far from the soma. GAP-43 also appears to be important during development, where high perinatal GAP-43 levels decrease until adulthood. However, mRNA and protein are still widely distributed in the adult brain (Benowitz et al., 1988; Yao et al., 1993).

These data have not established GAP-43 as a primary determinant of axon outgrowth. Therefore, a more generalized perspective could be generated by considering its biochemical properties. The aminoterminal of GAP-43 activates G_o and G_i proteins, of which the α and β subunits are enriched in growth cone membranes. Nevertheless, G protein activation was shown to retard axon outgrowth, which raises a conflict between the observed GAP-43 induction and its stimulating effect on G proteins (Strittmatter et al., 1992). A solution to this apparent contradiction could be seen in the palmitoylation of GAP-43, which blocks G protein activation and could also alter GAP-43 localization. The IQ motif of GAP-43 that is shared by members of the calpacitin family, and mediates calmodulin binding in the absence of calcium, is also involved in GAP-43 function. GAP-43 is a major substrate of protein kinase C (PKC) isoforms in the growth cone, and phosphorylation by PKCs abolishes calmodulin binding. The calcium/calmodulin activated phosphatase calcineurin, on the other hand, decreases the level of phosphorylated GAP-43. Phosphorylated GAP-43 stabilizes F-actin and localizes to growth cone lamellae.

Semaphorins

The semaphorin family of membrane bound or secreted chemotropic proteins was founded by collapsin (renamed to Sema3A), which induces growth cone collapse. Many members of this protein family have since been identified and implicated in axon guidance and patterning, but also in skeleton and heart formation during development. The phylogenetically highly conserved aminoterminal is characterized by the 500 amino acids containing the semaphorin domain with several conserved sequence stretches. The family has been subdivided into seven

classes, with the first two containing invertebrate semaphorins. Within the five vertebrate classes, comprising 20 members, the class specific carboxyterminus determines, whether semaphorins are secreted (class three), transmembrane (classes four to six) or GPI-anchored (class seven).

The cytosol facing carboxy terminals might also be involved in signalling, as for example SemaVib was shown to interact with the SH3 domain of c-src (Eckhardt et al., 1997). The repulsive actions of Sema3A are known to depend on furin convertase processing, which might therefore introduce the first level of axon repulsion modulation (Mark et al., 1997). The Sema3A induced collapse response stimulates endocytosis in growth cones. Endocytosis associated vacuoles at sites of altered F-actin organization contained the Sema3A receptors neuropilin-1 and plexin (mentioned below), and the Sema3A signalling molecule rac1 (Fournier et al., 2000).

Apart from mediating repulsion, like in the case of Sema3A, semaphorins are also known to mediate neurite attraction. Sema3C and Sema-1 mediated attraction was found in vertebrates (Bagnard et al., 1998) and in invertebrates (Wong et al., 1999), respectively. However, the observed guidance responses depend on an increasing gradient, as neither Sema3C mediated attraction, nor Sema3A mediated repulsion could be observed, if axons grew along decreasing semaphorin concentrations (Bagnard et al., 2000). Moreover, neurites from the same cell could respond in an opposite fashion towards a gradient of the axon repellent Sema3A. This semaphorin is suggested to be distributed in a gradient within the developing cortex (Polleux et al., 1998). Axons were shown to grow out along a decreasing Sema3A gradient, while dendrites of the same pyramidal cells moved upwards, requiring both Sema3A and neuropilin-1. In this case, asymmetrical distribution of soluble guanylate cyclase, being high at the apical side of the differentiating pyramidal cell, could explain the different behaviour of dendrites and axons towards cGMP gradients.

Other guidance molecules

The transmembrane receptors of the Roundabout (Robo) family are the receptors for the signalling molecule Slit, although there may be more Slit receptors. Together, Slit and Robo prevent longitudinal axons from crossing the midline as well as commissural axons from recrossing (Farmer et al., 2008).

The ephrins and Eph receptors are involved in the cell signalling pathway and animal development. The Eph receptor was identified in several regions in growth cones of spinal motor and oculomotor neurons (Pasquale et al., 1992).

The paired immunoglobulin-like receptor B (PirB) was found to be a second receptor (next to the Nogo receptor (NgR)) for the myelin inhibitors Nogo, MAG and OMgp (Atwal et al., 2008). Blocking both PirB and NgR leads to a release of neurites from myelin inhibition.

2.2.3 Known molecular reactions to nervous system injury

Unlike the CNS, the peripheral nervous system (PNS) does regenerate spontaneously after nerve injury. Thus, there are numerous studies describing changes in gene expression in the regenerating PNS (Bonilla et al., 2002; Bosse et al., 2006; Bosse et al., 2002; Cameron et al., 2003; Costigan et al., 2002; Fan et al., 2001; Kim et al., 2001; Maier et al., 2008; Nagarajan et al., 2002; Stam et al., 2007; Xiao et al., 2002). Most of these studies focused on transcriptional changes in cell bodies of axotomized sensory or spinal motor neurons, some also on gene expression alterations at the lesion site. Among the genes regulated in peripheral nerve regeneration are the growth associated protein 43 (GAP-43), v-jun sarcoma virus 17 oncogene homolog (c-jun), Galanin (GAL), activating transcription factor 3 (ATF3),

interleukin 6 (IL-6), neuropilin-1 (NRP1). It is likely that the presence or absence of some of the molecules necessary for successful PNS-regeneration play a part in CNS-regeneration failure.

Although a great number of studies investigated the gene expression response in the CNS after brain injury (Bareyre et al., 2002; Rall et al., 2003; Lu et al., 2004; Israelsson et al., 2006; Quintana et al., 2007a; Quintana et al., 2007b; Poulsen et al., 2005; Uhl et al., 1988; Somers and Beckstead, 1990; Salin and Chesselet, 1993, Salin and Chesselet, 1992; Raghavendra Rao et al., 2003), there is only little known about the regulatory response in the brain after spinal cord injury. Some studies suggest that CNS neurons do not respond to axotomy in the way PNS neurons do. For example, GAP-43, a regeneration/growth-associated gene of the PNS was only increased by cortical pyramidal neurons when subjected to a subcortical lesion, but not to a pyramidotomy (Tetzlaff et al., 1994). The same was shown for α -tubulin 1, which is known to be up-regulated in the regenerating PNS but is down-regulated in corticospinal neurons after axotomy (Mikucki and Oblinger, 1991). Interestingly, α -tubulin 1 is down-regulated in retinal ganglion cells (RGCs) after axotomy alone, but up-regulated when a peripheral nerve (PN) graft is applied to stimulate regeneration (Fournier and McKerracher, 1997). Beyond that data of Mason et al. (Mason et al., 2003) suggest that cortical neurons differentially change the injury-induced gene expression depending on the distance of the injury site to the cell body. Interestingly, the authors identified increased expression of a number of growth-associated genes like c-jun, L1, ATF3 and Krox-24 after intracortical but not after spinal axotomy of layer V pyramidal neurons. A recent study revealed no changes in expression of the myelin-associated inhibitors NgR1, NgR2, LINGO1, p75^{NTR} and TROY after severe T10 spinal cord contusion in any neuronal population of the mouse brain (Barrette et al., 2007). The above studies made use of *in situ* hybridisation (ISH)

and immunohistochemistry, in animal injury models without any further treatment. To date, no systematic studies on cortical gene expression profiles after SCI have been performed.

2.3 Lesion model and treatment

2.3.1 The lesion model of the axotomized corticospinal tract (CST)

Unlike in humans the CST in rats is mainly located in the anterior part of the posterior funiculus, between the fasciculi gracilis and cuneatus and the grey commissure. Though, uncrossed fibers from the pyramidal tract can also be found in lateral and ventral area of the spinal cord, the dorsal CST holds between 90-95% of all CST fibers in rats (Brösamle and Schwab, 1997). The main targets of the CST axons are neurons in the grey matter of the spinal cord. In humans these are alpha motoneurons which synapse directly to their target muscle.

The transection of the only the CST leads only to transient functional deficits in rats. Obviously the rubrospinal tract (RST) is able to compensate the functional deficits. Transection of the CST and RST simultaneously leads to permanent functional impairments (Kennedy, 1990). Lesion-caused functional restrictions and recovery of a CST-only lesion can still be observed by functional test like the BBB-score (Basso, Beattie, Bresnahan Locomotor Rating Scale Basso et al., 1995), the horizontal ladder (Metz et al., 2000) and the catwalk test (Gabriel et al., 2007).

2.3.2 Experimental strategies to suppress the collagen IV containing fibrous scar

The fibrous scar is mainly made of a complex extracellular matrix (for detailed review see: Yurchenco and Schittny, 1990). The underlying Coll IV network is connected to the laminin matrix via entactin. Integrins mediate the attachment of cells to this network.

Earlier studies on the proteolytic degradation of the Coll IV containing lesion scar led to extensive bleeding as the BM surrounding blood vessels was also degraded (Feringa et al., 1979). For this reason, an approach was developed to target only the *de novo* synthesis of Coll IV after lesion.

The collagen biosynthesis

In collagen-producing cells like fibroblasts (Berry et al., 1983), astrocytes (Liesi and Kauppila, 2002) and endothelial cells (Schwab et al., 2001) the procollagen is hydroxylated by the prolyl 4-hydroxylase. This reaction is essential to provide stable triple helices formations which are secreted into the ECM. Collagen triple helices spontaneously form networks, in the case of Coll IV sheet-like structures. One key enzyme in the collagen synthesis is the iron-dependent prolyl 4-hydroxylase. A deprivation of the cofactor iron would lead to a low hydroxylation rate and with that to a suppression of a stable collagen network formation.

Transient suppression of the collagen IV containing scar formation by the means of iron chelators

The regeneration supporting effect of transient scar suppression in the CNS could first be shown in the lesion model of fornix transection by local application of iron chelator 2,2'-dipyridyl (DPY, Stichel et al., 1999a). In the lesion model of spinal cord injury the injection of the more potent iron chelator 2,2'-bipyridine-5,5'-dicarboxylic acid (BPY-DCA) alone did not show significant suppression of Coll IV scar formation.

Inhibition of collagen IV producing cells

In the spinal cord meningeal fibroblasts invade the lesion site (Berry et al., 1983). The application of cAMP leads to a suppression of Coll IV production of these cells by interfering with the connective tissue growth factor (CTGF) mediated autocrine effect on proliferation and ECM production (Duncan et al., 1999).

2.3.3 The Anti Scarring Treatment (AST)

The AST-treatment is a combined application of the iron chelator BPY-DCA and 8-bromine-cAMP into the lesion site and an additional long-term release of BPY-DCA from an elvax copolymer placed onto the lesion site after operation. Klapka et al. (Klapka et al., 2005) could show delayed Coll IV expression and fibrous scar formation for up to 12–13 days after injury in treated animals. At 14 days after injury a Coll IV-positive fibrous scar had appeared in treated animals and resembled the collagenous scar in lesioned control animals.

Retrograde axonal Fluoro-Gold tracing of pyramidal neurons in layer V of primary somatosensory cortex projecting into the dorsal CST revealed a remarkable rescue effect of the scar-suppressing treatment in the cortical area of Bregma -1.1 to -2.1 mm.

The effect of scar suppressing treatment on axonal regeneration was tested by anterograde BDA-tracing of the CST. Axon growth was investigated for 10–12 weeks after surgery. In the group of treated animals extensive arborisation of BDA-traced axons could be observed in grey matter. High power magnification revealed that the axonal arborisations were decorated with numerous varicosities resembling presynaptic boutons adjacent to cell bodies located in grey matter. Interestingly, regenerating CST fibres in the distal stump were not restricted to grey matter.

2.3.4 Functional recovery

In Klapka et al. (2005) the functional benefit of fibrous scar-suppressing treatment by studying locomotor behaviour after SCI and treatment was investigated. BBB scores of the open-field tests, the CatWalk test as well as fine motor performance showed significantly improved locomotor performance of treated vs. lesioned control rats.

2.4 Concluding remarks

Increasing information on axon guidance associated protein families, has resulted in a remarkable gain of knowledge about nervous system wiring in the past years. This list reported here is still far from being complete and some guidance families had to be neglected in this introduction.

Though classical biochemical and genetic approaches are still very powerful to identify new guidance molecules and also some of their interaction partners, they fail to detect the highly complex downstream signalling machinery in the growth cone. The availability of genomics techniques enabled researchers to quantify the expression of known and unknown genes on a genomic scale (DeRisi et al., 1997). First, coexpression analysis in clusterograms helped to visualize thousands of genes, which are expressed together in different or similar experimental contexts (Eisen et al., 1998). As technology and the necessary analysis software evolved over time it is possible today to include multiple sources of information like functional annotations and protein interactions to the mere regulation data allowing additional findings on the level of systems biology.

Therefore, looking not only for regulated genes but also interpreting changes in functional group representation and shifts in regulation patterns can help to unravel the complex molecular reactions to axotomy and neuronal regeneration.

3. MATERIALS AND METHODS

3.1 Treatment paradigms and animal groups

To study changes in neocortical mRNA expression after axotomy to the CST in the thoracic spinal cord and to identify alterations in gene expression due to the AST-treatment, three experimental animal groups were examined and compared:

1. *Sham-operated* animals underwent laminectomy and opening of the dura but received no transection of the CST.
2. *Lesion-only* animals further received a CST transection resulting in a non-regenerating condition.
3. *AST-treated* animals received a CST transection followed by a combined treatment with BPY-DCA and cAMP resulting in complex regenerating reactions.

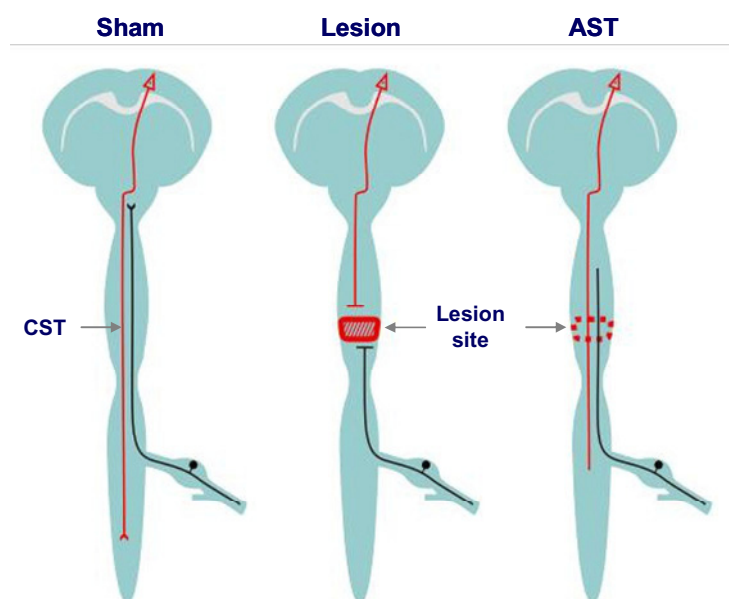


Fig. 1. Animal groups. Cortical tissue including directly affected pyramidal neurons was collected and analyzed from sham-operated, CST-lesioned as well as CST-lesioned and AST-treated animals.

The animals were sacrificed 1, 7, 21 or 60 days-post-operation (dpo). These time-points were chosen to obtain genetic profiles of distinct states of spinal cord injury and repair. While 1

day-post-lesion represents an acute phase, 7 days-post-lesion represents a phase of spontaneous axonal sprouting. At 21 dpo growth cones have reached the border of the lesion site and, in the case of the AST-treated animals, axons have entered the lesion area. At 60 dpo commencement of functional recovery could be observed in AST-treated animals (Klapka et al., 2005).

In this thesis, heterogeneous cortical tissue was used and, therefore, the higher expected variations had to compensate by increasing the number of test animals per experimental group and the type of analysis applied. For that reasons routinely 4-5 biological replicates (minimum 3) per condition were analysed. Samples were not pooled but each subject was hybridized to a separate microchip. Considerations concerning replicate numbers and pooling strategies can be found in section *Impact of experimental setup* (3.10.3). In addition, further technical aspects of this experiment required attention to achieve valuable data, e.g reproducibility of spinal cord axotomy, speed and accuracy of tissue preparation, extraction of quality RNA, optimal conditions for reverse transcription, labelling and hybridization.

3.2 Animals

Adult male Wistar rats (200-250g) were subjects for experimental cortico-spinal-tract transection. Animals were bred within the animal facility (Tierversuchsanlage, TVA) of the Heinrich-Heine-University, Düsseldorf and kept under specific pathogen free conditions until surgery. They were maintained in a temperature (21°C) and humidity (50+/- 5%) controlled animal housing, on a 12h light/dark cycle. Dry and pelleted animal food and water (pH 2), was available ad libitum.

3.3 Retrograde labelling of primary motoneurons which project into the CST

Application of tracer for retrograde tracing and identification of the cortical pyramidal cells (CPCs) was performed immediately after spinal cord injury and treatment by injecting 2 x 0.5 μ L of Fluoro-Gold (Fluorochrome LLC, Colorado, USA; 3% in aqua bideest) lateral to the CST at the most proximal end of segment Th7 using a 10- μ L Hamilton syringe with a 32-gauge canula. After 7 days brains of traced animals were dissected either for calibration of the cortical tissue preparation technique or for cell identification in combination with immunohistochemistry.

3.4 Corticospinal tract transection and Anti Scarring Treatment

Transection of the CST was carried out as previously described in (Klapka et al., 2005). In brief, laminectomy of vertebrae Th8 and Th9 was performed under isoflurane-mediated anaesthesia (Fig. 2a). The dura was opened with spring scissors and the dorsal columns and dorsal CST were cut with a Scouten Wire Knife (Bilaney, Germany; Fig. 2b). Animals with anti-scarring treatment received 2 mg solid 8-Br-cAMP into the lesion site before the dura was sutured (Fig. 2c). The iron chelator 2,2'-bipyridine-5,5'-dicarboxylic acid (BPY-DCA, 40 mM in Tris-buffer) was injected both into the lesion site (4 injections of 0.2 μ l) and at 1mm proximal to the lesion site (2 injections; Fig. 2d). After injection, 2 mg of 8-Br-cAMP were applied to the lesion area. Control animals received injections of Tris buffer without cAMP application. The lesion of treated animals was covered with a piece of ELVAX (ethylene-vinyl-) copolymer sheet loaded with BPY-DCA for slow release, whereas ELVAX copolymer in control animals contained Tris-buffer alone. Finally, the animals were sutured and treated with antibiotics (Baytril) for one week. If necessary, the bladders were emptied manually.

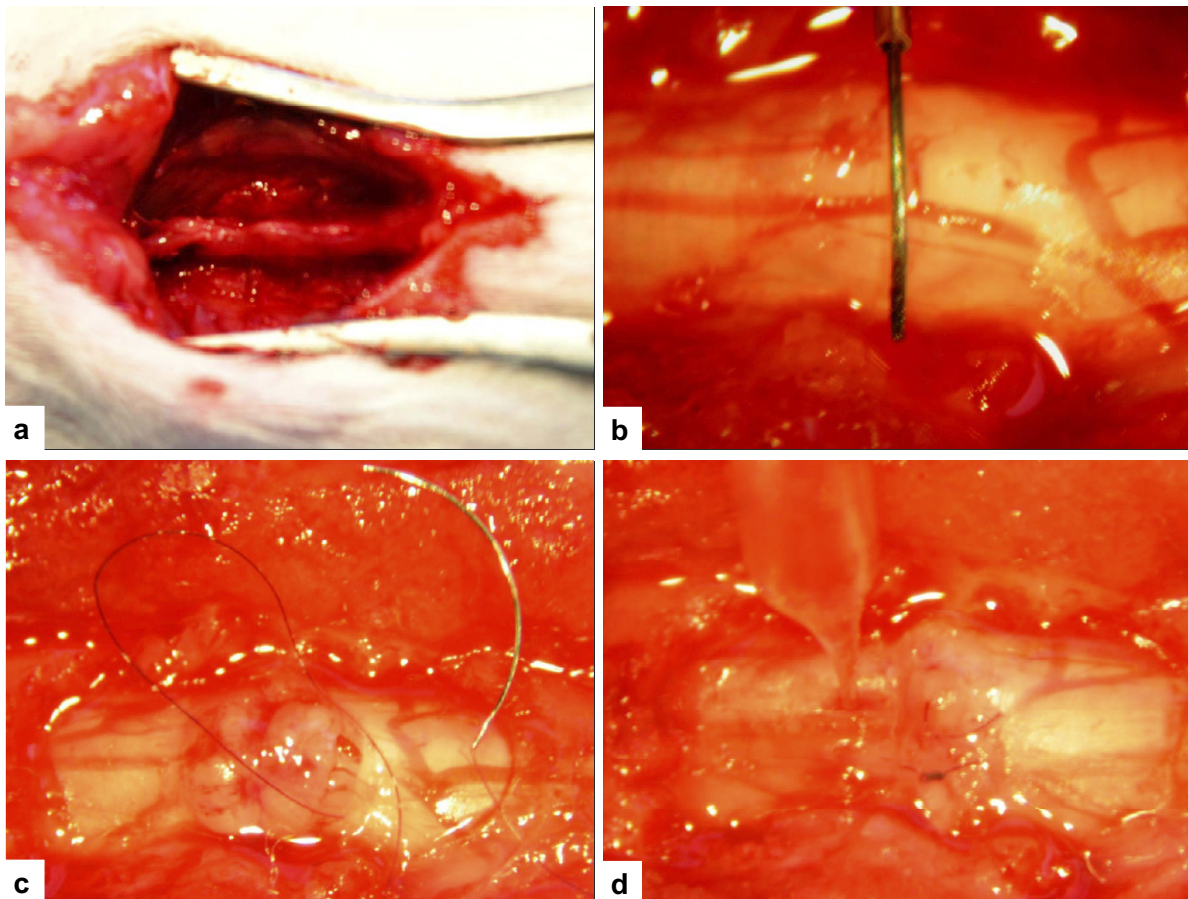


Fig. 2. (a) Laminectomy at thoracic level 8. (b) CST-transection with Scouten Wire Knife. (c) Stitching of the dura mater. (d) One of 6 Tris or BPY-DCA/cAMP injections into the lesion area. (With kind permission of Dr. N. Brazda)

3.5 Tissue preparation

3.5.1 Preparation of brain tissue

For the preparation of tissue for RNA extraction as well as retrogradely labelled tissue recovery each brain was quickly removed from the severed head in a cold room ($\sim 4^{\circ}\text{C}$). The left and right hemispheres were separated and snap-frozen in 2-methylbutan ($\sim -50^{\circ}\text{C}$). Frontal sections ($50\mu\text{m}$ thickness) were created using a cryostat (-25°).

3.5.2 Cortical tissue localization via retrograde labeling with Fluoro-Gold

The adequate cortical area for tissue preparation of pyramidal cells in layer V of the sensory-motor cortex was determined via retrograde labelling with Fluoro-Gold. The area from 0.5 to -1.5 mm Bregma showed the strongest labelling signal in all tested animals and assured reliable as well as reproducible coordinates for subsequent tissue preparation.

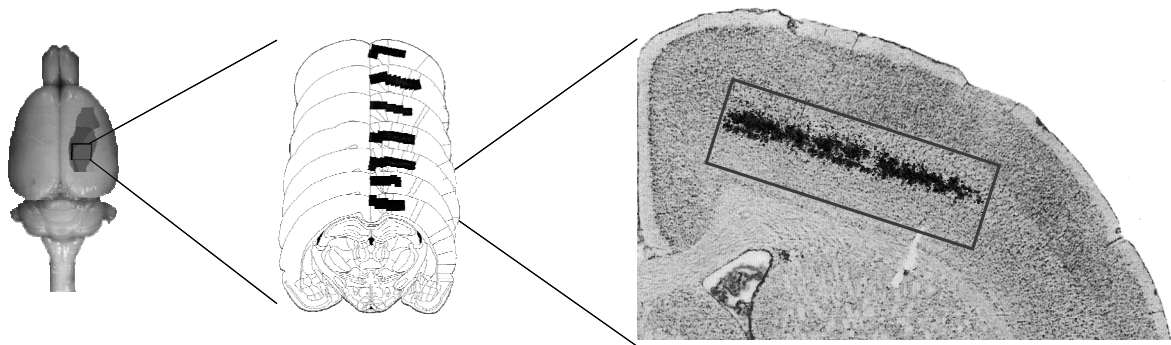


Fig. 3. Identification of the adequate cortical area. Left: 40 adjacent coronal cuts (50 μ m thickness, Bregma 0,5 to -1,5mm). Right: Preparation of cortical layer V and VI.

3.5.3 Preparation layer V sensorimotor cortex and total RNA isolation

For tissue collection the brains were removed in a cold room ($\sim 4^{\circ}\text{C}$) and directly frozen in isopropanol at -45 to -55°C . Using a cryotom 40 serial coronal brain slices of 50 μ m thickness were cut. The area of layer V containing the primary motor neurons and the subjacent part of layer VI were dissected at -20°C and collected in Qiazol. Cortical slices from lesioned adult rats (lesion-only and AST-treated), as well as from sham-operated rats were prepared. Tissue was rapidly removed and processed using the RNeasy Lipid Tissue Mini Kit (Qiagen). In

addition, DNase-I treatment and the RNeasy-clean up protocol (Qiagen) were applied in combination to devoid contamination with genomic deoxyribonucleic acid (DNA).

3.6 Utilized microarray platforms

Except for the one day timepoint the chip type A of the Affymetrix GeneChip® Rat Expression Set 230 was used. For the one day timepoint the Affymetrix GeneChip® Rat Genome 230 2.0 Array was used. The Affymetrix GeneChip® Rat Genome 230 2.0 is holding the same probesets as the combination of Affymetrix GeneChip® Rat Expression Set 230 A+B, approximately 30.000 probesets in total. Due to the fact that the different timepoints were not compared directly among each other differences in the chips are negligible for this study.

3.7 Probe labeling and array hybridization

Briefly, approx. 2 µg of total RNA were converted into labeled cRNA consecutively using Superscript Double-Stranded cDNA Synthesis Kit (Invitrogen) and BioArray High Yield RNA Transcript Labeling Kit (Enzo) for each condition. Following hybridization and several washing steps according to the manufacturer's protocol the hybridized Rat 230A microarrays (Affymetrix) were exposed to a scanner and the signals were digitalized. Signal intensities were determined and raw data quality was independently evaluated using *ArrayAssist* 4.2.0 Software (Stratagene).

3.8 Quantitative polymerase chain reaction (qPCR) procedures

Primers for real-time analysis of early growth response 2 (Krox-20), unc-5 homolog A (UNC5A), galanin (GAL1), vitamin D receptor (VDR), peroxiredoxin 2 (PRDX2), roundabout homolog 1 (ROBO1), colony stimulating factor 2 (CSF2), Bcl2-associated athanogene 1 (BAG1), syntaxin binding protein 1 (STXBP1), glial cell derived neurotrophic factor (GDNF) and kalirin (KALRN) were designed by using *PRIMER EXPRESS 2.0* software (Applied Biosystems) and tested for efficient amplification rates and specific amplicon generation. Real-time qPCR was performed by using SYBR green chemistry (Applied Biosystems) with Glyceraldehyde 3-phosphate dehydrogenase (GAPDH) and Ornithine decarboxylase 1 (ODC1) as reference genes. Reactions and readout were performed on an Applied Biosystems PRISM® 7000 Taqman sequence detection system, relative fold differences were determined with use of the Ct method as described by the manufacturer.

3.9 Immunohistochemistry

For immunohistochemistry rats were anaesthetised with Hypnorm (Janssen-Cilag, Germany) and Dormicum (Roche, Switzerland) and transcardially perfused with 4% paraformaldehyde. Brains were post-fixed in 4% paraformaldehyde, cryoprotected in 30% sucrose and cut on a cryostat for immunohistochemistry.

After microwave antigen retrieval (citrate buffer, 600W for 3x2 min) and blocking of nonspecific binding sites with blocking solution (5% donkey-serum; Sigma, USA, in PBS-T: PBS with 0,1% TritonX-100), 20 µm coronal brain sections were incubated at 4°C over night with rabbit anti-Galanin (1:100; Affinity BioReagents, USA), rabbit anti-VDR (1:750; Affinity BioReagents, USA), rabbit anti-GM-CSF (1:25; Santa Cruz Biotechnology, Inc.,

USA) and rabbit anti-Diablo (1:100; Calbiochem, USA) diluted in blocking solution. Staining was visualized using Avi-Alexa488-coupled secondary antibody (donkey anti-rabbit AviAlexa488, 1:200; Molecular Probes, USA) diluted in blocking solution. After 2 washing steps and elimination of lipofuscin autofluorescence with 0,3% Sudan Black B in 70% ethanol (7 min at room temperature), the brain sections were coverslipped with FluoromountG (Southern Biotech, USA).

As the Fluoro-Gold signal in retrogradely traced pyramidal neurons of sensorimotor cortex (see above) was lost during the immunohistochemical procedures, the sections were photographed before and after immuno staining at identical positions using a BZ-8000 digital microscope (Keyence, Japan).

3.10 Microarray data analysis

3.10.1 Affymetrix gene chip technology

Over the last 10 years, Affymetrix microarrays have become a standard in mRNA expression profiling. Using solid-phase chemical synthesis and photolithographic techniques employed in the semiconductor industry, 25-mer oligonucleotides are directly synthesized at specific locations on coated glass slides as probes for cRNA fragments (Lockhart et al., 1996; Lipshutz et al., 1999). Given the high density of probes due to their small feature size (from 50 down to 2 μm), chips with the size of a human thumbnail holding the whole transcribed genome of species like rat, mouse or human are available today (Affymetrix). To assess non-specific binding, each *perfect match* (*PM*) oligonucleotide sequence is accompanied by a *mismatch* (*MM*) probe in which an incorrect nucleotide is introduced at position 13 of the 25-

mer oligonucleotide. A *PM* probe and its reference *MM* probe make up a *probe pair*. To obtain reliable gene expression measures and background estimations multiple probe pairs are used for each mRNA expression measurement. Typically, on current Affymetrix arrays 11 different probe pairs make up such a so called *probe set*, related to a common gene or a fraction of a gene. Using the information of the multiple measurements of hybridization in each *probe set* allows a more robust measure of expression. However, calculating the expression is much more complex as compared to spotted arrays where each gene is represented by just one probe.

3.10.2 Variations

The measurand in microarray experiments is the amount of a specific transcript in a present sample from prepared tissue or cells of interest. The selective binding of cRNA fragments to their complementary chip probes is a function of this mRNA amount. Unfortunately, this function holds a number of unknown variables which lead to background noise. Among these variables are variations in the RNA extraction and reverse transcription efficiency, chip fabrication tolerances, background intensity fluctuations, non-uniform target labelling, pipetting errors, scanning deviations and so forth. The sources of these variations can be separated in three layers: biological variations, technical variations and measurement errors (Churchill, 2002). The biological variations are of interest for the investigator. This type of variation is intrinsic to all biological organisms and can be influenced by factors like tissue heterogeneity, genetic polymorphism, environmental factors, pooling of samples as well as by any type of treatment (Spruill et al., 2002; Whitney et al., 2003; Molloy et al., 2003; Oleksiak et al., 2002). Technical variations accumulate during handling of the biological samples such

as extraction, RNA preparation, labelling and probe hybridization. Measurement errors originate from the process of reading the fluorescence signals on the array. A complete elaboration of the different sources of variation can be found in Hartemink et al.(Hartemink et al., 2001). Given the fact that the ratio of interesting variations to obscuring variations has a significant impact on the usability of microarray data, minimising the technical variations by controlling the quality of the RNA samples and using well proven and efficient labelling and hybridization methods is crucial (Bakay et al., 2002; Brown et al., 2004; Dumur et al., 2004).

3.10.3 Impact of the experimental setup

The experimental setup has a great impact on the statistical power of the resulting data. This includes the choice of tissue and tissue preparation, number of and kind of replicates as well as the fact whether or not samples are pooled. Multiple replicates for each condition may tremendously increase the cost of a broad experimental setup, but, on the other hand, choosing too few replicates to bring down costs may render a still expensive study into an investigation lacking a reliable result. Various articles have assessed the effect of replicate numbers on the false positive rate(Hariharan, 2003; Pan et al., 2002) or to estimate the statistical power of experiments *a priori* (Seo et al., 2006). Hariharan showed that the number of false positives included to catch all 14 spike-in genes in the Affymetrix Latin Square dataset drops from 2.000 (2 replicates) to 50 (4 replicates).

Pooling biological samples seems to be appropriate to reduce the total number of microchips but keeps the number of animals up. The concept of pooling is to minimize subject-to-subject variations in order to identify substantial differences between the experimental groups (Simon and Dobbin, 2003; Churchill, 2002; Churchill and Oliver, 2001). Drawback of this approach

is the inability to identify and remove outliers and to approximate the variation within the population. While there are ways to minimize this effect by adequate pooling strategies where each group is split into overlapping subgroups, the advantages of pooling are limited to larger study designs and high amounts of samples (Kendziorski et al., 2005; Kendziorski et al., 2003; Shih et al., 2004).

3.10.4 Low-level analyses

To separate biological variations of interest from obscuring variations, the collected raw-data have to be pre-processed. This so called "low-level"-analysis normally includes background adjustment, normalization, *PM* correction and summarization. While background adjustment removes non-specific background from scanned images for each single array, normalization reduces non-specific, non-biological variations between multiple chips. *PM* correction is supposed to reduce the effects of non-specific binding or cross-hybridization by *MM* probe subtraction. The usefulness of this procedure is still controversially discussed in the literature, as several studies have shown that ignoring *MM* probes can lead to a lower variance (Bolstad et al., 2003; Irizarry et al., 2006b; Naef et al., 2002; Bolstad et al., 2004; Irizarry et al., 2003d; Millenaar et al., 2006; Wu and Irizarry, 2005; Cope et al., 2004). Finally, the summarization step generates a single expression value out of the multiple intensities of each *probe set*. Depending on the algorithm used, this can be done with a single chip or including data of multiple chips from one project. The steps of low-level analysis can not be separated by a clear cut as there are algorithmic approaches to solve two or more of these measures at once. There are also approaches that skip one or more steps like the background adjustment or, especially, the controversial issue of *PM* correction (Irizarry et al., 2006a).

In recent years it became more and more obvious that the way the oligonucleotide array data are pre-processed, dramatically influences the results that can be extracted from the experiments (Millenaar et al., 2006). Several studies tried to evaluate the performance of different pre-processing methods, mainly using "spike in" and "dilution" experiments (Hill et al., 2001; Schadt et al., 2000; Qin et al., 2006; Seo and Hoffman, 2006). Given the many different ways to perform the respective parts of low-level analysis and their countless combinations, making the right choice for pre-processing has become a scientific field of its own. Obviously, though coefficients like accuracy, precision and bias from a set of pre-processing combinations can be assessed, the overall "performance" is difficult to measure. The "performance" of low-level analyses mainly depends on the type of data to be processed, on factors like the number of chips, on the type of tissue that is to be analyzed and on the scientific goal that is pursued.

Microarray Suite (MAS)

Until 2001, GeneChip MAS 4.0 software used the average of the difference (*AvDiff*) of corresponding *PM* and *MM* intensities to calculate expression values. *AvDiff* is defined as

$$[1] \quad AvDiff = |A|^{-1} \sum_{\{j \in A\}} (PM_j - MM_j)$$

with *A* a set of suitable probe pairs. In about 1/3 of the probe pairs of an average array $MM \geq PM$ (Irizarry et al., 2003a). Thus, adjusting for non-specific binding and background noise by the *PM-MM* transformation leads to two obvious problems: about 5% of the resulting intensities of the *probe sets* are negative and data including negative values cannot be log transformed to account for the multiplicative measurement error. With introduction of MAS 5.0 in 2001 the *signal* was calculated as follows:

$$[2] \quad signal = Tukey\ Biweight\{\log(PM_j - MM_j^*)\}$$

with MM^* is a modified MM value to prevent adjusted expression values to become less or equal 0. Each probe pair has a "vote" in determining the *signal*; the probe pairs are weighted based on their distance from the *probe set* mean. Using the weighted intensity values, the adjusted mean for the *probe set* is determined (for detailed information on MAS 5.0 see Affymetrix, 2001). For background adjustment each chip is divided into 16 zones correcting the probe values by using (i) the second percentile of the probe values in that zone as background and (ii) the distance of the probe to the centre of its zone as a weight. To normalize the data of multiple chips MAS 5.0 uses linear regression, scaling the overall intensities of all chips to the same user-defined target intensity.

Model-based Expression Indexes (MBEI)

In 2001 Li and Wong (Li and Wong, 2001) showed that there are huge differences in the intensities of probes in the same *probe set*, though they all bind different segments of the same gene. However, the so called *probe set patterns* of genes are generally the same compared between different chips. The MBEI method, implemented in the dChip software package, uses this information to account for individual probe-specific effects as well as detection of outliers and image artefacts (Schadt et al., 2001). The *invariant set*, a large number of ad-hoc selected genes as references for non-linear normalization instead of a fixed catalogue of "housekeeping genes", is used for normalization (Li and Wong, 2001). Both a *PMMM* and *PM* mode are implemented in dChip, meaning that either the *PM/MM* differences are evaluated (*PMMM*) or ignored (*PM*).

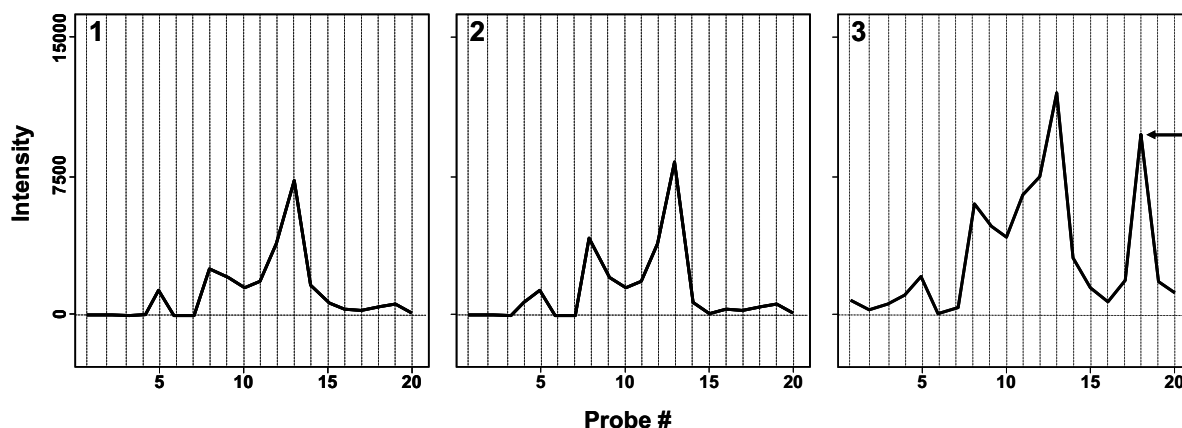


Fig. 4. Outlier detection by means of probe set patterns. The 20 PM intensity values of one probe set on three different arrays plotted against their probe numbers show almost the same profile. Irregular probes (black arrow) or chips can be identified. Figure modified from Li & Wong, 2001.

Several other low-level analyses have been developed from different groups. Most of them are based on the findings of Li and Wong (Li and Wong, 2001), namely strong probe effects in *PMMM*-adjusted intensity values, advantages of multi-array summaries for signal estimation as well as outlier detection and need for non-linear normalization.

Robust Multiarray Average (RMA)

In 2003, Irizarry et al. introduced RMA as a new method for low-level analysis (Irizarry et al., 2003a; Irizarry et al., 2003b). It is based on the discoveries made by Li and Wong, but uses different algorithms for each pre-processing step. Only *PM* values are used for the calculation, the *MM* values are ignored. The assumption is made that the observed *PM* intensity distribution is a combination of an exponentially distributed signal and a normally distributed background. The resulting background corrected probe intensities are then normalized using *quantile normalization*. Bolstad et al. (Irizarry et al., 2003a) demonstrated that data-driven *quantile normalization* is a fast and simple way of normalization. Moreover, *quantile normalization* showed good performance when compared to two other, already established

methods (*cyclic loess* and *contrast based*). All three normalization methods are referred to as "complete data methods", meaning that the data of all chips in an experiment are combined to form the normalization relation. *Quantile normalization* adjusts the data of all arrays to the same distribution. The method is based on the idea that a quantile-quantile plot of two data vectors shows a straight diagonal line if the distributions of the two vectors are the same. This suggests that projecting the data points of all n arrays in a n dimensional quantile-quantile plot onto the n -dimensional diagonal identity line leads to an equally distributed data set. Table 1 shows a simplified example: the expression values of each chip make up a column of a spreadsheet, each row representing a specific gene. Now each column is sorted in increasing order and the values of every cell are replaced with the row average. Finally, the columns are unsorted, each row representing a gene again. This method works well with most types of datasets and is stable against outliers. However, an extreme probe intensity value of a gene on a certain chip can influence the calculated expression values of different genes in the dataset of all the other chips. Therefore, *quantile normalization* should be performed before summarization in order to prevent such rare cases. Moreover, certain kinds of experimental setups can lead to a high error rate due to the assumption that there are no distribution changes over all chips. Looking at over 15.000 genes in one study, overall up- and down-regulation should be approximately the same. However, in studies involving malignant tumors, ageing or major interference of the transcriptional apparatus, this basal assumption made for *quantile normalization* may lead to aberrant biological results.

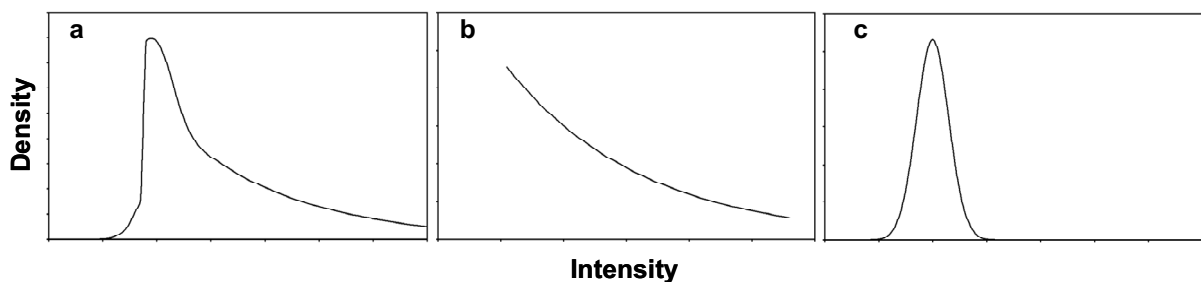


Fig. 5. Components of the measured intensity distribution. Detected density of probe intensities (a) includes two components, an exponentially distributed signal (b) and a normally distributed background (c).

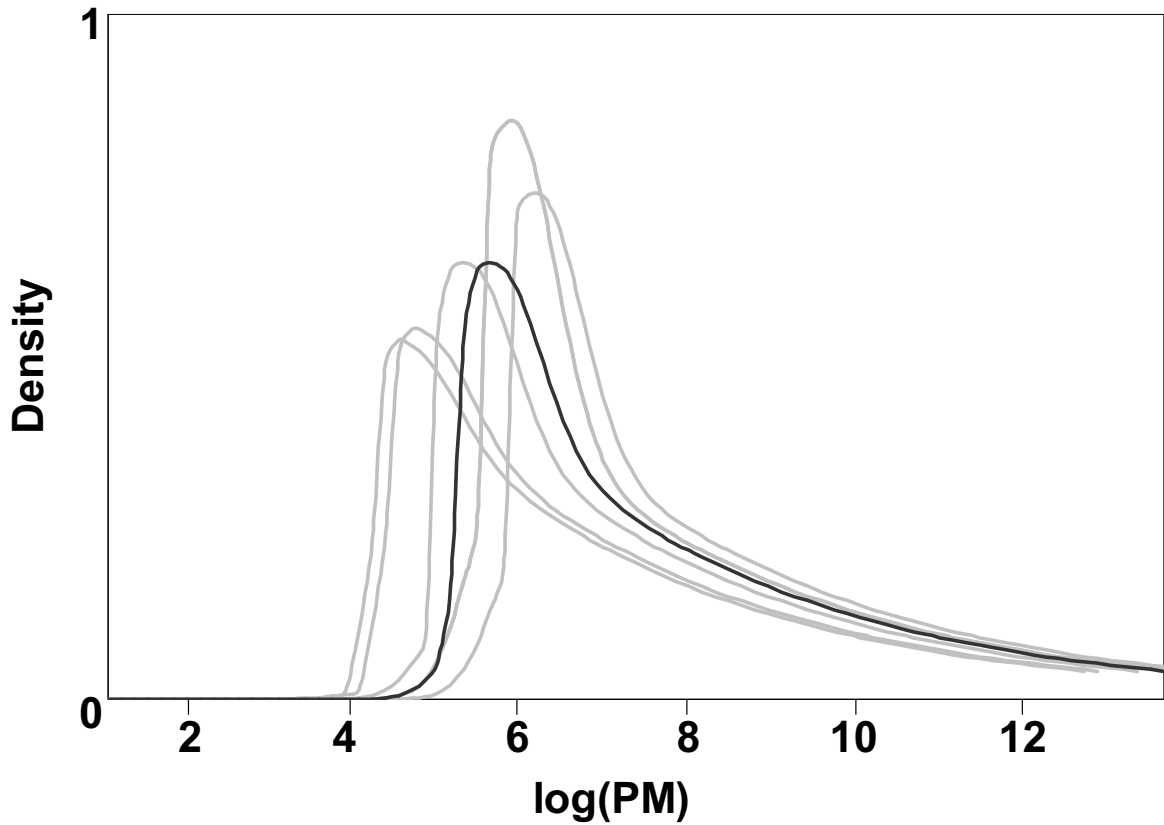


Fig. 6. Densities of *PM* probe intensities for spike-in datasets. Distributions before (grey) and after (black) quantile normalization are plotted. Figure modified from Bolstad et al., 2003.

After performing quantile normalization, RMA fits the background-adjusted, normalized and \log_2 -transformed *PM* intensities, denoted with Y , to a linear additive model:

$$[3] \quad Y_{ijn} = \mu_{in} + \alpha_{jn} + \varepsilon_{ijn}, \quad i = 1, \dots, I, \quad j = 1, \dots, J, \quad n = 1, \dots, n$$

with α_j standing for a probe affinity effect and ε_{ij} is an independent identical error term with mean 0. An estimated μ_i represents the log scale expression level for *probe set n* on array *i*.

The assumption that the average of each *probe set* is a representative measurement of the associated gene's expression leads to $\sum_j \alpha_j = 0$.

The model parameters are estimated using the robust *median polish* (Holder et al., 2001) procedure. A detailed comparison of MAS5.0, MBEI and RMA methods is given in Irizarry et al. (Irizarry et al., 2003c).

	Chip 1	Chip 2	Chip 3		mean	Chip 1	Chip 2	Chip 3
Gene 1	4	5	6	→	4	4	2	6
Gene 2	8	11	9		6	4	5	9
Gene 3	7	10	10		9	7	10	10
Gene 4	4	2	14		11	8	11	14

	Chip 1	Chip 2	Chip 3		mean	Chip 1	Chip 2	Chip 3
Gene 1	4	6	4	←	4	4	4	4
Gene 2	11	11	6		6	6	6	6
Gene 3	9	9	9		9	9	9	9
Gene 4	6	4	11		11	11	11	11

Table 1. Example for *quantile normalization*. Columns representing chip data are sorted in ascending order, the values in each row replaced by the rows mean and finally the columns unsorted. After *quantile normalization* each chip shows the same distribution, due to the same values in every column. For example gene 2 seems to be lower expressed in the sample on chip 3, though the original values do not show that directly. Extreme outliers can influence corrected values of other genes on other chips.

GC-RMA

In 2004, Wu and Irizarry (Wu et al., 2003) added a new way of background adjustment to the RMA method, using probe sequence information to estimate the affinity of the probe for non-specific binding (NSB). This approach, called GC-RMA, was designed to resolve the

drawback of RMA. While the precision of RMA is high, it lacks accuracy in estimating fold changes. The new GC-RMA method not simply uses the GC content but the position of each base type (A, T, G or C) in the 25-mer oligonucleotide sequence to determine the affinity of each probe. Two effects come in to play here. First, G-C pairs form three hydrogen bonds as opposed to two in the case of A-T pairs, leading to a stronger hybridization. Second, the purines U and C in the mRNA are labelled, leading to weaker hybridization (Naef and Magnasco, 2003).

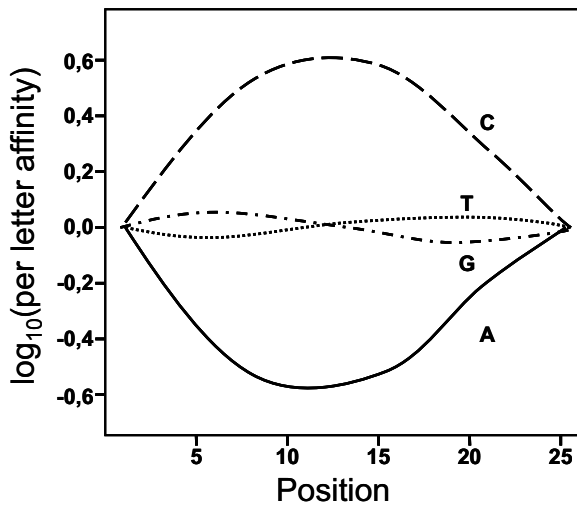


Fig. 7. Effect of bases A, T, G and C in position k on the affinity and brightness of probes. Position 1 corresponds to the first base on the glass slide. Figure modified from Naef & Magnasco, 2003 and Wu et al., 2003.

The original model introduced by Naef and Magnasco (2003) described the probe affinity α as the sum of position-dependent base effects:

$$[4] \quad \alpha = \sum_{k=1}^{25} \sum_{j \in \{A, T, G, C\}} \mu_{j,k} 1_{b_k=j} \quad \text{with} \quad \mu_{j,k} = \sum_{l=0}^3 \beta_{j,l} k^l,$$

where $k=1, \dots, 25$ represents the position along the probe, j indicates the base letter, b_k indicates the base at position k , $1_{b_k=j}$ is 1 when the k -th base is of type j and 0 otherwise, and $\mu_{j,k}$ indicates the contribution to affinity of base j in position k . The effect $\mu_{j,k}$ for fixed j is assumed to be polynomial of degree 3. This model is adapted to describe the NSB in GC-RMA. It is assumed that PM is the sum of optical noise O_{PM} , NSB noise N_{PM} and the signal S while MM is the sum of optical noise O_{MM} and NSB noise N_{MM} only. *Maximum Likelihood*

Estimate (MLE) or *Empirical Bayes Estimate* (EB) is used to estimate S . GC-RMA implementing an empirical Bayes approach outperforms RMA for low expressed genes.

Probe Logarithmic Intensity Error (PLIER)

Affymetrix introduced PLIER in the year 2005 (Affymetrix, 2005). Because of the complex interactions leading to measured intensities, the analyzed parameters are termed *feature responses* instead of *probe affinities* as in Irizarry et al. (Irizarry et al., 2006a). The PLIER algorithm does not utilize probe sequence information. It rather generates an empirical *probe set specific feature response pattern* that is supposed not only to incorporate the different thermodynamic properties and binding efficiencies, but also other factors like labelling, non-equilibrium washes, and density of synthesis. This *feature response pattern* can be compared to the *probe set pattern* introduced in MBEI. *Feature response patterns* across multiple arrays are utilized to identify poorly performing features with erratic hybridization characteristics. The PLIER algorithm additionally accounts for heteroskedacity of the data. It is assumed that in *probe sets* with a mean close to the background, probes with the highest *feature response* are those most informative. In the process of signal generation each feature receives a weight, the most informative features providing the strongest contribution to the signal. The weight is depending on the consistency of the feature over multiple arrays and the median feature intensity, favouring higher *feature responses* at the low end of target abundance. The error estimation also includes abundance information. While at low abundance the largest component of the measured intensity is most likely background, at high abundance it is specific target response. This is also true for the error contained in the intensity. To avoid underestimation of error at the lower end of abundance, PLIER implements an error model, which smoothly transitions between a low abundance "arithmetic" to a high abundance "multiplicative" form. This design leads to a high sensitivity for low expressors and a low

false positive rate (Seo and Hoffman, 2006). A detailed description of the underlying M-estimator calculation can be found at:

http://www.affymetrix.com/support/technical/technotes/plier_technote.pdf

3.10.5 Statistical analysis

Once the data have been background corrected, transformed into log scale, normalized and summarized, expression values for every gene are obtained. The main purpose for microarray experiments is to assess information about differences of gene expression. Thus, a decision has to be made which genes will be accounted for as regulated/differently expressed based on their expression values. The easiest way is to calculate the ratio of the group's mean expression values, the so called fold change, and set a threshold above which the genes will be considered as regulated. This method was widely used at the beginning of the microarray era. The fold change cut-off, however, has major drawbacks, because it does neither accommodate for the actual level of expression values nor for their variance. While at small intensities slight changes of the signal due to background noise can already lead to a massive fold change, highly expressed, truly regulated genes on the other hand may not reach the fold change cut-off, potentially already running into a saturation effect. Furthermore, the resulting fold change value is highly dependent on the preceding low-level analysis. By changing the type of background adjustment the fold change could change dramatically (Seo and Hoffman, 2006).

Additionally, comparison of actual RNA amounts to resulting fold changes measured in spike-in experiments showed that the ratios assessed by microarray data greatly underestimate the actual RNA fold changes (Cope et al., 2004). Taking into account that these changes could

be caused by only a subgroup of cells in heterogeneous tissue samples, biologically relevant gene regulations may show fold changes lower than 1.5.

The t-test can be used to prove significance in differential gene expression between two experimental groups. The t-statistic t_g is calculated for each gene g with e_1, e_2 representing the mean expression values, s_1, s_2 the standard deviations, and n_1, n_2 the number of arrays for group 1 and 2:

$$[5] \quad t_g = \frac{e_1 - e_2}{\sqrt{\frac{s_1^2}{n_1} + \frac{s_2^2}{n_2}}}$$

The t_g value can be transformed into a more convenient p-value using the Student's t-distribution. The assumption is made that the expression values in each group are normally distributed and the variances of these two distributions are the same. Thousands of genes are tested at once, leading to a severe inflation of the *type I error rate* increasing the chance for false positives. To neutralize this effect several p-value correction methods have been introduced. The p-value correction methods based on the family wide error rate (FWER) tend to be rather conservative leading to a higher number of false negatives. The FWER controls the chance of having one false positive in the group of regulated genes. Given the nature of microarray studies with thousands of analyzed genes and often hundreds of regulated genes the less conservative p-value correction method controlling the false discovery rate (FDR) is often advisable. This method does not control the chance of having one false positive but it controls the chance of having a given percentage (normally 5%) of false positives.

If more than two conditions have to be analyzed a comparison of all possible individual pairs of conditions could be performed using the t-test. But increasing the number of tests will subsequently rise the number of false positives. Another parametric test, the *analysis of variance* (ANOVA), is not bound to a comparison of only two groups and might thus be

beneficial in such a study. The ANOVA follows the null hypothesis that the population means μ for all conditions are the same:

$$[6] \quad H_0 : \mu_1 = \mu_2 = \dots \mu_k$$

with H_0 is the null hypothesis and k the number of conditions. Basically, ANOVA compares two estimates of variance (σ^2), the *Mean Square Error (MSE)* and the *Mean Square Between (MSB)*. The *MSE* is based on the variances within the sample's and is an estimate of σ^2 no matter if the null hypothesis is true or not. The *MSB* is based on differences among the samples means and is only an estimate of σ^2 if the null hypothesis is true, otherwise it will be larger. Therefore, if $MSB \gg MSE$, it is likely that at least one mean of the population is different to the rest. The ratio of *MSB* and *MSE* can be used to calculate the corresponding p-value for this difference using the *F distribution*. Just like the t-test, the ANOVA assumes independence, normal distribution and homogeneity of variance. Although the distribution of microarray data of interest may not be known, ANOVA is quite robust to violations of these assumptions, tending to be rather conservative. To completely avoid these problems, non-parametric methods like *Mann-Whitney U* for two conditions or *Kruskal-Wallis* for more than two conditions are suitable tests for statistical analysis.

3.10.6 Biological pathways and ontology information

Fitting a list of regulated genes to already known pathway maps of biological processes provides an approach towards the understanding of the biological function of the observed gene regulations. Projects like the *Kyoto Encyclopedia of Genes and Genomes (KEGG)* database of biological systems; (<http://www.genome.jp/kegg/>) may help to unravel putative molecular interactions and signalling networks. Tools like *PathwayArchitect* use known

connections between genes and their products elucidate putative functional pathways out of a given group of genes.

In information science, ontology describes a set of individuals and the relationships between these individuals within a domain. In the case of gene ontology (GO) the individuals are different genes which belong to certain classes, like "cytoskeleton" or "neurotransmitter secretion". Linked by the two relationships *is-a* and *part-of* these GO-classes build a tree-like structure holding information about biological processes, cellular components and molecular functions in a species-independent manner. While annotation binds biological information to specific genes, ontology provides a framework of structured, controlled vocabulary to do this. Using gene ontology annotation information is a simple way for a high-level analysis of gene functions based on microarray data. Web-based tools like *David* (<http://david.abcc.ncifcrf.gov>) or *L2L* (<http://depts.washington.edu/l2l/>) enable the scientist to identify functional annotations, which are significantly enriched in a given list of *probe set* IDs as described in the following example: Imagine that a functional group F which is represented by 100 genes on a chip with 10.000 different *probe sets* hitting at least one of the terms in the GO-database. By chance, about 1% of the genes in a list of regulated genes belongs to F . If the outcome of a virtual array experiment results in a much higher proportion of regulated genes of that functional group F , it would be strong evidence for a possible biological function of that specific group in the analyzed paradigm. One handicap of this procedure is that only one gene list is analyzed at a time. For a more detailed description of high-level analysis measures see Kruse et al. (*Kruse et al., 2008*).

4. RESULTS

4.1 Lesion model and tissue preparation

This work demonstrates that cortical gene expression profiles after thoracical CST transection as well as after thoracical CST transection and regeneration promoting treatment can be assessed by the means of microarray hybridisations. The lesion model is adequate to produce test animals with comparable lesions resulting in animal groups with similar cortical gene expression. The tissue preparation methods using cryo-dissected slices and microscope aided scalpel tissue preparation led to well-preserved total RNA as well as adequate and reproducible localization of tissue-blocks. The comparability of the resulting animal groups in the different conditions was checked by correlation analysis and principal component analysis (PCA).

4.2 Difficulties and solutions in microarray experiments

4.2.1 From raw data to biological meaning

The presented comprehensive study on differential genomic responses in sensorimotor cortex after CST transection with or without pharmacological intervention implies several factors which complicated the identification of differentially expressed genes. As noted above heterogeneous cortical tissue was studied, a fact which implies the advantageous potential to analyse both neuronal and glial reactions to CST lesion. However, this approach leads to a

decrease in signal detection, because gene expression changes in one particular cell type are diluted by the other cells. As well, counteracting responses in different cell types may mask each other. In the case of the CST lesion, only a proportion of cells in the analyzed cortical tissue, the primary motor neurons of layer V, are directly affected by the lesion. Furthermore, only a subpopulation of these neurons will regenerate, depending on the condition examined. Nevertheless, to assure accurate and reproducible results an increased number of biological replicates per condition were used and in the subsequent data analysis a broad spectrum of pre-processing methods was implemented. Gene regulations involved in regeneration processes, apoptosis and survival were identified and distinct AST treatment-mediated modifications were observed.

4.2.2 Data processing

Initial data analysis has been performed using the Stratagene softwares *ArrayAssist* and *PathwayArchitect*. Using *ArrayAssist* the investigator can choose between the 5 well established algorithms for low-level analysis, MAS5, MBEI, PLIER, RMA and GC-RMA. To ensure a fast and flexible workflow, scripts based on the programming language *Python* to automatically and reproducibly process the analysis of different sets of arrays were developed. The raw data was imported separating the chips into groups according to their experimental conditions. The *Python* scripts automatically performed the corresponding sets of background correction, normalization, variance stabilization and log transformation and carried out statistical analyses for all five algorithms. When finished the resulting data sets were exported to *Excel* file format by the *Python* scripts. Further analysis was done in *Microsoft Excel* using a package of self-provided *Visual Basic for Applications* (VBA)-based tools which was termed ChipChat. The resulting lists of regulated genes additional information from external

databases like *David* (<http://david.abcc.ncifcrf.gov>) or *L2L* (<http://depts.washington.edu/l2l/>) could be accessed via the VBA-tool for high-level analysis, functional grouping and clustering.

4.2.3 Combination of pre-processing methods

Five of the most commonly used pre-processing methods have been described above. Depending on multiple factors all algorithms will be able to find more or less overlapping and accurate groups of regulated genes. Using only one pre-processing algorithm will lead to biased data depending on the accuracy and precision of the algorithm and the type of background adjustment, normalization and summarization steps. To narrow down the group of false negatives without including too many false positives a combination of multiple analysis methods appears beneficial in the majority of cases (Irizarry et al., 2006a).

Box 1: Error types

Two different types of errors can be differentiated, *statistical* and *systematic errors*. Although the statistical error is caused by random variations, the systematic error is the result of nonrandom variations of an unknown source.

The statistical error can be divided into two types:

- *Type I* is the error of accepting a difference when in truth there is none (*false positive*).
- *Type II* is the error of accepting the null hypothesis when in truth there is a difference (*false negative*)

For each experiment, a reasonable balance between *type I* and *type II errors* (Box 1) has to be found, based on the data and the scientific aim. If only a few new candidate genes are to be identified a higher false negative rate can be accepted. In a systemic approach, on the other hand, a slightly higher false positive rate will not disturb the overall regulation pattern, but, e.g., an algorithm-specific non-sensitivity for low-level expression changes will do so. In this

thesis a method implementing five well-described algorithms with different weights on the "vote" for regulation was developed that can be used to utilize the advantages of all algorithms while holding the disadvantages in check. As multiple statistical tests based on the resulting data of each pre-processing method are performed, the p-value thresholds need to be adapted to compensate for the resulting *type I error* increase.

ChipChat software tool

Due to the complex experimental setup, including multiple analyzed conditions and timepoints as well as the heterogenous brain tissue samples, the analysis of the microarray data had to be adjusted. By incorporating the whole data derived from the five different pre-processing methods used into the ChipChat software tool, the five resulting lists of regulated genes can be compared directly. Moreover, the setting of separately changeable thresholds for crucial criteria, like p-values and fold changes enables widespread analyses and comparisons. Overlaps of lists were calculated and information regarding ranks or percentages of genes which have a proper p-value but do not meet the fold change threshold can be assessed. In the "vote" for regulated gene expression the different algorithms could be rated by selectable weightings. A concluding results sheet was then generated representing the calculated expression information of all algorithms for each regulated gene including the respective fold changes and p-values. For each gene in each comparison a *regulation index* is calculated based on the number of pre-processing methods which account for the gene to be regulated, the weights given for the respective analysis type and the direction of regulation. This *regulation index* offers the excellent capability for fast semi-automated identification of genes that, e.g., satisfied specific threshold criteria in at least three of the pre-processing procedures.

Additionally, genes comprising similar regulation patterns can be identified. These calculations can be performed with multiple worksheets at once, which enables the user of ChipChat to quickly compare different datasets and further simplifies an informed decision what data sets are reliable.

Implemented thresholds

Using the ANOVA statistical test additional lists of genes were generated, which were significantly regulated at least in one of the analyzed conditions. To specify the time-point and experimental condition at which a particular gene is regulated t-tests were applied. Using the information gained from t-test cross-comparisons genes were classified (i) as regulated in response to the injury, (ii) as boosted or counter-regulated due to AST-treatment when compared to lesion-only, (iii) or exclusively regulated in the AST-treated. The results shown here were acquired using a one-way-ANOVA for the 7, 21 and 60 dpo time-points (with a p-value threshold of 0.02 after GC-RMA and PLIER low-level analysis). The 1 dpo time-point contained only two conditions, therefore t-tests were run p-value thresholds of 0.02 and fold change thresholds of 1.3. At 1 dpo a gene was considered to be regulated if the calculations met the thresholds in at least 2 out of the 5 low-level analysis methods described, and if one of the fulfilling methods was GC-RMA or PLIER. Using these analysis settings resulted in reliable list of regulated genes. These regulations could be confirmed for selected genes by qPCR. Additionally, the list of regulated genes are verified by the results of the high-level analysis below.

4.2.4 Resulting guidelines for microarray data low-level and statistical analysis

When planning a study based on microarray data, it is fundamental to define the goals of this study. As the group sizes, the appropriate low-level analysis as well as statistical analysis depend on the type of tissue or samples as well as the experimental setup, the thresholds depend on the scientific goals of the study. Generally, thresholds that should be considered are minimum expression values, the fold-change cut-off, the p-value cut-off as well as combination of multiple low-level analysis types in an *and* or *or* connection. If the goal is to identify only a handful of strongly regulated candidates associated with a certain condition these thresholds should be chosen in a wider range. However, if the goal is to identify a broad spectrum of regulation for further high-level analysis a less conservative strategy is reasonable to a certain degree, as potential false positives should not interfere with high-level analysis results.

Quality control is a crucial step in microarray data analysis as the chip failure rate, e.g. for Affymetrix chips, lies at about 10%. Checking internal controls, correlation plots and PCA visualisations helps to identify potential outlier chips.

To minimize the inflation of the error type I rate, prefiltering is recommended. The stricter the filter criteria are in these steps, the higher is the percentage of identified significant regulations in the remaining dataset. Next to filtering for minimum expression levels and fold-change cut-offs it can be advisable to additionally filter for the genes which can be found significantly regulated by multiple low-level analysis algorithms.

The statistical evaluation depends on the experimental setup, the number of groups and their dependencies. In most cases, where more than two conditions are studied, a uni- or multi-variant statistical test like ANOVA followed by an adequate post-hoc test can be used. By

using a FDR-based error correction, the experimenter is able to directly control the type I error rate without losing high numbers of accurate results.

4.3 Cortical gene expression profiles following spinal cord injury

In order to characterize the changes in cortical mRNA expression profile after thoracic spinal cord injury RNA samples from cortical layer V of CST-transected adult rats to that of sham-operated animals were compared (Fig. 1 a,b). Significantly regulated genes comprising stage-specific molecular responses over a period of 1, 7, 21 and 60 dpo (Table 2) were identified. Out of a total of ~11.000 genes represented on the chip, approximately 3.100 genes were detected that showed significant regulation at least at one of the selected timepoints.

	Total	Lesion vs. Sham			AST vs. Lesion		
		regulated	up	down	regulated	up	down
1 dpo	917	521	41%	59%	430	25%	75%
7 dpo	1404	853	44%	56%	732	68%	32%
21 dpo	2035	1199	27%	73%	1167	55%	45%
60 dpo	1582	959	56%	44%	866	51%	49%

Table 2. Numbers of regulated genes in sensorimotor cortex of sham, lesioned-only and AST-treated rats at four different timepoints (1, 7, 21, 60 days) after surgical treatment. The numbers and proportions of up- and down-regulated genes are shown. While the numbers of regulated genes identified at each timepoint are very similar for the lesion and AST group, a strong imbalance of up- vs. down-regulations was observed at 1 and 7 dpo in the AST-group and at 21 dpo in the lesion-only group.

Significantly enriched functional groups of regulated genes after SCI

1 dpo	7 dpo	21 dpo	60 dpo
apoptosis	response to oxidative stress	translation	apoptosis
response to wounding	macromolecule metabolic process	biosynthetic process	protein metabolic process
protein folding	brain development	ribosome	structural constituent of ribosome
cytoskeleton organization	neurological process	cytoskeleton organization	synaptic transmission
regulation of neurogenesis	glutamate receptor activity	signal transduction	
	neurotransmitter transport	synapse part	
		ion channel activity	
		postsynaptic membrane	

Table 3. Significantly enriched functional groups of regulated genes after SCI. Differentially regulated genes were checked for GO-term enrichments. The cortical regulatory response to CST-lesion shows a timepoint-specific profile of strongly modulated functional clusters.

As early as one day after CST transection 521 genes were significantly regulated in Layer V despite of the distance of several centimetres from the lesion site in spinal cord (at thoracic level 8) to the sensorimotor cortex from which the RNA was isolated (Table 2). Later (7 - 60 dpo) the number of regulated genes was further increased and showed a maximum of 1.199 genes at three weeks after injury. Notably, the proportion of up- and down- regulations varied over time. While at 1, 7 and 60 dpo close to 50% of the genes were regulated in either direction, at 21 dpo nearly 75% of the regulated genes were repressed (Table 2).

Analysing the enrichment of regulated genes in functional groups of the GO-tree, the analysis indicated strong stage-specific dynamic modulation of different functional processes (Table 3). At 1 dpo affected processes included, among others, “wounding responses”, “growth-associated cytoskeletal reorganization” and “cell survival”, whereas at 7 dpo “metabolic and transport processes” and genes involved in “oxidative stress responses” were concerned. Later on, functional groups involved in “protein biosynthesis” and “synaptic reorganization” were enriched at 21 and 60 dpo. Likewise, “apoptotic processes” were strongly modulated at 60 dpo.

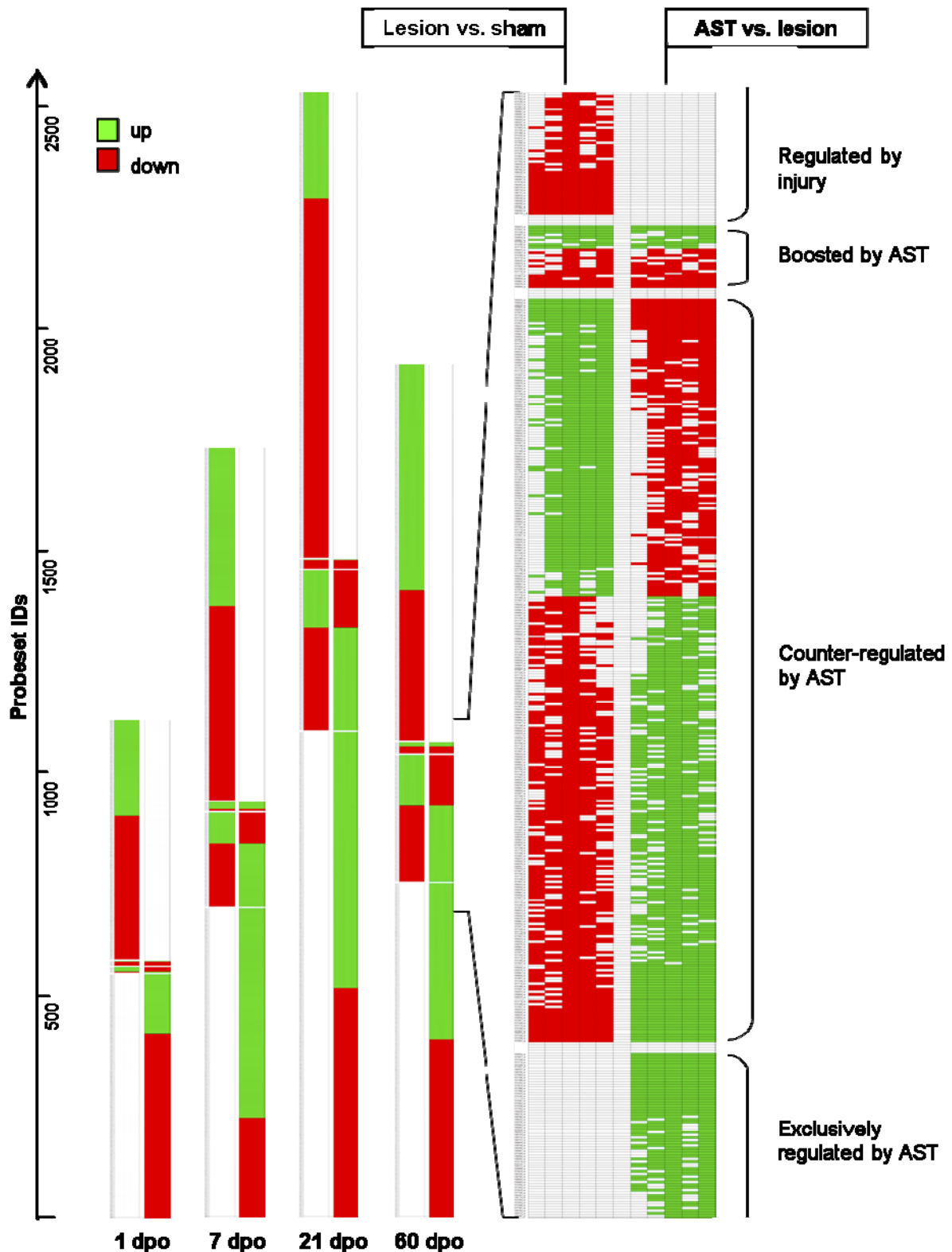


Fig. 8 Schematic representation of expression changes in lesioned animals compared to sham animals and in AST animals compared to lesion controls illustrates the various regulation patterns. In comparison to lesion-induced regulations, AST-induced regulations showed four different responses: (i) probesets “Regulated by injury” are strictly altered by SCI regardless of an additional AST treatment (no significant regulation in the comparison AST vs. Lesion); (ii) “Boosted by AST” are probesets with altered expression by injury that become

further up- or down-regulated by AST; (iii) “Counter-regulated by AST” represents probesets which are regulated back to or beyond sham-level by AST; (iv) probesets “Exclusively regulated by AST” show no significant Lesion vs. Sham regulation. The detailed view on the left illustrates the results of all the five implemented algorithms (Mas5, LiWong, Plier, RMA and GC-RMA) for each comparison (Kruse et al., 2008).

4.4 Modulation of the cortical lesion-triggered gene expression profile by AST

Direct comparison of gene expression in AST animals with lesion-only control rats revealed a strong modulation of lesion-triggered gene expression profiles by the regeneration promoting treatment (Table 2). Similar to lesion-only animals the number of significantly regulated genes in AST-treated animals increased over time reaching a peak at 21 dpo (1167 genes, Table 2). Over the entire period (1-60dpo) approximately 2.800 genes were significantly altered in treated compared to lesioned animals. While at 1 dpo only 25% of the regulated genes in AST animals were up-regulated, nearly 70% of the regulated genes were up-regulated at 7 dpo. Interestingly, the total number of regulated genes at each timepoint corresponded among the groups of lesion-only and the AST animals. Thus, the detected regulatory complexities of cortical reactions to SCI on the one hand and the time-dependent alterations of these lesion-triggered modifications by AST-treatment are in the same order of magnitude.

4.4.1 Principle time- and treatment-specific changes in gene expression patterns

Differences in gene regulations were analyzed in two groups. The groups were: (i) *Lesion vs. Sham*, where the transcriptome of cortical layer V of spinal cord injured rats is compared to that of unlesioned (sham) animals, and (ii) the *AST vs. Lesion* comparison where treatment-elicited regulations were identified which accompany the AST-triggered axonal regeneration

and functional improvement as previously described in detail (Klapka et al., 2005). In the following, gene regulations discovered in the *Lesion vs. Sham* comparison are referred to as lesion-triggered while regulations in AST-treated animals are based on significant changes identified in the *AST vs. Lesion* comparison.

In principle, AST-triggered alterations of gene expression may lead (i) to no significant differences compared to lesion-only animals (injury-specific gene regulation), (ii) to an even higher or even lower expression level of the respective probeset found to be regulated in lesion-only animals (genes boosted further up or down by AST), (iii) to a counter-regulation back to or beyond the basal sham expression level (genes counter-regulated by AST), or (iv) to genes exclusively regulated in AST-treated animals showing no changes in transcript level by spinal cord lesion only. As shown in figure 3 all groups (i-iv) of differential gene regulation were observed. Interestingly, the group of AST-boosted probesets comprised only a small proportion (~1%) of the regulated transcripts at all timepoints examined. In contrast, the proportion of AST-counter-regulated transcripts clearly increased over time to more than 15% (Fig. 8). The proportion of AST-specific transcripts of the overall detected regulated probesets was surprisingly high (40-46%, Fig. 8). At each timepoint the amount of injury-specific and of AST-specific regulated transcripts were very similar.

4.4.2 Identification of time- and treatment-specific clusters of regulated genes

The overlap between timepoints of groups of regulated genes was low (<20%), indicating distinct regulation profiles at the observed stages. For further insight into the gene regulation patterns, the data was checked for significant overlaps between groups of regulated genes in lesion-only and AST-treated animals at all timepoints. The number of overlapping genes expected by chance was calculated based on the group sizes and the total number of genes

present on the microarray and then compared to the actual number of overlaps found between the respective groups. Those overlapping groups of regulated genes that differed significantly from the overlaps expected by chance were, therefore, considered to be significantly over- or under-represented in the experimental procedures. Table 4 summarizes the overlaps between lesion- and AST-regulated genes. For example, it is shown that genes which are up-regulated at 1 dpo in lesioned animals were significantly enriched in the groups of AST-suppressed genes at 1 dpo (259%) and 7 dpo (331%). Thus, although total overlap was low, the data shown in Table 4 revealed a number of specific regulations pointing to significant differences in regulatory processes between lesion-only and AST animals.

		Lesion vs. Sham								AST vs. Lesion								
		up				down				up				down				
		1	7	21	60	1	7	21	60	1	7	21	60	1	7	21	60	
Lesion vs. Sham	up	1		180	195	135		108	112	148	95	94	114	95	259	331	167	182
		7	180		295	120	114		94	126	108	71	143	121	156	688	245	138
	21	195	295		160	78	122		115	127	125	27	463	129	220	771	32	
	60	135	120	160		146	158	79		94	115	138	65	57	104	101	383	
down	1		114	78	146		119	190	127	131	186	134	146	133	91	115	133	
	7	108		122	158	119		99	153	147	490	122	78	107	78	83	124	
	21	112	94		79	190	99		279	92	78	366	48	82	133	50	190	
	60	148	126	115		127	153	279		96	173	123	815	65	145	148	73	
AST vs. Lesion	up	1	95	108	127	94	131	147	92	96		284	221	69		86	115	95
		7	94	71	125	115	186	490	78	173	284		118	146	90		101	140
		21	114	143	27	138	134	122	366	123	221	118		212	123	154		105
		60	95	121	463	65	146	78	48	815	69	146	212		133	85	185	
	down	1	259	156	129	57	133	107	82	65		90	123	133		190	221	96
		7	331	688	220	104	91	78	133	145	86		154	85	190		177	208
		21	167	245	771	101	115	83	50	148	115	101		185	221	177		117
		60	182	138	32	383	133	124	190	73	95	140	105		96	208	117	

Table 4. Overlaps between gene regulations in Lesion and AST paradigms at different timepoints. The given overlap between groups of regulated genes is shown as percentage of the expected number of overlapping genes based on the group sizes and the total number of genes on the chip. Each possible comparison for the timepoint-specific sets of up- and down-regulated genes in the groups Lesion vs. Sham and AST vs. Lesion is illustrated. Overlaps showing a significant over- or under-representation are shown in orange (over-representation) and blue (under-representation), respectively. Interestingly, some effects are not constricted to the same timepoint. For example a significant proportion of lesion-induced genes at 1 dpo is down-regulated by AST at 1 (259%) and also at 7 (331%) dpo.

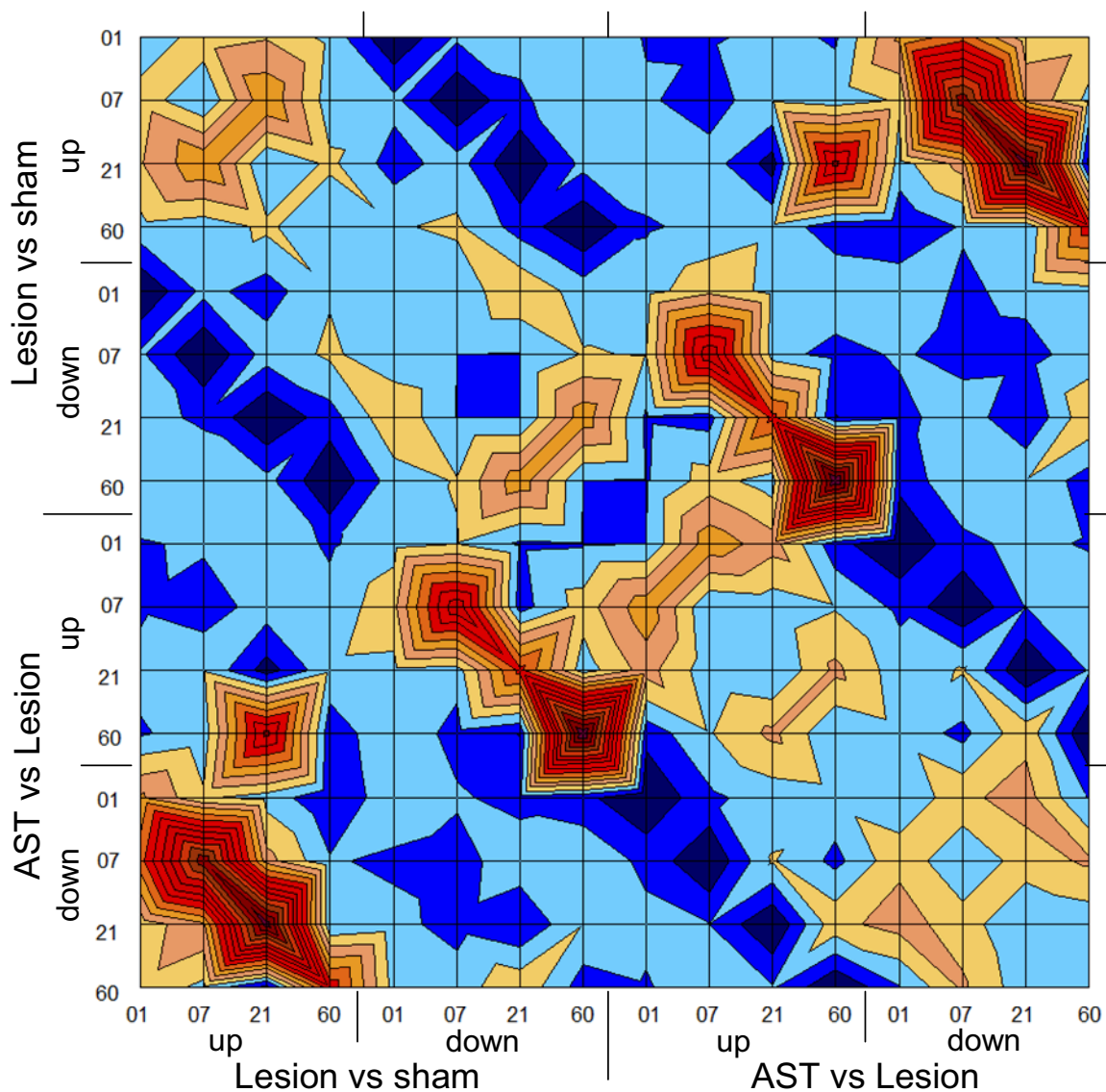


Fig. 9. “Topographic” map illustrating overlaps between sets of regulated genes with respect to kind of treatment, direction of regulation and timepoint of the respective gene regulation. Overlaps between groups of regulated genes for each timepoint, direction of regulation and the comparison of Lesion versus Sham and AST versus Lesion have been calculated. The given number of overlaps is shown as percentage of the expected number of overlaps. Overlaps smaller than 150% of the expectancy value are illustrated in light to dark blue, over-representations in overlaps higher than 150% of the expectancy value are illustrated in light to dark red. For example AST-counter-regulations of lesion-induced genes at 7 and 21 dpo lead to the ridge structure in the lower left and in mirror image in the upper right corner of the topographic map. The corresponding values of the over- or under-representations including the level of significance are shown in Table 4.

The “topographic” map in Fig. 9 visualizes the data presented in Table 4. Structures containing significant high overlaps representing processes like counter-regulation or genes

continuously regulated over time can be easily identified. Many of these over- or under-representations might be expected, as for example genes cannot be up- and down-regulated at the same timepoint in one condition. Therefore, the overlaps of these groups will be zero as indicated by a blue pit. Additional dark blue areas denote the low amount of AST-boosted regulations. On the other hand, AST-counter-regulations were very common over all timepoints, leading to ridge-like structures. For example, the lesion-triggered up-regulations which are counter-regulated in treated animals are shown as prominent ridges in the lower left corner (Fig. 9). Within the lesion group the highest overlap among up-regulated genes was displayed between 7 and 21 dpo. In contrast, down-regulated genes in this group overlapped strongest between 21 and 60 dpo. On the other hand, within the AST group up-regulations, e.g., exhibited a high overlap between 1 and 7 as well as between 21 and 60 dpo. Down-regulated genes in the AST group, however, showed a broad overlap between the timepoints 1, 7 and 21 dpo. This indicates a remarkable difference for the regulatory control of repressed and induced genes over the analyzed time frame.

Another noticeable observation was the singular sharp peak representing a significant high overlap between genes found up-regulated at 21 dpo in the lesioned animals and genes up-regulated at 60 dpo in AST-treated animals. Studying this group of regulated genes in more detail showed that a very high proportion of AST counter-regulated genes at 21 dpo were exclusively AST-induced at 60 dpo. Among the group of genes which showed this striking kind of regulation were candidates such as Fas apoptotic inhibitory molecule 2 (FAIM2), claudin 11 (CLDN11), peroxisome proliferative activated receptor delta (PPARD), dihydropyrimidinase-like 5 (DPYSL5), BCL2-like 1 (BCL2L1), statin-like (STNL), syntaxin binding protein 1 (STXBP1), unc-5 homolog A (UNC5A) and neuronal d4 domain family member (NeuD4).

The peaks of overlap were analyzed for the enrichment of functional gene groups. AST counter-regulated genes at 7 dpo were significantly enriched in functional groups involved in "developmental processes". At 21 dpo AST-induced counter-regulated genes were enriched in functional groups like "protein synthesis" and "synaptic function", while genes which were only induced in lesioned animals at this timepoint were enriched in genes associated with "plasticity of the dendritic tree".

4.5 Functional groups of regulated genes

In a further step, functional groups of genes, which showed an over- or under-representation of GO-categories (Ashburner et al., 2000) have been analyzed to reveal biological processes that were activated or repressed during regeneration. A selection of significantly over- and under-represented functional groups is shown in Table 5. Several genes are part of many GO-classes and may be connected to multiple groups.

Interestingly, in the group of regulated genes linked to the GO-term "apoptosis" there was a clear difference in the over- and under-representation of genes that were associated with induction or negative regulation of apoptosis, respectively. In lesioned animals, numerous genes responsible for induction of cell death were significantly enriched in the group of up-regulated genes. In contrast, in AST-treated animals both up-regulated anti-apoptotic or neuroprotective genes and down-regulated genes involved in induction of apoptosis were significantly enriched. Down-regulation of pro-apoptotic genes was observed most strongly at 1 dpo (data not shown). The amount of up-regulated anti-apoptotic or neuroprotective genes in treated animals increased over time (Fig. 10).

	Lesion versus Sham			AST versus Lesion			Significance level:			
	overall	up	down	overall	up	down	<0.01	<0.001	<0.01	<0.001
	2060	893	1167	2036	1175	861	overrepresentation		underrepresentation	
	%			%						
227	144	116	165	158	164	148	apoptosis anti-apoptosis negative regulation of apoptosis induction of apoptosis by extracellular signals <i>induction of apoptosis via death domain receptors</i>			
101	75	104	53	148	172	117				
120	76	102	56	154	178	121				
33	184	266	122	117	81	165				
11	276	399	183	175	61	331				
416	109	120	100	155	173	131	cell adhesion homophilic cell adhesion			
52	80	101	65	170	218	105				
70	147	138	153	198	209	182	cell morphogenesis axonogenesis axon guidance			
32	59	27	84	216	292	114				
40	57	22	84	202	167	250				
3539	129	121	134	120	133	103	cellular metabolic process protein metabolic process positive regulation of biological process <i>positive regulation of cellular biosynthetic process</i>			
1739	132	124	138	110	114	105				
676	119	137	104	127	141	109				
30	51	29	67	51	89	0				
179	130	147	116	159	168	147				
1761	91	104	81	93	86	102	signal transduction Wnt receptor signaling pathway GTPase activity			
56	156	204	120	192	250	114				
128	107	116	100	177	187	163				
467	108	115	103	132	180	66	structural molecule activity structural constituent of myelin sheath			
5	152	175	134	231	400	0				
21	199	125	256	73	127	0	tissue regeneration			
466	122	141	108	133	154	103	transcription regulation of transcription <i>positive regulation of transcription</i> <i>negative regulation of transcription</i>			
1000	129	132	127	123	143	97				
159	108	110	105	126	176	57				
148	128	107	145	140	140	141				
224	137	102	165	125	184	45				
							translation			

Table 5. A selection of significantly over- and under-represented functional groups of genes. The first column states the total number of genes on the chip associated with the corresponding functional group (right column) followed by the proportion (%) of number of genes found / expected number of genes. The upper row shows the total number of regulated genes (overall, up- and down-regulated) in the given comparison. The colour indicates the significance level calculated via the hypergeometric distribution. The names of the functional groups in the right column are given as in the GO-tree.

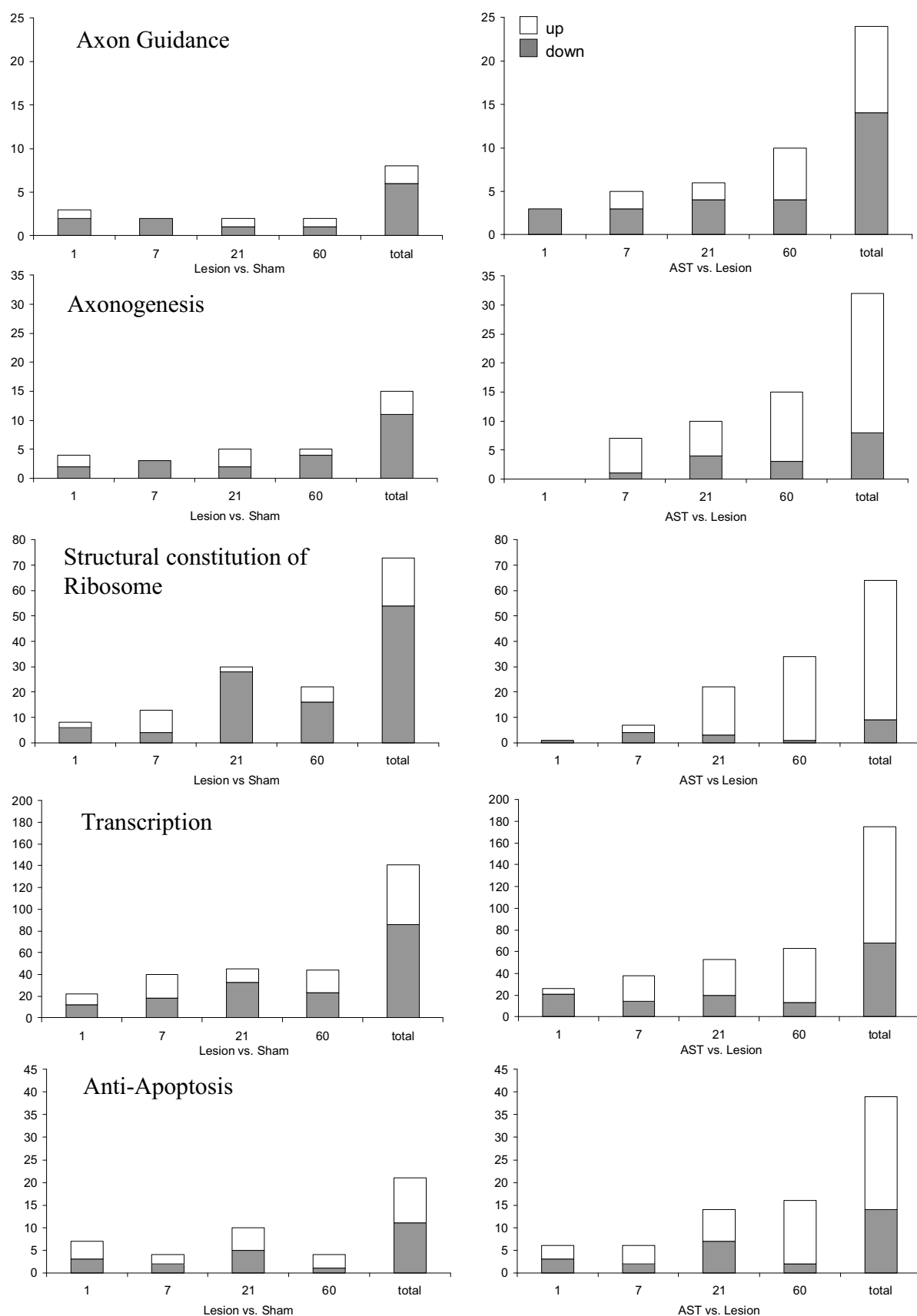


Fig. 10. Examples of functional groups which were strongly modulated by AST-treatment. The number of significantly regulated genes associated with the GO-terms “axon guidance”, “axonogenesis”, “structural

constitution of ribosome”, “transcription” and “anti-apoptosis” are shown at each timepoint and over all timepoints (total). Note that the number of axon guidance genes that is altered by AST compared to lesion is higher than the total number of axon guidance genes regulated due to the lesion itself (up-regulation: white bar; down-regulation: grey bar).

The GO-term “cell morphogenesis” displayed significant over-representations. Its subgroups “axonogenesis” and “axon guidance” were of particular interest. Both terms were under-represented among lesion-induced genes (Table 5). The low amounts of regulated genes in both processes were detected at all timepoints. In contrast, the AST-induced genes related to “axonogenesis” and “axon guidance” were increasingly over-represented over time (Table 5). In treated animals the profile of regulation for “axon guidance” changed from a solely down-regulation at 1 dpo to a predominant up-regulation at 60 dpo. In the case of “axonogenesis” an increased regulation from 7 to 60 dpo was detected (Fig. 10).

In the group of lesion-triggered down-regulations genes linked to the GO-term “tissue regeneration” were significantly enriched. However, not a single gene linked to this GO-term was found to be regulated in AST animals. This indicated that the genes in this group are regulated as a response to injury, regardless of treatment.

In addition, genes associated with “membrane organization and biogenesis” could be identified to be over-represented in the groups of up-regulated genes in both lesioned and AST-treated animals (Table 5). It was very surprising, however, that in AST-treated animals up-regulated “structural constituents of the myelin sheath” were significantly over-represented at 21 and 60 dpo (data not shown).

Genes linked to the GO-term “transcription” were significantly enriched in the group of lesion-triggered up-regulations. Interestingly, this enrichment peaked at 7 dpo and declined at the later timepoints. In addition to this enrichment of lesion-triggered transcription-associated up-regulations, AST-treated animals further showed significant over-representation of up-regulated genes in this functional group as compared to lesion-only animals. These AST-

triggered effects increased over time peaking at 60 dpo. The same profile was observed for “structural constitution of ribosome” (Fig. 10). Thus, transcriptional and translational activity in the cortex is enhanced after SCI but further stimulated after AST-treatment (Table 5).

4.6 Identification of regulated genes associated with AST-dependent responses

One goal of this study was to characterize novel gene products that were regulated in the injury paradigm and the regeneration-failure following SCI. However, the major aim of this work was to identify regulated genes that could be associated with successful AST-promoted axonal regeneration (Table 6).

4.6.1 Axon outgrowth and guidance

Genes affecting processes involved in axon growth, like galanin (GAL1), glial cell derived neurotrophic factor (GDNF), kalirin (KALRN), LIM domain only 4 (Lmo4), galectin 1 (LGALS1), mitogen activated protein kinase 8 interacting protein (Mapk8ip), actin beta (ACTB), interleukin 4+6 (IL-4+6), vitamin D receptor (VDR), enabled homolog (ENAH) and S100 calcium binding protein beta (S100B) were up-regulated in the AST animals (Table 6).

Genes involved in axonal guidance, like roundabout homolog 1 (ROBO1), reticulon 4 receptor (RTN4R), unc-5 homolog A+B (UNC5A+5B), dihydropyrimidinase-like 5 (DPYSL5/CRMP5), paired-Ig-like receptor B (PirB), neuropilin 1 (NRP1), receptor-like tyrosine kinase (RYK), cyclin-dependent kinase 5 (CDK5), semaphorin 6B (Sema6B), contactin 2 (axonal, CNTN2), neural cell adhesion molecule L1 (NCAML1), fasciculation and elongation protein zeta 1 (FEZ1) and activated leukocyte cell adhesion molecule

(ALCAM) also showed AST-triggered changes in expression. Of these genes, ROBO1, UNC5A+B, DPYSL5, RTN4R, PirB and NRP1 which are all known to be involved in growth cone repulsion and/or collapse, were down-regulated in AST-treated compared to lesion-only animals in at least one of the observed timepoints (Table 6). On the other hand, genes like CNTN2, FEZ1 and ALCAM, which are positively involved in outgrowth and axon targeting, were up-regulated in the AST-group. Sema6B was up-regulated in the cortex in AST-treated rats late at 60 dpo.

Like Mason et al. (2003) and others before (Reh et al., 1987; Tetzlaff et al., 1994) no significant cortical up-regulation of GAP-43 in lesioned-only nor in AST-treated animals was found. On the other hand, the down-regulation of two regulated genes, far upstream element binding protein 1 (FUBP1) and polypyrimidine tract binding protein 2 (PTBP2, Table 6) was detected, which are known to be involved in GAP-43 mRNA binding, thereby influencing its stability (Irwin et al., 1997). Both genes are down-regulated in AST-treated animals, FUBP1 at 1 and 7 dpo, PTBP2 at 60dpo.

4.6.2 Apoptosis, Protection and Stress response

Apoptosis-associated genes like Bcl2l1, BCL2-like 13 (apoptosis facilitator, Bcl2l13), BTB (POZ) domain containing 14B (BTBD14B), diablo homolog, Drosophila (Diablo), corticotropin releasing hormone (CRH), Tnf receptor-associated factor 2 (Traf2), BH3 interacting domain (Bid3), v-akt murine thymoma viral oncogene homolog 1 (Akt1), Bcl2-associated athanogene 1 (Bag1), peroxiredoxin 2 (PRDX2), superoxide dismutase 1 (SOD1), colony stimulating factor 2 (CSF2) and signal transducer and activator of transcription 5A (STAT5A) were regulated by AST-treatment (Table 6). Of these genes, Bcl2l13, BTBD14B, Diablo, CRH, Traf2 and Bid3, which are associated with pro-apoptotic processes, were

exclusively down-regulated in treated animals. On the other hand, genes described to comprise anti-apoptotic and/or neuro cell-protective properties like Akt1, Bag1, PRDX2, SOD1, CSF2 and STAT5A, were found up-regulated in the AST animals compared to lesion controls.

4.6.3 Myelin associated genes

Interestingly, myelin-associated genes like claudin 11 (CLDN11), peripheral myelin protein 22 (PMP22), myelin-associated oligodendrocyte basic protein (MOBP), myelin basic protein (MBP), cyclic nucleotide phosphodiesterase 1 (Cnp1) and early growth response 2 (EGR2, Krox-20) were all up-regulated due to AST-treatment at later timepoints (21 and/or 60 dpo; Table 6). Except for EGR2 all of these genes encode for proteins essential for compact myelin structures. EGR2 is a transcription factor regulating several genes which are relevant for myelin formation and maintenance.

1	dpo			Gene/protein name
	7	21	60	
<i>Outgrowth / Axon guidance</i>				
↑	↑	↑	↑	galanin (GAL)
↑		↑		glial cell derived neurotrophic factor (GDNF)
	↑		↑	kalirin, RhoGEF kinase (KALRN)
	↑			activated leukocyte cell adhesion molecule (ALCAM)
		↓		neural cell adhesion molecule L1 (NCAML1)
	↑			interleukin-6 (IL6)
		↑		interleukin-4 (IL4)
		↓	↑	microtubule-associated protein 1 A (Mtap1a)
			↑	mitogen activated protein kinase 8 interacting protein (Mapk8ip)
			↑	early growth response 1 (EGR1, krox-24)
↓	↓			far upstream element binding protein 1 (FUBP1)
			↓	polypyrimidine tract binding protein 2 (PTBP2)
<i>Growth inhibitory / Repulsive</i>				
↓		↓		neuropilin 1 (NRP1)
↓			↑	reticulon 4 receptor (RTN4R)
	↓		↓	roundabout, axon guidance receptor, homolog 1 (ROBO1)
	↓		↑	unc-5 homolog B (UNC5B)
		↓	↑	unc-5 homolog A (UNC5A)
		↓	↓	paired-Ig-like receptor B (PirB)
			↓	3F8 chondroitin sulfate proteoglycan (Phosphacan, PTPRZ1)
			↑	semaphorin 6B (Sema6b)
<i>Survival / Anti-Apoptotic</i>				
↑	↑			vitamin D (1,25- dihydroxyvitamin D3) receptor (VDR)
↑			↑	v-akt murine thymoma viral oncogene homolog 1 (Akt1)
↑	↑			colony stimulating factor 2 (CSF2)
	↑			signal transducer and activator of transcription 5A (STAT5A)
		↑		ciliary neurotrophic factor (CNTF)
		↓	↑	Bcl2-like 1 (BCL2L1)
		↑	↑	peroxiredoxin 2 (PRDX2)
			↑	superoxide dismutase 1 (SOD1)
		↑		Bcl2-associated athanogene 1 (Bag1)
		↑		clusterin (CLU)
<i>Pro-Apoptotic</i>				
↓				diablo homolog (Diablo)
↓			↓	corticotropin releasing hormone (CRH)
↓				BH3 interacting domain (Bid3)
↓				Tnf receptor-associated factor2 (Traf2)
	↓	↓	↓	G protein α q (GNAQ)
<i>Myelin-associated</i>				
		↑		peripheral myelin protein 22 (PMP22)
		↑	↑	myelin-associated oligodendrocyte basic protein (MOBP)
			↑	cyclic nucleotide phosphodiesterase 1 (Cnp1)
			↑	myelin basic protein (MBP)
		↓	↑	claudin 11 (CLDN11)
		↑	↑	early growth response 2 (EGR2, krox-20)
		↓		POU domain, class 3, transcription factor 1 (Oct-6, SCIP)

Table 6. Sensorimotor cortical regulation of selected genes in the AST vs. Lesion comparison are displayed for selected functional groups. The arrows indicate the significant up- or down-regulation of the corresponding gene at the given timepoints in AST compared to lesioned-only animals. Next to genes involved in axonal outgrowth

and guidance, survival and apoptosis a surprisingly high number of cortically regulated genes associated with myelin was detected. The majority of these genes were up-regulated at 60 dpo.

4.7 qPCR validation

To verify the validity of the microarray data of selected genes, real-time quantitative PCR was performed (qPCR, Fig. 11). For most genes, the qPCR data confirmed the microarray results, both in temporal pattern as in magnitude of regulation. The fold change of regulation detected by qPCR was in general about 1.5 to 2 times greater than in the array based data. Genes from several relevant functional groups were chosen for validation. CSF2, Bag1, KALRN, PRDX2, VDR, EGR2, ROBO1, UNC5A, and GDNF showed the same significant regulation patterns with qPCR as compared to the arrays. Galanin 1 (GAL1) and Syntaxin binding protein (STXBP1) even showed qPCR-based regulation at more timepoints as was originally detected by microarrays. Possibly due to differences in sensitivity between the methods, the detected degree in change of gene expression varied somewhat. In the case of Diablo, NRP1 and Zfp281, the significance of the array-based regulation could be reproduced for some but not all timepoints. In general, the qPCR analysis suggests that the regulations observed by microarrays are trustworthy.

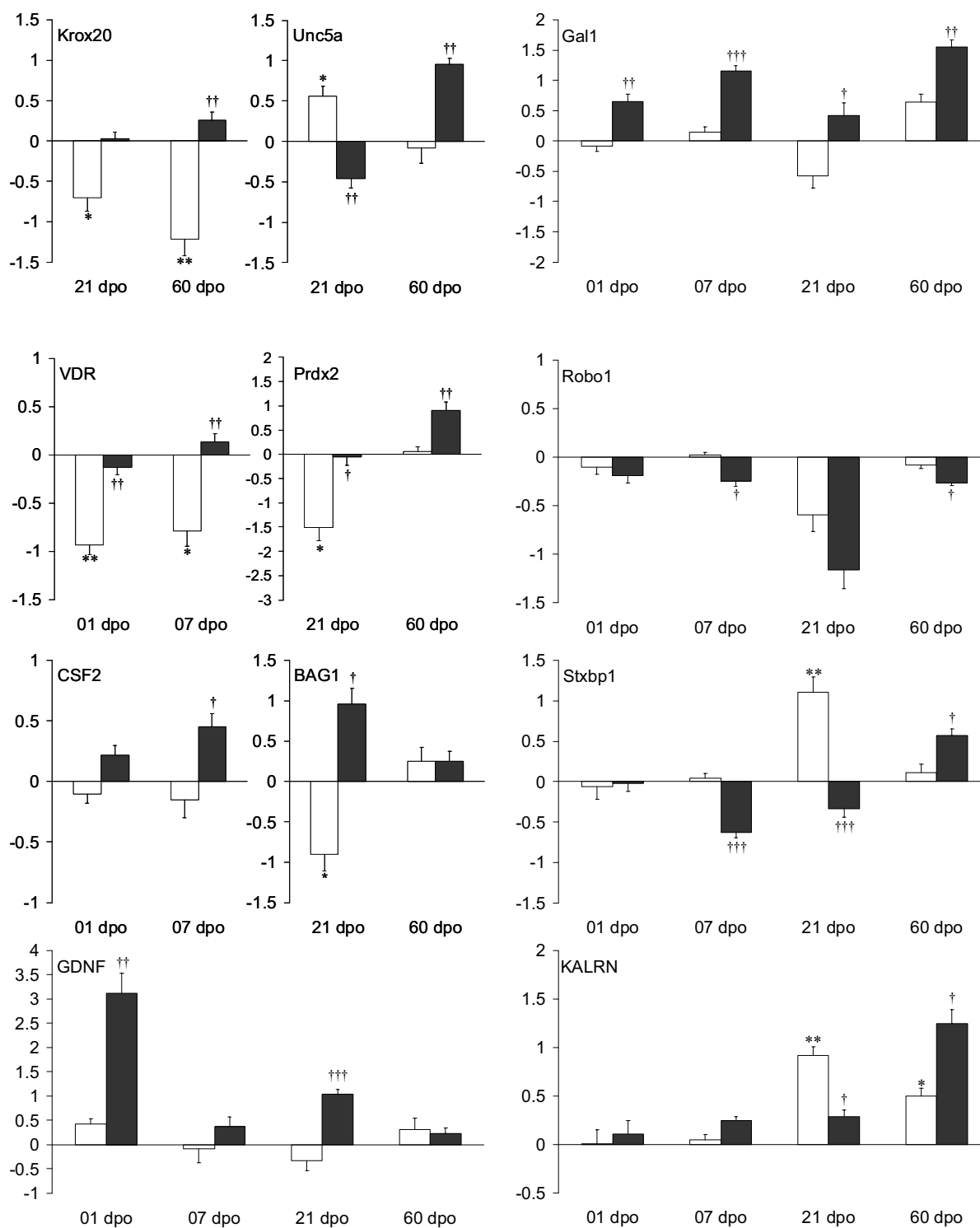


Fig. 11. Validation by quantitative qPCR for a subset of regulated cortical genes identified by the GeneChip analysis. For selected timepoints the mRNA-expression levels of cortical tissues from either lesion-only (white bars) or AST- treated (black bars) were compared to sham-operated animals. Abbreviations: early growth response 2 (Krox-20), unc-5 homolog A (UNC5A), galanin (GAL1), vitamin D receptor (VDR), peroxiredoxin 2 (PRDX2), roundabout homolog 1 (ROBO1), colony stimulating factor 2 (CSF2), Bcl2-associated athanogene 1 (BAG1), syntaxin binding protein 1 (STXBP1), glial cell derived neurotrophic factor (GDNF), kalirin (KALRN). Note: Significance was calculated for the comparisons Lesion-only vs. Sham-operated (corrected p-

value < 0.05 *, <0.01 **, <0.001 ***) and AST-treated vs. Lesion-only (corrected p-value < 0.05 †, <0.01 ††, <0.001 †††).

4.8 Cellular localisation

To understand the complexity of cellular responses leading to regeneration-failure or regeneration-success in the injured CNS, the cellular localisation of the transcripts and/or proteins encoded by the regulated genes is instrumental. The Allen Brain Atlas was used to gain insight into the anatomical expression pattern of most of the genes of interest. In addition, neuronal localization of GAL1, CSF2, Diablo and VDR by immunohistochemistry in retrograde labelled pyramidal cells of layer V in sensorimotor cortex was performed by Dipl. Biol. Marcia Gasis. She found all tested genes to be expressed in unlesioned as well as transected identified pyramidal cells in layer V. In these cells the proteins GAL and CSF2 showed a homogenous cytoplasmatic localisation while the spot-like distribution of Diablo in the cytoplasm supported its known mitochondrial localization. Immune staining of VDR was predominantly detected in the nucleus.

5. DISCUSSION

5.1 Lesion model and tissue preparation

The lesion model for CST transection as well as the described tissue preparation proved reliable and feasible to study cortical gene expression profiles. The great impact of SCI as well as of AST on gene expression in the cortex especially at the early timepoint is surprising. Taking the fast and early cortical response to lesion and most notably to treatment into account it could be beneficial to start potential treatments in human patients within hours of the incident.

The requirements for complete successful regeneration have been stated in the Introduction (2.1.1). Interestingly, the AST treatment obviously affects more processes than “tissue repair in the lesion site” (respectively the suppression of scar formation) and the “survival of axotomized neurons”. As soon as at 1 dpo several genes involved in axonal outgrowth and cell survival are regulated in treated animals (Table 6). Over time, numerous regulations indicate that all the other requirements for successful regeneration, “stimulation of axonal outgrowth”, “correct pathfinding of outgrowing axon”, and “functional reinnervation”, are also positively influenced by AST (Table 3): How the components of the AST-treatment induce such a fundamentally different regeneration program compared to the lesion-only reaction still needs to be studied.

The way of signal transduction from the lesion site to the cortex to transport the information of an axotomy is still unclear. Fast signal transduction after peripheral nerve injury to the facial nucleus via the ciliary neurotropic factor (CNTF) and STAT3 in less than 12 hours has

been described (Kirsch et al., 2003). Still, how the AST-treatment induces positive effects at this early timepoint has to be further studied.

The possibilities in applying these methods to other lesion models, treatments or timeframes are self-evident. For example, ongoing experiments in our lab are the analysis of cortical reactions to the separate treatment with BPY-DCA and cAMP as well as cortical reactions to SCI treatment with olfactory ensheathing cells. The comparison of the reactions to BPY-DCA as well as to cAMP treatment will help to understand how the combined treatment including both components leads to functional recovery. The comparison of gene expression profiles after SCI lesion and treatment with either AST or olfactory ensheathing cells could help to identify treatment specific and regeneration associated patterns.

Furthermore, the DRGs of the used test animals have been collected and utilized for microarray experiments. Thus, the regulation pattern of cortical and DRG tissue after SCI with and without treatment can be compared. Another approach to unravel the regulatory reactions after axotomy are ongoing experiments in our lab focusing on the PNS. Analysis of the expression profiles of affected DRGs after sciatic nerve crush, transection as well as reanastomosis are being identified. Comparing the resulting data sets will help to identify similarities and differences in the regeneration programs of the central and peripheral nervous system.

In future work, the described tissue preparation method could easily be used to compare several different SCI treatment approaches like stem cell implantation or tube grafts. In addition to functional studies, this could help to understand the underlying regeneration potential.

For this study, the complete layer V of the sensorimotor cortex was dissected to prepare total RNA from lesioned-affected cortical tissue. Alternatively, individual retrogradely labelled and identified pyramidal cells from layer V of the cerebral cortex could be collected via laser

capture microdissection. The advantage of laser microdissection is the cellular purity of the resulting samples as well as that all gene regulations detected by subsequent microarray analysis can be ascribed to neurons directly affected by the transection. The drawback of this approach is however, the necessity of RNA amplification due to the limited amount of collected material, leading to additional technical variations. On the other hand, using a tissue-block to harvest a defined cortical layer does not only give insight into the reactions of pyramidal neurons but also into the secondary responses of the surrounding glial cells. For this reason as well as the refrain from RNA amplification the tissue-block preparation method was performed. However, experiments with detailed focus regeneration phase based on single cell laser capture microdissection to collect identified pyramidal cells of cortical layer V, which have regenerated across the lesion site, are being planned.

One example for potential glial reactions is the several myelin-associated genes found to be up-regulated at the 60 dpo timepoint (Table 6). Although, some of these myelin genes have been described to also be expressed in pyramidal neurons (e.g. SCIP) others are only known to be expressed in oligodendrocytes (e.g. CLDN11). Furthermore, the time pattern and enrichment of these expression changes at the late timepoints suggests myelination associated processes in oligodendrocytes. Interestingly, Ryu et al. (2007) showed in the PNS that the expression of SCIP has to stay low for successful myelination by Schwann cells, as it decreases the levels of myelin protein-zero (MPZ), MBP and Pmp22 mRNA. In this thesis, SCIP is found down-regulated in treated animals at 21 dpo, while all three genes, MPZ, MBP, and Pmp22, are up-regulated at the 21 and/or 60 dpo timepoint (MPZ is up-regulated in lesioned and treated animals at 60 dpo). Thus, the detected expression changes could indicate similarities between Schwann cell and oligodendrocyte regulations in regard to myelination respectively remyelination, including timepoint-specific down-regulation of SCIP.

5.2 Data analysis and data verification

One of the drawbacks of the numerous microarray gene-profiling studies published to date is the nonconformity of applied data analysis procedures. Countless possible options for low-level analysis and statistical evaluation make the results hard to compare. Additionally, basic rules for proper data analysis based on the size and the goal of the experiment as well as the resulting data are not always taken into account. One example is the implemented normalization type. Though quantile normalization has been established as the standard normalization method for microarray data, it works under the assumption that there are no distribution changes over all chips. Thus, it generates a high error rate in cases where strongly differing tissue samples (like tumor vs. healthy tissue) are compared.

The inflation type I error rate is also often underestimated. The investigator often neglects the fact that the number of found significantly regulated genes is higher if the data is filtered prior to the statistical test, resulting in a smaller list giving more results. Focusing on relevant test groups and prefiltering the data for genes which are above given expression and fold-change thresholds drastically enhances the power of the resulting output.

The impact of the low-level analysis on the resulting data has been described above (3.10.4). Due to the fact that each algorithm has its strength and weaknesses a combination of the multiple resulting data sets can be useful. For example, PLIER is especially powerful in detecting low-abundance expression changes but underestimates the regulation fold change. While GCRMA has been shown to calculate less biased fold changes it will most likely not detect numerous low-abundance regulations. A combination of the two datasets helps to solve these problems.

Verification of the microarray results by qPCR documented a very good analogy. This indicates the quality of the presented data sets. First analysis trials with the standard settings

for analysis in the *ArrayAssist* software using only RMA for low-level analysis and a FWER-based correction method for the statistical evaluation resulted in a handful of regulated genes. None of the genes that were verified by qPCR was in this list. Thus, using this standard analysis approach it would have not been possible to detect hundreds of relevant and significantly regulated genes nor to define both distinct phase- and treatment-dependent associated regulation patterns.

The tools and procedures for microarray data low-level, statistical and high-level analysis developed in this thesis lead to reliable and robust results even in the case of complex experimental setups and challenging samples like heterogeneous brain tissue. They have proven their scientific usefulness by contributing to several publications (Kruse et al., 2008; Barbaria et al., 2009; Heinen et al., 2008; Kury et al., 2004; Kruse et al., 2009; Bosse et al., in preparation).

5.3 Comparison to optic nerve regeneration

The optic nerve, like the CST, represents a CNS pathway that does not regenerate spontaneously (Benowitz and Yin, 2008). Though the retinal ganglion cells (RGCs) show a transitory sprouting response after injury, this response does not lead to long-distance regeneration through the optic nerve. However, if an inflammatory reaction is induced in the eye (e.g. by lens injury), resulting in trophic factors being secreted by macrophages, RGCs are able to regenerate axons through the optic nerve (Fischer et al., 2004). Interestingly, the regenerating RGCs seem to undergo gene expression changes comparable to those seen in regenerating peripheral neurons (Fischer et al., 2004). For example, GAP-43 is strongly induced in regenerating RGCs. Although the regulation patterns of regenerating RGCs and cortical pyramidal cells (CPCs) in layer V are fundamentally different, there are also

similarities. For example, the genes GAL1 and SOCS3 are both strongly up-regulated in regenerating RGCs as well as in CPCs. As GAL1 is involved in outgrowth and SOCS3 is involved in cell survival an overlap in these basic processes of regeneration is plausible. Nonetheless, as the regeneration in RGCs is induced by increased inflammation and AST-treatment in the spinal cord is thought to decrease the inflammatory response, differences in the resulting regulatory reaction are not all-too surprising.

5.4 Cortical molecular response after CST axotomy and AST-treatment

In this work, for the first time, gene expression profiles with high temporal resolution in layer V of sensorimotor cortex following spinal cord injury were analyzed and compared to gain insight into changes in CNS neuronal gene regulation related to axotomy and successful axon outgrowth and regeneration. The goal was to find regulated genes in the sensorimotor cortex of sham-operated, lesion-only and AST-treated rats following dorsal hemisection in thoracic spinal cord. RNA was isolated from the sensorimotor cortex at 1, 7, 21 and 60 days after CST transection. By comparing the mRNA expression profiles from lesioned animals lacking axonal regeneration to cortical expression patterns of animals receiving the regeneration-promoting AST treatment (Klapka et al., 2005), regeneration-associated profiles of gene expression have been identified.

Besides genes of known axon growth-promoting proteins, which are likely to take part in the observed functional recovery in AST-treated animals, genes with thus far unknown or multiple known functions could be classified for their putative role in corticospinal axon regeneration leading to functional improvement.

Lesion and AST-triggered gene expression changes in cortical layer V were observed as early as 1 dpo. These early regulations involved more than 900 genes including functional groups

of genes particularly related to wounding, apoptosis, regulation of neurogenesis and cytoskeletal reorganization, which are significantly over-represented. With respect to the great distance between the lesion site at mid-thoracic spinal cord level and the analyzed cortical tissue the huge number of genes affected in injured and AST-treated animals within one day is very surprising. At present, it is unclear how the lesion- and AST-triggered local signals are transmitted from the side of injury in spinal cord to sensorimotor cortex. The number of regulated genes is further increased over time in both lesion-only and AST animals reaching a maximum at three weeks after injury and treatment, respectively.

Besides possible direct effects of the iron chelator and cAMP on the injured CST axons, putative indirect neuroprotective effects of the iron chelator through inhibition of the Fenton reaction (suppression of reactive oxygen species, ROS) and/or growth stimulating effects of cAMP indirectly influence cortical responses in AST animals are possible. As scar suppression itself is unlikely to have an effect on cortical gene expression at this early timepoint, systemic effects or changes in the lesion rim, for example due to the injected cAMP or changes in the inflammatory reaction are feasible explanations for these results.

The very large proportions of AST-counter-regulated and AST-specific gene regulations clearly demonstrate that the regeneration promoting treatment AST causes a massive change in the cortical gene expression profile that is normally induced after CST-lesion only. This finding indicates that AST causes a fundamental alteration of the lesion-induced gene expression program in cortical neurons of control animals towards a regeneration-associated profile. Obviously, AST does not slightly modify a lesion-induced regeneration program but the gene expression profile triggered by AST leading to successful regeneration and functional improvement differs fundamentally from that of lesion-only animals.

5.5 Important timepoint and treatment-specific regulation pattern

The overlaps between groups of regulated genes over the observed time period were analyzed in order to detect specific processes taking place in the different experimental paradigms. In addition, this method provided an important systematic tool to pinpoint interesting events in the vast amount of data microarray studies provide. An example of such an event is the unexpectedly high overlap between genes, which were up-regulated in lesioned cortex at 21 dpo and in treated animals at 60 dpo. As mentioned before these genes were mainly counter-regulated by AST at 21 dpo and exclusively up-regulated in treated animals at 60 dpo. This suggests that for this subgroup of genes there is a general regulation pattern, which is switched on exclusively in lesioned-only animals at 21 dpo and in treated animals at 60 dpo. The genes following this pattern could not be assigned to a specific functional group. Interestingly, at 7 dpo genes which were lesion-repressed and AST-induced were significantly enriched for the function “developmental process”. This is remarkable as in the adult CNS dedifferentiation is a requirement for processes like axonal outgrowth, axon guidance and myelination to take place. At 21 dpo the counter-regulated group of AST-induced genes were significantly enriched for protein synthesis and synaptic function. On the other hand, AST-counter-regulated genes, which were lesion-induced at the same timepoint, were significantly enriched for the functional group plasticity of dendritic tree. Thus, the process of synaptic stripping could be involved. This loss of synaptic buttons after axotomy or functional detachment of motoneurons from their target has been described to increase between 4 to 35 days after detachment (Pastor et al., 1997). This fits the interpretation that in lesioned animals at 21 dpo dendritic reorganisation as well as reduced metabolic activity takes place whereas in treated animals heightened protein synthesis and synaptic function indicates ongoing functional axonal regeneration.

5.6 Over- and underrepresentation of functional groups of regulated genes

An AST-triggered over-representation of anti-apoptotic genes and a down-regulation of pro-apoptotic genes were found (Table 3). This indicates that AST drives gene expression into protection against apoptosis. This correlates with the published neuroprotective effects of AST. Interestingly, the AST triggered changes in the genes involved in apoptosis occurred mainly at early as well as late timepoints (Table 6), indicating that there may be two phases after SCI where the neurons need protection: the acute, early phase, where neurons are just injured and the late phase, where neurons try to reach their targets.

Additionally, AST-triggered up-regulation of genes involved in axon guidance and axonogenesis were observed (Fig. 10). These up-regulations increase over time and could be part of the cortical molecular reaction responsible for the published axonal regeneration. As there are only very few genes regulated in these functional groups in lesion-only animals this emphasizes that in these animals there is no detectable long-lasting regeneration program initiated.

Compared to lesion-only animals the cortical expression in treated animals of genes associated with transcriptional and translational processes increases drastically over time (Fig. 10). For example, ribosomal genes are strongly down-regulated in lesioned animals at 21 dpo, nearly all of these regulations are counter-regulated in AST-treated animals. In treated animals, there are more ribosomal genes up-regulated at 60 dpo alone than in lesioned-only animals in all timepoints taken together. On the other hand, there are two times more ribosomal genes with significantly reduced expression in lesioned animals at 60 dpo than in treated animals at all timepoints taken together.

The described expression changes of these functional groups indicate the regeneration failure as well as cortical cell atrophy and metabolic restructuring in lesion-only animals. On the other hand, in treated animals influenced functional groups characterize the effort for ongoing outgrowth and axonal regeneration.

5.7 Regulated genes with known roles in regeneration

To date, studies on cortical gene expression after SCI showed no changes in genes of known relevance to regeneration. In contrast to the findings of Mason et al. (2003) the work presented here has identified significantly regulated genes in the cortex of CST-transected rats. In the earlier study the authors showed that no changes of expression after cervical axotomy could be identified in layer V pyramidal neurons for the genes GAP-43, CAP-23, SGC10, L1, CHL1, c-jun, ATF3 or krox-24 using *in situ*-hybridisations. Each of these genes is associated with the cell body response to a proximal, but not to a distal, axotomy. Except for CAP-23 and krox-24 all of these genes were up-regulated in corticospinal neurons in layer V after a proximal intracortical lesion, indicating that cortical neurons are capable of the same response to axotomy like neurons which successfully regenerate. In this study, c-jun and krox-24 were found regulated after CST lesion at Th8, indicating that, with the microarray method which is more sensitive than ISH, a response to injury can be observed. Furthermore, in treated animals L1 was found to be down-regulated.

No significant change in GAP-43 mRNA levels has been found. While GAP-43 is known to be expressed at high levels in neuronal growth cones during development and during axonal regeneration its role in injured CNS neurons is not clear. As functional recovery after AST treatment was observed, this might indicate that up-regulation of GAP-43 transcript in pyramidal cells may not be essential for corticospinal tract regeneration. Previous work on

striatal reactions to cortical lesion showed unchanged or decreased GAP-43 mRNA and protein levels (Szele et al., 1995; Pasinetti et al., 1993). However, the regulation of FUBP1 and PTBP2, two RNA binding proteins binding to GAP-43 mRNA (Irwin et al., 1997), might lead to accumulation or deprivation of GAP-43 on protein level, without requiring significant expression changes of its mRNA. Both respective proteins seem to compete for binding GAP-43 mRNA, leading to antagonistic effects regarding mRNA-lifetime, thus influencing GAP-43 protein concentrations. As FUBP1 is thought to destabilize GAP-43 mRNA (Irwin et al., 1997) its down-regulation at 1 and 7 dpo in AST-treated animals could lead to higher cortical GAP-43 protein levels. Although these potential changes in GAP-43 protein levels fit phases of axonal outgrowth and functional recovery, an essential function of GAP-43 in corticospinal regeneration still needs to be shown.

The transcription factor c-jun has been associated with neuronal regeneration after axotomy as well as with programmed cell death in other experimental paradigms (Herdegen et al., 1997). The AST-triggered counter-regulation of c-Jun mRNA back down to sham-level indicates that in corticospinal neurons the function in apoptotic cell death may be predominant, or alternatively that c-jun up-regulation may not be necessary for layer V pyramidal neuron regeneration. This observation would fit the findings of Chaisuksunt et al. (*Chaisuksunt et al., 2000*), who showed that purkinje cells close to peripheral nerve grafts do up-regulate c-jun without showing any regenerative response. These data suggest that there are both parallels and differences in the genes regulated in central and peripheral regeneration.

Among others, the up-regulation of the genes KALRN, GDNF and GAL1 has been verified via qPCR. Kalirin was first discovered as a protein interacting with huntingtin-associated protein 1 (HAP1) and is known to be involved in neuronal shape and growth. It has the ability to interact with numerous other proteins. GDNF is a potent neurotrophic factor for motor neurons and has been shown to prevent apoptosis of motor neurons after axotomy. Galanin

has been described as a “regenerating axon” marker in peripheral nerve lesion studies (Suarez et al., 2006). The up-regulation of galanin in the cortex of treated animals in every observed timepoint could be an indicator for long-term axon regeneration. Interestingly, in lesioned animals there was only an up-regulation of galanin at 60 dpo, which was boosted even higher in AST-animals. The fact that there is nearly no regulation of such proteins in lesion-only animals further underlines the hypothesis that there is a profound difference between the cortical reaction to axotomy and an expression profile that leads to successful regeneration as observed in the treated animals.

Several of the genes described above are also known to be involved in other neurodegenerative diseases, like Alzheimer disease (AD) or Multiple Sclerosis. For example, KALRN, CDK5, S100, CRH are involved in AD. Though the function of KALRN in AD is not resolved, it has been found to be under-expressed in the hippocampus of Alzheimer patients.

Interestingly, a number of AST-triggered gene regulation, which are detected in multiple timepoints change the direction of regulation. For example, in Table 6 each functional group except “pro-apoptotic” holds one gene that is regulated in different directions at 21 and 60 dpo (Mtap1a, UNC5A, BCL2L1, CLDN11). This taken together with the small overall overlap between the different timepoints underlines the distinct timepoint-specific cortical regulation patterns.

5.8 Summary and outlook

In summary, this thesis showed that corticospinal transection leads to massive regulatory reaction of the transected pyramidal neurons and surrounding cortical tissue. This reaction could be detected as early as 1 dpo. While early regulations were enriched for functional

groups like apoptosis and wound response, later timepoints showed enrichment for genes involved in brain development, biosynthesis and cytoskeletal reorganisation. This thesis also presents evidence that AST-treatment leading to functional recovery induced extensive changes in this cortical regulatory response, including modulation of genes involved in processes like axonal outgrowth, axon guidance, survival, apoptosis and myelination. Genes known to promote axon growth and survival are AST-induced, while growth inhibitory, repulsive and pro-apoptotic genes are repressed in treated animals.

The tissue preparation method and data analysis tools developed in this thesis lead to reliable and convincing results. Ongoing experiments are based on the presented findings and the data analysis tools have contributed to several publications.

In future work, the presented data will be compared to expression profiles in DRGs after central as well as after peripheral lesion. A comparison with another regeneration supporting approach, the application of olfactory ensheathing cells, is underway. Thus, the presented work is a building block in unravelling and understanding the complex reactions to nervous system injury and regeneration.

6. REFERENCES

Affymetrix. www.affymetrix.com.

Affymetrix (2001). Statistical Algorithms Reference Guide.

Affymetrix (2005). Guide to Probe Logarithmic Intensity Error (PLIER) Estimation.

Allen Brain Atlas. Seattle (WA): Allen Institute for Brain Science. © 2008. <http://www.brain-map.org>.

Ashburner, M., Ball, C.A., Blake, J.A., Botstein, D., Butler, H., Cherry, J.M., Davis, A.P., Dolinski, K., Dwight, S.S. and Eppig, J.T., et al. (2000). Gene ontology: tool for the unification of biology. The Gene Ontology Consortium. *Nat Genet* 25, 25–29.

Atwal, J.K., Pinkston-Gosse, J., Syken, J., Stawicki, S., Wu, Y., Shatz, C. and Tessier-Lavigne, M. (2008). PirB is a functional receptor for myelin inhibitors of axonal regeneration. *Science* 322, 967–970.

Aubert, I., Ridet, J.L., Schachner, M., Rougon, G. and Gage, F.H. (1998). Expression of L1 and PSA during sprouting and regeneration in the adult hippocampal formation. *J Comp Neurol* 399, 1–19.

Bagnard, D., Lohrum, M., Uziel, D., Puschel, A.W. and Bolz, J. (1998). Semaphorins act as attractive and repulsive guidance signals during the development of cortical projections. *Development* 125, 5043–5053.

Bagnard, D., Thomasset, N., Lohrum, M., Puschel, A.W. and Bolz, J. (2000). Spatial distributions of guidance molecules regulate chemorepulsion and chemoattraction of growth cones. *J Neurosci* 20, 1030–1035.

Bakay, M., Chen, Y.W., Borup, R., Zhao, P., Nagaraju, K. and Hoffman, E.P. (2002). Sources of variability and effect of experimental approach on expression profiling data interpretation. *BMC.Bioinformatics*. 3, 4.

Bandtlow, C.E. and Loschinger, J. (1997). Developmental changes in neuronal responsiveness to the CNS myelin-associated neurite growth inhibitor NI-35/250. *Eur J Neurosci* 9, 2743–2752.

Barbaria, E.M., Kohl, B., Buhren, B.A., Hasenpusch-Theil, K., Kruse, F., Küry, P., Martini, R. and Müller, H.W. (2009). The alpha-chemokine CXCL14 is up-regulated in the sciatic nerve of a mouse model of Charcot-Marie-Tooth disease type 1A and alters myelin gene expression in cultured Schwann cells. *Neurobiol. Dis.* 33, 448–458.

Bareyre, F.M., Haudenschild, B. and Schwab, M.E. (2002). Long-lasting sprouting and gene expression changes induced by the monoclonal antibody IN-1 in the adult spinal cord. *J. Neurosci.* 22, 7097–7110.

- Barrette, B., Vallières, N., Dubé, M. and Lacroix, S. (2007). Expression profile of receptors for myelin-associated inhibitors of axonal regeneration in the intact and injured mouse central nervous system. *Mol. Cell. Neurosci.* 34, 519–538.
- Basso, D.M., Beattie, M.S. and Bresnahan, J.C. (1995). A sensitive and reliable locomotor rating scale for open field testing in rats. *J. Neurotrauma* 12, 1–21.
- Becker, T., Bernhardt, R.R., Reinhard, E., Wullimann, M.F., Tongiorgi, E. and Schachner, M. (1998). Readiness of zebrafish brain neurons to regenerate a spinal axon correlates with differential expression of specific cell recognition molecules. *J. Neurosci.* 18, 5789–5803.
- Becker, T., Wullimann, M.F., Becker, C.G., Bernhardt, R.R. and Schachner, M. (1997). Axonal regrowth after spinal cord transection in adult zebrafish. *J. Comp. Neurol.* 377, 577–595.
- Benfey, M. and Aguayo, A.J. (1982). Extensive elongation of axons from rat brain into peripheral nerve grafts. *Nature* 296, 150–152.
- Benowitz, L.I., Apostolides, P.J., Perrone-Bizzozero, N., Finklestein, S.P. and Zwiers, H. (1988). Anatomical distribution of the growth-associated protein GAP-43/B-50 in the adult rat brain. *J. Neurosci.* 8, 339–352.
- Benowitz, L. and Yin, Y. (2008). Rewiring the injured CNS: lessons from the optic nerve. *Exp. Neurol.* 209, 389–398.
- Berry, M., Maxwell, W.L., Logan, A., Mathewson, A., McConnell, P., Ashhurst, D.E. and Thomas, G.H. (1983). Deposition of scar tissue in the central nervous system. *Acta Neurochir. Suppl (Wien.)* 32, 31–53.
- Bisby, M.A. and Tetzlaff, W. (1992). Changes in cytoskeletal protein synthesis following axon injury and during axon regeneration. *Mol. Neurobiol.* 6, 107–123.
- Bolstad, B.M., Collin, F., Simpson, K.M., Irizarry, R.A. and Speed, T.P. (2004). Experimental design and low-level analysis of microarray data. *Int. Rev. Neurobiol.* 60, 25–58.
- Bolstad, B.M., Irizarry, R.A., Astrand, M. and Speed, T.P. (2003). A comparison of normalization methods for high density oligonucleotide array data based on variance and bias. *Bioinformatics.* 19, 185–193.
- Bonilla, I.E., Tanabe, K. and Strittmatter, S.M. (2002). Small proline-rich repeat protein 1A is expressed by axotomized neurons and promotes axonal outgrowth. *J. Neurosci.* 22, 1303–1315.
- Boran, B.O., Colak, A. and Kutlay, M. (2005). Erythropoietin enhances neurological recovery after experimental spinal cord injury. *Restor. Neurol. Neurosci.* 23, 341–345.
- Bosse, F., Küry, P. and Müller, H.W. (2002). Gene expression profiling and molecular aspects in peripheral nerve regeneration. *Restor. Neurol. Neurosci.* 19, 5–18.
- Bosse, F., Hasenpusch-Theil, K., Küry, P. and Müller, H.W. (2006). Gene expression profiling reveals that peripheral nerve regeneration is a consequence of both novel injury-dependent and reactivated developmental processes. *J. Neurochem.* 96, 1441–1457.

- Brösamle, C. and Schwab, M.E. (1997). Cells of origin, course, and termination patterns of the ventral, uncrossed component of the mature rat corticospinal tract. *J. Comp. Neurol.* 386, 293–303.
- Brown, J.S., Kuhn, D., Wisser, R., Power, E. and Schnell, R. (2004). Quantification of sources of variation and accuracy of sequence discrimination in a replicated microarray experiment. *Biotechniques* 36, 324–332.
- Brummendorf, T., Kenwrick, S. and Rathjen, F.G. (1998). Neural cell recognition molecule L1: from cell biology to human hereditary brain malformations. *Curr Opin Neurobiol* 8, 87–97.
- Bundesen, L.Q., Scheel, T.A., Bregman, B.S. and Kromer, L.F. (2003). Ephrin-B2 and EphB2 regulation of astrocyte-meningeal fibroblast interactions in response to spinal cord lesions in adult rats. *J. Neurosci.* 23, 7789–7800.
- Burden-Gulley, S.M., Pendergast, M. and Lemmon, V. (1997). The role of cell adhesion molecule L1 in axonal extension, growth cone motility, and signal transduction. *Cell Tissue Res* 290, 415–422.
- Cameron, A.A., Vansant, G., Wu, W., Carlo, D.J. and Ill, C.R. (2003). Identification of reciprocally regulated gene modules in regenerating dorsal root ganglion neurons and activated peripheral or central nervous system glia. *J. Cell. Biochem.* 88, 970–985.
- Campanot, R.B. (1994). NGF and the local control of nerve terminal growth. *J Neurobiol* 25, 599–611.
- Caroni, P. and Schwab, M.E. (1989). Codistribution of neurite growth inhibitors and oligodendrocytes in rat CNS: appearance follows nerve fiber growth and precedes myelination. *Dev Biol* 136, 287–295.
- Castellani, V., Angelis, E. de, Kenwrick, S. and Rougon, G. (2002). Cis and trans interactions of L1 with neuropilin-1 control axonal responses to semaphorin 3A. *EMBO J.* 21, 6348–6357.
- Chaisuksunt, V., Zhang, Y., Anderson, P.N., Campbell, G., Vaudano, E., Schachner, M. and Lieberman, A.R. (2000). Axonal regeneration from CNS neurons in the cerebellum and brainstem of adult rats: correlation with the patterns of expression and distribution of messenger RNAs for L1, CHL1, c-jun and growth-associated protein-43. *Neuroscience* 100, 87–108.
- Chen, D.F., Schneider, G.E., Martinou, J.C. and Tonegawa, S. (1997). Bcl-2 promotes regeneration of severed axons in mammalian CNS. *Nature* 385, 434–439.
- Chen, M.S., Huber, A.B., van der Haar, M.E., Frank, M., Schnell, L., Spillmann, A.A., Christ, F. and Schwab, M.E. (2000). Nogo-A is a myelin-associated neurite outgrowth inhibitor and an antigen for monoclonal antibody IN-1. *Nature* 403, 434–439.
- Chen, X.Y., Wolpaw, J.R., Jakeman, L.B. and Stokes, B.T. (1996). Operant conditioning of H-reflex in spinal cord-injured rats. *J Neurotrauma* 13, 755–766.
- Chiba, Y., Kuroda, S., Maruichi, K., Osanai, T., Hokari, M., Yano, S., Shichinohe, H., Hida, K. and Iwasaki, Y. (2009). Transplanted bone marrow stromal cells promote axonal

- regeneration and improve motor function in a rat spinal cord injury model. *Neurosurgery* 64, 991-9; discussion 999-1000.
- Churchill, G.A. (2002). Fundamentals of experimental design for cDNA microarrays. *Nat.Genet.* 32 Suppl, 490–495.
- Churchill, G.A. and Oliver, B. (2001). Sex, flies and microarrays. *Nat.Genet.* 29, 355–356.
- Cope, L.M., Irizarry, R.A., Jaffee, H.A., Wu, Z. and Speed, T.P. (2004). A benchmark for Affymetrix GeneChip expression measures. *Bioinformatics.* 20, 323–331.
- Corset, V., Nguyen-Ba-Charvet, K.T., Forcet, C., Moyses, E., Chedotal, A. and Mehlen, P. (2000). Netrin-1-mediated axon outgrowth and cAMP production requires interaction with adenosine A2b receptor. *Nature* 407, 747–750.
- Costigan, M., Befort, K., Karchewski, L., Griffin, R.S., D'Urso, D., Allchorne, A., Sitarski, J., Mannion, J.W., Pratt, R.E. and Woolf, C.J. (2002). Replicate high-density rat genome oligonucleotide microarrays reveal hundreds of regulated genes in the dorsal root ganglion after peripheral nerve injury. *BMC neuroscience* 3, 16.
- Cristante, A.F., Barros-Filho, T.E.P., Tatsui, N., Mendrone, A., Caldas, J.G., Camargo, A., Alexandre, A., J Teixeira, W.G., Oliveira, R.P. and Marcon, R.M. (2009). Stem cells in the treatment of chronic spinal cord injury: evaluation of somatosensitive evoked potentials in 39 patients. *Spinal Cord*.
- Dahlin, L.B. (1995). Prevention of macrophage invasion impairs regeneration in nerve grafts. *Brain Res* 679, 274–280.
- Davenport, R.W., Thies, E. and Cohen, M.L. (1999). Neuronal growth cone collapse triggers lateral extensions along trailing axons. *Nat Neurosci* 2, 254–259.
- Davies, S.J., Fitch, M.T., Memberg, S.P., Hall, A.K., Raisman, G. and Silver, J. (1997). Regeneration of adult axons in white matter tracts of the central nervous system. *Nature* 390, 680–683.
- Decherchi, P. and Gauthier, P. (1996). In vitro pre-degenerated nerve autografts support CNS axonal regeneration. *Brain Res* 726, 181–188.
- DeRisi, J.L., Iyer, V.R. and Brown, P.O. (1997). Exploring the metabolic and genetic control of gene expression on a genomic scale. *Science* 278, 680–686.
- DeVivo, M.J., Kartus, P.L., Stover, S.L. and Fine, P.R. (1990). Benefits of early admission to an organised spinal cord injury care system. *Paraplegia* 28, 545–555.
- DiProspero, N.A., Meiners, S. and Geller, H.M. (1997). Inflammatory cytokines interact to modulate extracellular matrix and astrocytic support of neurite outgrowth. *Exp Neurol* 148, 628–639.
- Dobkin, B.H., Curt, A. and Guest, J. (2006). Cellular transplants in China: observational study from the largest human experiment in chronic spinal cord injury. *Neurorehabilitation and neural repair* 20, 5–13.

- Dumur, C.I., Garrett, C.T., Archer, K.J., Nasim, S., Wilkinson, D.S. and Ferreira-Gonzalez, A. (2004). Evaluation of a linear amplification method for small samples used on high-density oligonucleotide microarray analysis. *Anal.Biochem.* 331, 314–321.
- Duncan, M.R., Frazier, K.S., Abramson, S., Williams, S., Klapper, H., Huang, X. and Grotendorst, G.R. (1999). Connective tissue growth factor mediates transforming growth factor beta-induced collagen synthesis: down-regulation by cAMP. *FASEB J.* 13, 1774–1786.
- Eckhardt, F., Behar, O., Calautti, E., Yonezawa, K., Nishimoto, I. and Fishman, M.C. (1997). A novel transmembrane semaphorin can bind c-src. *Mol Cell Neurosci* 9, 409–419.
- Eisen, M.B., Spellman, P.T., Brown, P.O. and Botstein, D. (1998). Cluster analysis and display of genome-wide expression patterns. *Proc Natl Acad Sci U S A* 95, 14863–14868.
- Faissner, A. (1997). The tenascin gene family in axon growth and guidance. *Cell Tissue Res.* 290, 331–341.
- Fan, J., Mansfield, S.G., Redmond, T., Gordon-Weeks, P.R. and Raper, J.A. (1993). The organization of F-actin and microtubules in growth cones exposed to a brain-derived collapsing factor. *J Cell Biol* 121, 867–878.
- Fan, M., Mi, R., Yew, D.T. and Chan, W.Y. (2001). Analysis of gene expression following sciatic nerve crush and spinal cord hemisection in the mouse by microarray expression profiling. *Cell. Mol. Neurobiol.* 21, 497–508.
- Farmer, W.T., Altick, A.L., Nural, H.F., Dugan, J.P., Kidd, T., Charron, F. and Mastick, G.S. (2008). Pioneer longitudinal axons navigate using floor plate and Slit/Robo signals. *Development* 135, 3643–3653.
- Fawcett, J.W. and Asher, R.A. (1999a). The glial scar and central nervous system repair. *Brain Res. Bull.* 49, 377–391.
- Fawcett, J.W. and Asher, R.A. (1999b). The glial scar and central nervous system repair. *Brain Res Bull* 49, 377–391.
- Fehlings, M.G. (2001). Editorial: recommendations regarding the use of methylprednisolone in acute spinal cord injury: making sense out of the controversy. *Spine* 26, S56-7.
- Feringa, E.R., Kowalski, T.F., Vahlsing, H.L. and Frye, R.A. (1979). Enzyme treatment of spinal cord transected rats. *Ann. Neurol.* 5, 203–206.
- Fischer, D., Pavlidis, M. and Thanos, S. (2000). Cataractogenic lens injury prevents traumatic ganglion cell death and promotes axonal regeneration both in vivo and in culture. *Invest Ophthalmol Vis Sci* 41, 3943–3954.
- Fischer, D., Petkova, V., Thanos, S. and Benowitz, L.I. (2004). Switching mature retinal ganglion cells to a robust growth state in vivo: gene expression and synergy with RhoA inactivation. *J. Neurosci.* 24, 8726–8740.
- Fitch, M.T. and Silver, J. (1997). Activated macrophages and the blood-brain barrier: inflammation after CNS injury leads to increases in putative inhibitory molecules. *Exp Neurol* 148, 587–603.

- Fouad, K., Schnell, L., Bunge, M.B., Schwab, M.E., Liebscher, T. and Pearse, D.D. (2005). Combining Schwann cell bridges and olfactory-ensheathing glia grafts with chondroitinase promotes locomotor recovery after complete transection of the spinal cord. *J. Neurosci.* 25, 1169–1178.
- Fournier, A.E., GrandPre, T. and Strittmatter, S.M. (2001). Identification of a receptor mediating Nogo-66 inhibition of axonal regeneration. *Nature* 409, 341–346.
- Fournier, A.E. and McKerracher, L. (1997). Expression of specific tubulin isotypes increases during regeneration of injured CNS neurons, but not after the application of brain-derived neurotrophic factor (BDNF). *J. Neurosci.* 17, 4623–4632.
- Fournier, A.E., Nakamura, F., Kawamoto, S., Goshima, Y., Kalb, R.G. and Strittmatter, S.M. (2000). Semaphorin3A enhances endocytosis at sites of receptor-F-actin colocalization during growth cone collapse. *J Cell Biol* 149, 411–422.
- Fu, S.Y. and Gordon, T. (1997). The cellular and molecular basis of peripheral nerve regeneration. *Mol Neurobiol* 14, 67–116.
- Gabriel, A.F., Marcus, M.A.E., Honig, W.M.M., Walenkamp, G.H.I.M. and Joosten, E.A.J. (2007). The CatWalk method: a detailed analysis of behavioral changes after acute inflammatory pain in the rat. *J. Neurosci. Methods* 163, 9–16.
- Giger, R.J., Pasterkamp, R.J., Heijnen, S., Holtmaat, A.J. and Verhaagen, J. (1998). Anatomical distribution of the chemorepellent semaphorin III/collapsin-1 in the adult rat and human brain: predominant expression in structures of the olfactory-hippocampal pathway and the motor system. *J Neurosci Res* 52, 27–42.
- Giszter, S.F. (2008). Spinal cord injury: present and future therapeutic devices and prostheses. *Neurotherapeutics : the journal of the American Society for Experimental NeuroTherapeutics* 5, 147–162.
- Gitler, D. and Spira, M.E. (1998). Real time imaging of calcium-induced localized proteolytic activity after axotomy and its relation to growth cone formation. *Neuron* 20, 1123–1135.
- GrandPre, T., Nakamura, F., Vartanian, T. and Strittmatter, S.M. (2000). Identification of the Nogo inhibitor of axon regeneration as a Reticulon protein. *Nature* 403, 439–444.
- GrandPré, T., Nakamura, F., Vartanian, T. and Strittmatter, S.M. (2000). Identification of the Nogo inhibitor of axon regeneration as a Reticulon protein. *Nature* 403, 439–444.
- Green, B.A., Kahn, T. and Klose, K.J. (1980). A comparative study of steroid therapy in acute experimental spinal cord injury. *Surg Neurol* 13, 91–97.
- Grill, R., Murai, K., Blesch, A., Gage, F.H. and Tuszynski, M.H. (1997). Cellular delivery of neurotrophin-3 promotes corticospinal axonal growth and partial functional recovery after spinal cord injury. *J Neurosci* 17, 5560–5572.
- Hains, B.C., Black, J.A. and Waxman, S.G. (2003). Primary cortical motor neurons undergo apoptosis after axotomizing spinal cord injury. *J.Comp Neurol.* 462, 328–341.
- Hariharan, R. (2003). The analysis of microarray data. *Pharmacogenomics.* 4, 477–497.

- Harkey, H.L., al-Mefty, O., Marawi, I., Peeler, D.F., Haines, D.E. and Alexander, L.F. (1995). Experimental chronic compressive cervical myelopathy: effects of decompression. *J Neurosurg* 83, 336–341.
- Hartemink, A.J., Gifford, D.K., Jaakkola, T.S. and Young, R.A. (2001). Maximum Likelihood Estimation of Optimal Scaling Factors for Expression Array Normalization. *SPIE BiOS* 2001.
- Heiduschka, P. and Thanos, S. (2000). Aurintricarboxylic acid promotes survival and regeneration of axotomised retinal ganglion cells in vivo. *Neuropharmacology* 39, 889–902.
- Heinen, A., Kremer, D., Göttle, P., Kruse, F., Hasse, B., Lehmann, H., Hartung, H.P. and Küry, P. (2008). The cyclin-dependent kinase inhibitor p57kip2 is a negative regulator of Schwann cell differentiation and in vitro myelination. *Proc. Natl. Acad. Sci. U.S.A.* 105, 8748–8753.
- Hendricks, W.A., Pak, E.S., Owensby, J.P., Menta, K.J., Glazova, M., Moretto, J., Hollis, S., Brewer, K.L. and Murashov, A.K. (2006). Predifferentiated embryonic stem cells prevent chronic pain behaviors and restore sensory function following spinal cord injury in mice. *Mol. Med.* 12, 34–46.
- Herdegen, T., Brecht, S., Mayer, B., Leah, J., Kummer, W., Bravo, R. and Zimmermann, M. (1993). Long-lasting expression of JUN and KROX transcription factors and nitric oxide synthase in intrinsic neurons of the rat brain following axotomy. *J. Neurosci.* 13, 4130–4145.
- Herdegen, T., Skene, P. and Bähr, M. (1997). The c-Jun transcription factor--bipotential mediator of neuronal death, survival and regeneration. *Trends Neurosci.* 20, 227–231.
- Hill, A.A., Brown, E.L., Whitley, M.Z., Tucker-Kellogg, G., Hunter, C.P. and Slonim, D.K. (2001). Evaluation of normalization procedures for oligonucleotide array data based on spiked cRNA controls. *Genome Biol.* 2, RESEARCH0055.
- Holder, D., Raubertas, R.F., Pikounis, V.B., Svetnik, V. and Soper, K. (2001). Statistical analysis of high density oligonucleotide arrays: a SAFER approach. *Proceedings of the ASA Annual Meeting* 2001.
- Hollis, E.R., Jamshidi, P., Löw, K., Blesch, A. and Tuszynski, M.H. (2009). Induction of corticospinal regeneration by lentiviral trkB-induced Erk activation. *Proc. Natl. Acad. Sci. U.S.A.* 106, 7215–7220.
- Holmes, T.C., Lacalle, S. de, Su, X., Liu, G., Rich, A. and Zhang, S. (2000). Extensive neurite outgrowth and active synapse formation on self-assembling peptide scaffolds. *Proc Natl Acad Sci U S A* 97, 6728–6733.
- Houweling, D.A., Bar, P.R., Gispen, W.H. and Joosten, E.A. (1998a). Spinal cord injury: bridging the lesion and the role of neurotrophic factors in repair. *Prog Brain Res* 117, 455–471.
- Houweling, D.A., Bär, P.R., Gispen, W.H. and Joosten, E.A. (1998b). Spinal cord injury: bridging the lesion and the role of neurotrophic factors in repair. *Prog. Brain Res.* 117, 455–471.

- Houweling, D.A., Lankhorst, A.J., Gispen, W.H., Bar, P.R. and Joosten, E.A. (1998c). Collagen containing neurotrophin-3 (NT-3) attracts regrowing injured corticospinal axons in the adult rat spinal cord and promotes partial functional recovery. *Exp Neurol* 153, 49–59.
- Ide, C. (1996). Peripheral nerve regeneration. *Neurosci Res* 25, 101–121.
- Irizarry, R.A., Bolstad, B.M., Collin, F., Cope, L.M., Hobbs, B. and Speed, T.P. (2003a). Summaries of Affymetrix GeneChip probe level data. *Nucleic Acids Res.* 31, e15.
- Irizarry, R.A., Cope, L.M. and Wu, Z. (2006a). Feature-level exploration of a published Affymetrix GeneChip control dataset. *Genome Biol.* 7, 404.
- Irizarry, R.A., Gautier, L. and Cope, L. (2003b). An R package for analysis of Affymetrix oligonucleotide arrays. In *The Analysis of Gene Expression Data: Methods and Software* (Berlin: Springer), pp. 102–119.
- Irizarry, R.A., Hobbs, B., Collin, F., Beazer-Barclay, Y.D., Antonellis, K.J., Scherf, U. and Speed, T.P. (2003c). Exploration, normalization, and summaries of high density oligonucleotide array probe level data. *Biostatistics.* 4, 249–264.
- Irizarry, R.A., Ooi, S.L., Wu, Z. and Boeke, J.D. (2003d). Use of mixture models in a microarray-based screening procedure for detecting differentially represented yeast mutants. *Stat.Appl.Genet.Mol.Biol.* 2, Article 1.
- Irizarry, R.A., Wu, Z. and Jaffee, H.A. (2006b). Comparison of Affymetrix GeneChip expression measures. *Bioinformatics.* 22, 789–794.
- Irwin, N., Baekelandt, V., Goritchenko, L. and Benowitz, L.I. (1997). Identification of two proteins that bind to a pyrimidine-rich sequence in the 3'-untranslated region of GAP-43 mRNA. *Nucleic Acids Res.* 25, 1281–1288.
- Israelsson, C., Lewén, A., Kylberg, A., Usoskin, D., Althini, S., Lindeberg, J., Deng, C.-X., Fukuda, T., Wang, Y. and Kaartinen, V., et al. (2006). Genetically modified bone morphogenetic protein signalling alters traumatic brain injury-induced gene expression responses in the adult mouse. *J. Neurosci. Res.* 84, 47–57.
- Itoh, Y., Mizoi, K. and Tessler, A. (1999). Embryonic central nervous system transplants mediate adult dorsal root regeneration into host spinal cord. *Neurosurgery* 45, 849-56; discussion 856-8.
- Ivins, J.K., Raper, J.A. and Pittman, R.N. (1991). Intracellular calcium levels do not change during contact-mediated collapse of chick DRG growth cone structure. *J Neurosci* 11, 1597–1608.
- Jakeman, L.B., Wei, P., Guan, Z. and Stokes, B.T. (1998). Brain-derived neurotrophic factor stimulates hindlimb stepping and sprouting of cholinergic fibers after spinal cord injury. *Exp Neurol* 154, 170–184.
- Jeffery, D.R., Absher, J., Pfeiffer, F.E. and Jackson, H. (2000). Cortical deficits in multiple sclerosis on the basis of subcortical lesions. *Mult Scler* 6, 50–55.

- Kalderon, N. and Fuks, Z. (1996). Severed corticospinal axons recover electrophysiologic control of muscle activity after x-ray therapy in lesioned adult spinal cord. *Proc Natl Acad Sci U S A* 93, 11185–11190.
- Keirstead, H.S., Dyer, J.K., Sholomenko, G.N., McGraw, J., Delaney, K.R. and Steeves, J.D. (1995). Axonal regeneration and physiological activity following transection and immunological disruption of myelin within the hatchling chick spinal cord. *J Neurosci* 15, 6963–6974.
- Kendziorski, C., Irizarry, R.A., Chen, K.S., Haag, J.D. and Gould, M.N. (2005). On the utility of pooling biological samples in microarray experiments. *Proc.Natl.Acad.Sci.U.S.A* 102, 4252–4257.
- Kendziorski, C.M., Zhang, Y., Lan, H. and Attie, A.D. (2003). The efficiency of pooling mRNA in microarray experiments. *Biostatistics*. 4, 465–477.
- Kennedy, P.R. (1990). Corticospinal, rubrospinal and rubro-olivary projections: a unifying hypothesis. *Trends Neurosci*. 13, 474–479.
- Kim, D.S., Lee, S.J., Park, S.Y., Yoo, H.J., Kim, S.H., Kim, K.J. and Cho, H.J. (2001). Differentially expressed genes in rat dorsal root ganglia following peripheral nerve injury. *Neuroreport* 12, 3401–3405.
- Kirsch, M., Terheggen, U. and Hofmann, H.-D. (2003). Ciliary neurotrophic factor is an early lesion-induced retrograde signal for axotomized facial motoneurons. *Mol. Cell. Neurosci*. 24, 130–138.
- Klapka, N., Hermanns, S., Straten, G., Masanneck, C., Duis, S., Hamers, F.P., Müller, D., Zuschratter, W. and Müller, H.W. (2005). Suppression of fibrous scarring in spinal cord injury of rat promotes long-distance regeneration of corticospinal tract axons, rescue of primary motoneurons in somatosensory cortex and significant functional recovery. *Eur.J Neurosci*. 22, 3047–3058.
- Koenig, E., Kinsman, S., Repasky, E. and Sultz, L. (1985). Rapid mobility of motile varicosities and inclusions containing alpha-spectrin, actin, and calmodulin in regenerating axons in vitro. *J Neurosci* 5, 715–729.
- Kruse, F., Brazda, N., Bosse, F., Vogelaar, C.F., Küry, P., Gasis, M. and Müller, H.W. (2009). Cortical gene expression profiling in spinal cord repair: insight into the complexity of the neural regeneration program. Submitted.
- Kruse, F., Brazda, N., Küry, P., Bosse, F. and Müller, H.W. (2008). Analyzing complex gene expression profiles in sensorimotor cortex following spinal cord injury and regeneration promoting treatment. In *Neural Degeneration and Repair. Gene Expression Profiling, Proteomics and Systems Biology*, H.W. Müller, ed., pp. 61–89.
- Kubasak, M.D., Jindrich, D.L., Zhong, H., Takeoka, A., McFarland, K.C., Muñoz-Quiles, C., Roy, R.R., Edgerton, V.R., Ramón-Cueto, A. and Phelps, P.E. (2008). OEG implantation and step training enhance hindlimb-stepping ability in adult spinal transected rats. *Brain* 131, 264–276.

- Kugler, S., Klocker, N., Kermer, P., Isenmann, S. and Bahr, M. (1999). Transduction of axotomized retinal ganglion cells by adenoviral vector administration at the optic nerve stump: an in vivo model system for the inhibition of neuronal apoptotic cell death. *Gene Ther* 6, 1759–1767.
- Kuhn, T.B., Brown, M.D., Wilcox, C.L., Raper, J.A. and Bamberg, J.R. (1999). Myelin and collapsin-1 induce motor neuron growth cone collapse through different pathways: inhibition of collapse by opposing mutants of rac1. *J Neurosci* 19, 1965–1975.
- Kury, P., Abankwa, D., Kruse, F., Greiner-Petter, R. and Muller, H.W. (2004). Gene expression profiling reveals multiple novel intrinsic and extrinsic factors associated with axonal regeneration failure. *Eur.J.Neurosci.* 19, 32–42.
- La Houssaye, B.A. de, Mikule, K., Nikolic, D. and Pfenninger, K.H. (1999). Thrombin-induced growth cone collapse: involvement of phospholipase A(2) and eicosanoid generation. *J Neurosci* 19, 10843–10855.
- Lee, M.S., Kwon, Y.T., Li, M., Peng, J., Friedlander, R.M. and Tsai, L.H. (2000). Neurotoxicity induces cleavage of p35 to p25 by calpain. *Nature* 405, 360–364.
- Li, C. and Wong, W.H. (2001). Model-based analysis of oligonucleotide arrays: expression index computation and outlier detection. *Proc.Natl.Acad.Sci.U.S.A* 98, 31–36.
- Li, Y., Field, P.M. and Raisman, G. (1998). Regeneration of adult rat corticospinal axons induced by transplanted olfactory ensheathing cells. *J Neurosci* 18, 10514–10524.
- Li, Y. and Raisman, G. (1994). Schwann cells induce sprouting in motor and sensory axons in the adult rat spinal cord. *J. Neurosci.* 14, 4050–4063.
- Liesi, P. and Kauppila, T. (2002). Induction of type IV collagen and other basement-membrane-associated proteins after spinal cord injury of the adult rat may participate in formation of the glial scar. *Exp.Neurol.* 173, 31–45.
- Lipshutz, R.J., Fodor, S.P., Gingeras, T.R. and Lockhart, D.J. (1999). High density synthetic oligonucleotide arrays. *Nat.Genet.* 21, 20–24.
- Lockhart, D.J., Dong, H., Byrne, M.C., Follettie, M.T., Gallo, M.V., Chee, M.S., Mittmann, M., Wang, C., Kobayashi, M. and Horton, H., et al. (1996). Expression monitoring by hybridization to high-density oligonucleotide arrays. *Nat.Biotechnol.* 14, 1675–1680.
- Logan, A., Berry, M., Gonzalez, A.M., Frautschy, S.A., Sporn, M.B. and Baird, A. (1994). Effects of transforming growth factor beta 1 on scar production in the injured central nervous system of the rat. *Eur J Neurosci* 6, 355–363.
- Loschinger, J., Bandtlow, C.E., Jung, J., Klostermann, S., Schwab, M.E., Bonhoeffer, F. and Kater, S.B. (1997). Retinal axon growth cone responses to different environmental cues are mediated by different second-messenger systems. *J Neurobiol* 33, 825–834.
- Lu, J., Ashwell, K.W. and Waite, P. (2000). Advances in secondary spinal cord injury: role of apoptosis. *Spine* 25, 1859–1866.

- Lu, X.-C.M., Williams, A.J., Yao, C., Berti, R., Hartings, J.A., Whipple, R., Vahey, M.T., Polavarapu, R.G., Woller, K.L. and Tortella, F.C., et al. (2004). Microarray analysis of acute and delayed gene expression profile in rats after focal ischemic brain injury and reperfusion. *J. Neurosci. Res.* 77, 843–857.
- Maier, I.C., Baumann, K., Thallmair, M., Weinmann, O., Scholl, J. and Schwab, M.E. (2008). Constraint-induced movement therapy in the adult rat after unilateral corticospinal tract injury. *J. Neurosci.* 28, 9386–9403.
- Mansour, H., Asher, R., Dahl, D., Labkovsky, B., Perides, G. and Bignami, A. (1990). Permissive and non-permissive reactive astrocytes: immunofluorescence study with antibodies to the glial hyaluronate-binding protein. *J. Neurosci. Res.* 25, 300–311.
- Mark, M.D., Lohrum, M. and Puschel, A.W. (1997). Patterning neuronal connections by chemorepulsion: the semaphorins. *Cell Tissue Res* 290, 299–306.
- Mason, M.R.J., Lieberman, A.R. and Anderson, P.N. (2003). Corticospinal neurons up-regulate a range of growth-associated genes following intracortical, but not spinal, axotomy. *Eur. J. Neurosci.* 18, 789–802.
- McDonald, J.W., Liu, X.Z., Qu, Y., Liu, S., Mickey, S.K., Turetsky, D., Gottlieb, D.I. and Choi, D.W. (1999). Transplanted embryonic stem cells survive, differentiate and promote recovery in injured rat spinal cord. *Nat Med* 5, 1410–1412.
- McKerracher, L., Essagian, C. and Aguayo, A.J. (1993). Marked increase in beta-tubulin mRNA expression during regeneration of axotomized retinal ganglion cells in adult mammals. *J Neurosci* 13, 5294–5300.
- Metz, G.A., Merkler, D., Dietz, V., Schwab, M.E. and Fouad, K. (2000). Efficient testing of motor function in spinal cord injured rats. *Brain Res.* 883, 165–177.
- Mikucki, S.A. and Oblinger, M.M. (1991). Corticospinal neurons exhibit a novel pattern of cytoskeletal gene expression after injury. *J. Neurosci. Res.* 30, 213–225.
- Millenaar, F.F., Okyere, J., May, S.T., van, Z.M., Voesenek, L.A. and Peeters, A.J. (2006). How to decide? Different methods of calculating gene expression from short oligonucleotide array data will give different results. *BMC.Bioinformatics.* 7, 137.
- Ming, G.L., Song, H.J., Berninger, B., Holt, C.E., Tessier-Lavigne, M. and Poo, M.M. (1997). cAMP-dependent growth cone guidance by netrin-1. *Neuron* 19, 1225–1235.
- Miranda, J.D., White, L.A., Marcillo, A.E., Willson, C.A., Jagid, J. and Whittemore, S.R. (1999). Induction of Eph B3 after spinal cord injury. *Exp Neurol* 156, 218–222.
- Molloy, M.P., Brzezinski, E.E., Hang, J., McDowell, M.T. and VanBogelen, R.A. (2003). Overcoming technical variation and biological variation in quantitative proteomics. *Proteomics.* 3, 1912–1919.
- Morgenstern, D.A., Asher, R.A. and Fawcett, J.W. (2002). Chondroitin sulphate proteoglycans in the CNS injury response. *Prog.Brain Res.* 137, 313–332.

- Naef, F., Hacker, C.R., Patil, N. and Magnasco, M. (2002). Empirical characterization of the expression ratio noise structure in high-density oligonucleotide arrays. *Genome Biol.* 3, RESEARCH0018.
- Naef, F. and Magnasco, M.O. (2003). Solving the riddle of the bright mismatches: labeling and effective binding in oligonucleotide arrays. *Phys.Rev.E.Stat.Nonlin.Soft.Matter Phys.* 68, 11906.
- Nagarajan, R., Le, N., Mahoney, H., Araki, T. and Milbrandt, J. (2002). Deciphering peripheral nerve myelination by using Schwann cell expression profiling. *Proc. Natl. Acad. Sci. U.S.A.* 99, 8998–9003.
- Oleksiak, M.F., Churchill, G.A. and Crawford, D.L. (2002). Variation in gene expression within and among natural populations. *Nat.Genet.* 32, 261–266.
- Olson, L. (1993). NGF and the treatment of Alzheimer's disease. *Exp Neurol* 124, 5–15.
- Pan, W., Lin, J. and Le, C.T. (2002). How many replicates of arrays are required to detect gene expression changes in microarray experiments? A mixture model approach. *Genome Biol.* 3, research0022.
- Pasinetti, G.M., Cheng, H.W., Morgan, D.G., Lampert-Etchells, M., McNeill, T.H. and Finch, C.E. (1993). Astrocytic messenger RNA responses to striatal deafferentation in male rat. *Neuroscience* 53, 199–211.
- Pasquale, E.B., Deerinck, T.J., Singer, S.J. and Ellisman, M.H. (1992). Cdk5, a membrane receptor-type tyrosine kinase, is in neurons of the embryonic and postnatal avian brain. *J. Neurosci.* 12, 3956–3967.
- Pastor, A.M., Moreno-López, B., La Cruz, R.R. de and Delgado-García, J.M. (1997). Effects of botulinum neurotoxin type A on abducens motoneurons in the cat: ultrastructural and synaptic alterations. *Neuroscience* 81, 457–478.
- Pettigrew, D.B. and Crutcher, K.A. (1999). White matter of the CNS supports or inhibits neurite outgrowth in vitro depending on geometry. *J Neurosci* 19, 8358–8366.
- Pfurtscheller, G., Müller, G.R., Pfurtscheller, J., Gerner, H.J. and Rupp, R. (2003). 'Thought'--control of functional electrical stimulation to restore hand grasp in a patient with tetraplegia. *Neurosci. Lett.* 351, 33–36.
- Polleux, F., Giger, R.J., Ginty, D.D., Kolodkin, A.L. and Ghosh, A. (1998). Patterning of cortical efferent projections by semaphorin-neuropilin interactions. *Science* 282, 1904–1906.
- Poulsen, C.B., Penkowa, M., Borup, R., Nielsen, F.C., Cáceres, M., Quintana, A., Molinero, A., Carrasco, J., Giralt, M. and Hidalgo, J. (2005). Brain response to traumatic brain injury in wild-type and interleukin-6 knockout mice: a microarray analysis. *J. Neurochem.* 92, 417–432.
- Prinjha, R., Moore, S.E., Vinson, M., Blake, S., Morrow, R., Christie, G., Michalovich, D., Simmons, D.L. and Walsh, F.S. (2000). Inhibitor of neurite outgrowth in humans. *Nature* 403, 383–384.

- Qian, T., Campagnolo, D. and Kirshblum, S. (2000). High-dose methylprednisolone may do more harm for spinal cord injury. *Med. Hypotheses* 55, 452–453.
- Qian, T., Guo, X., Levi, A.D., Vanni, S., Shebert, R.T. and Sipski, M.L. (2005). High-dose methylprednisolone may cause myopathy in acute spinal cord injury patients. *Spinal Cord* 43, 199–203.
- Qin, L.X., Beyer, R.P., Hudson, F.N., Linford, N.J., Morris, D.E. and Kerr, K.F. (2006). Evaluation of methods for oligonucleotide array data via quantitative real-time PCR. *BMC.Bioinformatics*. 7, 23.
- Quintana, A., Giralt, M., Molinero, A., Campbell, I.L., Penkowa, M. and Hidalgo, J. (2007a). Analysis of the cerebral transcriptome in mice subjected to traumatic brain injury: importance of IL-6. *Neuroimmunomodulation* 14, 139–143.
- Quintana, A., Molinero, A., Florit, S., Manso, Y., Comes, G., Carrasco, J., Giralt, M., Borup, R., Nielsen, F.C. and Campbell, I.L., et al. (2007b). Diverging mechanisms for TNF-alpha receptors in normal mouse brains and in functional recovery after injury: From gene to behavior. *J. Neurosci. Res.* 85, 2668–2685.
- Raghavendra Rao, V.L., Dhodda, V.K., Song, G., Bowen, K.K. and Dempsey, R.J. (2003). Traumatic brain injury-induced acute gene expression changes in rat cerebral cortex identified by GeneChip analysis. *J. Neurosci. Res.* 71, 208–219.
- Rall, J.M., Matzilevich, D.A. and Dash, P.K. (2003). Comparative analysis of mRNA levels in the frontal cortex and the hippocampus in the basal state and in response to experimental brain injury. *Neuropathol. Appl. Neurobiol.* 29, 118–131.
- Ramer, M.S., Priestley, J.V. and McMahon, S.B. (2000). Functional regeneration of sensory axons into the adult spinal cord. *Nature* 403, 312–316.
- Ramon y Cajal (1928). *Degeneration and regeneration of the nervous system*. London: Oxford University Press.
- Ramon-Cueto, A., Cordero, M.I., Santos-Benito, F.F. and Avila, J. (2000). Functional recovery of paraplegic rats and motor axon regeneration in their spinal cords by olfactory ensheathing glia. *Neuron* 25, 425–435.
- Rapalino, O., Lazarov-Spiegler, O., Agranov, E., Velan, G.J., Yoles, E., Fraidakis, M., Solomon, A., Gepstein, R., Katz, A. and Belkin, M., et al. (1998). Implantation of stimulated homologous macrophages results in partial recovery of paraplegic rats. *Nat Med* 4, 814–821.
- Reh, T.A., Redshaw, J.D. and Bisby, M.A. (1987). Axons of the pyramidal tract do not increase their transport of growth-associated proteins after axotomy. *Brain Res.* 388, 1–6.
- Reier, P., Stensaas, L. and Guth, L. (1983). The astrocytic scar as an impediment to regeneration in the central nervous system. In *Spinal cord reconstruction*, C.C. Kao and R.P. Bunge, eds. (New York: Raven Pr.), pp. 163–195.
- Richardson, P.M., McGuinness, U.M. and Aguayo, A.J. (1980). Axons from CNS neurons regenerate into PNS grafts. *Nature* 284, 264–265.

- Rubio, M.-P., Muñoz-Quiles, C. and Ramón-Cueto, A. (2008). Adult olfactory bulbs from primates provide reliable ensheathing glia for cell therapy. *Glia* 56, 539–551.
- Salin, P. and Chesselet, M.F. (1992). Paradoxical increase in striatal neuropeptide gene expression following ischemic lesions of the cerebral cortex. *Proc. Natl. Acad. Sci. U.S.A.* 89, 9954–9958.
- Salin, P. and Chesselet, M.F. (1993). Expression of GAD (M(r) 67,000) and its messenger RNA in basal ganglia and cerebral cortex after ischemic cortical lesions in rats. *Exp. Neurol.* 119, 291–301.
- Savio, T. and Schwab, M.E. (1990). Lesioned corticospinal tract axons regenerate in myelin-free rat spinal cord. *Proc Natl Acad Sci U S A* 87, 4130–4133.
- Schadt, E.E., Li, C., Ellis, B. and Wong, W.H. (2001). Feature extraction and normalization algorithms for high-density oligonucleotide gene expression array data. *J.Cell Biochem.Suppl Suppl* 37, 120–125.
- Schadt, E.E., Li, C., Su, C. and Wong, W.H. (2000). Analyzing high-density oligonucleotide gene expression array data. *J.Cell Biochem.* 80, 192–202.
- Schnell, L., Schneider, R., Kolbeck, R., Barde, Y.A. and Schwab, M.E. (1994). Neurotrophin-3 enhances sprouting of corticospinal tract during development and after adult spinal cord lesion. *Nature* 367, 170–173.
- Schnell, L. and Schwab, M.E. (1993). Sprouting and regeneration of lesioned corticospinal tract fibres in the adult rat spinal cord. *Eur J Neurosci* 5, 1156–1171.
- Schwab, J.M., Beschorner, R., Nguyen, T.D., Meyermann, R. and Schluesener, H.J. (2001). Differential cellular accumulation of connective tissue growth factor defines a subset of reactive astrocytes, invading fibroblasts, and endothelial cells following central nervous system injury in rats and humans. *J.Neurotrauma* 18, 377–388.
- Scremin, A.M., Kurta, L., Gentili, A., Wiseman, B., Perell, K., Kunkel, C. and Scremin, O.U. (1999). Increasing muscle mass in spinal cord injured persons with a functional electrical stimulation exercise program. *Archives of physical medicine and rehabilitation* 80, 1531–1536.
- Seidl, E.C. (2000). Promising pharmacological agents in the management of acute spinal cord injury. *Pharm Pract Manag Q* 20, 21–27.
- Selkoe, D.J. (1999). Translating cell biology into therapeutic advances in Alzheimer's disease. *Nature* 399, A23-31.
- Seo, J., Gordish-Dressman, H. and Hoffman, E.P. (2006). An interactive power analysis tool for microarray hypothesis testing and generation. *Bioinformatics.* 22, 808–814.
- Seo, J. and Hoffman, E.P. (2006). Probe set algorithms: is there a rational best bet? *BMC.Bioinformatics.* 7, 395.
- Shih, J.H., Michalowska, A.M., Dobbin, K., Ye, Y., Qiu, T.H. and Green, J.E. (2004). Effects of pooling mRNA in microarray class comparisons. *Bioinformatics.* 20, 3318–3325.

- Simon, R.M. and Dobbin, K. (2003). Experimental design of DNA microarray experiments. *Biotechniques Suppl*, 16–21.
- Skaper, S.D. and Walsh, F.S. (1998). Neurotrophic molecules: strategies for designing effective therapeutic molecules in neurodegeneration. *Mol Cell Neurosci* 12, 179–193.
- Skene, J.H. (1989). Axonal growth-associated proteins. *Annu Rev Neurosci* 12, 127–156.
- Skene, J.H. and Willard, M. (1981). Characteristics of growth-associated polypeptides in regenerating toad retinal ganglion cell axons. *J Neurosci* 1, 419–426.
- Smith, G.M. and Hale, J.H. (1997). Macrophage/Microglia regulation of astrocytic tenascin: synergistic action of transforming growth factor-beta and basic fibroblast growth factor. *J Neurosci* 17, 9624–9633.
- Somers, D.L. and Beckstead, R.M. (1990). Striatal preprotachykinin and preproenkephalin mRNA levels and the levels of nigral substance P and pallidal Met5-enkephalin depend on corticostriatal axons that use the excitatory amino acid neurotransmitters aspartate and glutamate: quantitative radioimmunocytochemical and in situ hybridization evidence. *Brain Res. Mol. Brain Res.* 8, 143–158.
- Song, H., Ming, G., He, Z., Lehmann, M., McKerracher, L., Tessier-Lavigne, M. and Poo, M. (1998). Conversion of neuronal growth cone responses from repulsion to attraction by cyclic nucleotides. *Science* 281, 1515–1518.
- Spruill, S.E., Lu, J., Hardy, S. and Weir, B. (2002). Assessing sources of variability in microarray gene expression data. *Biotechniques* 33, 916-3.
- Stam, F.J., MacGillavry, H.D., Armstrong, N.J., Gunst, M.C.M. de, Zhang, Y., van Kesteren, R.E., Smit, A.B. and Verhaagen, J. (2007). Identification of candidate transcriptional modulators involved in successful regeneration after nerve injury. *Eur. J. Neurosci.* 25, 3629–3637.
- Stein, E., Zou, Y., Poo, M. and Tessier-Lavigne, M. (2001). Binding of DCC by netrin-1 to mediate axon guidance independent of adenosine A2B receptor activation. *Science* 291, 1976–1982.
- Steuer, H., Fadale, R., Muller, E., Muller, H.W., Planck, H. and Schlosshauer, B. (1999). Biohybride nerve guide for regeneration: degradable polylactide fibers coated with rat Schwann cells. *Neurosci Lett* 277, 165–168.
- Stichel, C.C., Hermanns, S., Luhmann, H.J., Lausberg, F., Niermann, H., D'Urso, D., Servos, G., Hartwig, H.G. and Müller, H.W. (1999a). Inhibition of collagen IV deposition promotes regeneration of injured CNS axons. *Eur.J.Neurosci.* 11, 632–646.
- Stichel, C.C., Kappler, J., Junghans, U., Koops, A., Kresse, H. and Müller, H.W. (1995). Differential expression of the small chondroitin/dermatan sulfate proteoglycans decorin and biglycan after injury of the adult rat brain. *Brain Res* 704, 263–274.
- Stichel, C.C. and Müller, H.W. (1994). Relationship between injury-induced astrogliosis, laminin expression and axonal sprouting in the adult rat brain. *J. Neurocytol.* 23, 615–630.

- Stichel, C.C., Niermann, H., D'Urso, D., Lausberg, F., Hermanns, S. and Müller, H.W. (1999b). Basal membrane-depleted scar in lesioned CNS: characteristics and relationships with regenerating axons. *Neurosci.* 93, 321–333.
- Strittmatter, S.M., Vartanian, T. and Fishman, M.C. (1992). GAP-43 as a plasticity protein in neuronal form and repair. *J Neurobiol* 23, 507–520.
- Stromberg, I., Bygdeman, M. and Almqvist, P. (1992). Target-specific outgrowth from human mesencephalic tissue grafted to cortex or ventricle of immunosuppressed rats. *J Comp Neurol* 315, 445–456.
- Suarez, V., Guntinas-Lichius, O., Streppel, M., Ingorokva, S., Grosheva, M., Neiss, W.F., Angelov, D.N. and Klimaschewski, L. (2006). The axotomy-induced neuropeptides galanin and pituitary adenylate cyclase-activating peptide promote axonal sprouting of primary afferent and cranial motor neurones. *Eur. J. Neurosci.* 24, 1555–1564.
- Szele, F.G., Alexander, C. and Chesselet, M.F. (1995). Expression of molecules associated with neuronal plasticity in the striatum after aspiration and thermocoagulatory lesions of the cerebral cortex in adult rats. *J. Neurosci.* 15, 4429–4448.
- Tatagiba, M., Brosamle, C. and Schwab, M.E. (1997). Regeneration of injured axons in the adult mammalian central nervous system. *Neurosurgery* 40, 541-6; discussion 546-7.
- Tessier-Lavigne, M. and Goodman, C.S. (1996). The molecular biology of axon guidance. *Science* 274, 1123–1133.
- Tetzlaff, W., Kobayashi, N.R., Giehl, K.M., Tsui, B.J., Cassar, S.L. and Bedard, A.M. (1994). Response of rubrospinal and corticospinal neurons to injury and neurotrophins. *Prog. Brain Res.* 103, 271–286.
- Timpl, R. (1994). Proteoglycans of basement membranes. *EXS* 70, 123–144.
- Trapp, B.D., Ransohoff, R. and Rudick, R. (1999). Axonal pathology in multiple sclerosis: relationship to neurologic disability. *Curr Opin Neurol* 12, 295–302.
- Tuszynski, M.H., Weidner, N., McCormack, M., Miller, I., Powell, H. and Conner, J. Grafts of genetically modified Schwann cells to the spinal cord: survival, axon growth, and myelination. *Cell transplantation* 7, 187–196.
- Uhl, G.R., Navia, B. and Douglas, J. (1988). Differential expression of preproenkephalin and preprodynorphin mRNAs in striatal neurons: high levels of preproenkephalin expression depend on cerebral cortical afferents. *J. Neurosci.* 8, 4755–4764.
- Varga, Z.M., Bandtlow, C.E., Erulkar, S.D., Schwab, M.E. and Nicholls, J.G. (1995). The critical period for repair of CNS of neonatal opossum (*Monodelphis domestica*) in culture: correlation with development of glial cells, myelin and growth-inhibitory molecules. *Eur J Neurosci* 7, 2119–2129.
- Viollet, C. and Doherty, P. (1997). CAMs and the FGF receptor: an interacting role in axonal growth. *Cell Tissue Res* 290, 451–455.

- Weidner, N., Blesch, A., Grill, R.J. and Tuszynski, M.H. (1999). Nerve growth factor-hypersecreting Schwann cell grafts augment and guide spinal cord axonal growth and remyelinate central nervous system axons in a phenotypically appropriate manner that correlates with expression of L1. *J Comp Neurol* 413, 495–506.
- Whitney, A.R., Diehn, M., Popper, S.J., Alizadeh, A.A., Boldrick, J.C., Relman, D.A. and Brown, P.O. (2003). Individuality and variation in gene expression patterns in human blood. *Proc.Natl.Acad.Sci.U.S.A* 100, 1896–1901.
- Victorin, K., Brundin, P., Gustavii, B., Lindvall, O. and Bjorklund, A. (1990). Reformation of long axon pathways in adult rat central nervous system by human forebrain neuroblasts. *Nature* 347, 556–558.
- Wilson, M.A., Gaze, R.M., Goodbrand, I.A. and Taylor, J.S. (1992). Regeneration in the *Xenopus* tadpole optic nerve is preceded by a massive macrophage/microglial response. *Anat Embryol (Berl)* 186, 75–89.
- Winter, F. de, Oudega, M., Lankhorst, A.J., Hamers, F.P., Blits, B., Ruitenberg, M.J., Pasterkamp, R.J., Gispen, W.H. and Verhaagen, J. (2002). Injury-induced class 3 semaphorin expression in the rat spinal cord. *Exp.Neurol.* 175, 61–75.
- Woerly, S., Petrov, P., Sykova, E., Roitbak, T., Simonova, Z. and Harvey, A.R. (1999). Neural tissue formation within porous hydrogels implanted in brain and spinal cord lesions: ultrastructural, immunohistochemical, and diffusion studies. *Tissue Eng* 5, 467–488.
- Wong, J.T., Wong, S.T. and O'Connor, T.P. (1999). Ectopic semaphorin-1a functions as an attractive guidance cue for developing peripheral neurons. *Nat Neurosci* 2, 798–803.
- Wu, Z., Irizarry, R., Gentleman, R., Murillo, F. and Spencer, F. (2003). A Model Based Background Adjustment for Oligonucleotide Expression Arrays. Technical Report, John Hopkins University, Department of Biostatistics Working Papers, Baltimore.
- Wu, Z. and Irizarry, R.A. (2005). Stochastic models inspired by hybridization theory for short oligonucleotide arrays. *J.Comput.Biol.* 12, 882–893.
- Xiao, H.-S., Huang, Q.-H., Zhang, F.-X., Bao, L., Lu, Y.-J., Guo, C., Yang, L., Huang, W.-J., Fu, G. and Xu, S.-H., et al. (2002). Identification of gene expression profile of dorsal root ganglion in the rat peripheral axotomy model of neuropathic pain. *Proc. Natl. Acad. Sci. U.S.A.* 99, 8360–8365.
- Xie, X.Y. and Barrett, J.N. (1991). Membrane resealing in cultured rat septal neurons after neurite transection: evidence for enhancement by Ca(2+)-triggered protease activity and cytoskeletal disassembly. *J Neurosci* 11, 3257–3267.
- Yao, G.L., Kiyama, H. and Tohyama, M. (1993). Distribution of GAP-43 (B50/F1) mRNA in the adult rat brain by in situ hybridization using an alkaline phosphatase labeled probe. *Brain Res Mol Brain Res* 18, 1–16.
- Yurchenco, P.D. and Schittny, J.C. (1990). Molecular architecture of basement membranes. *FASEB J.* 4, 1577–1590.

Zhou, L., Connors, T., Chen, D.F., Murray, M., Tessler, A., Kambin, P. and Saavedra, R.A. (1999). Red nucleus neurons of Bcl-2 over-expressing mice are protected from cell death induced by axotomy. *Neuroreport* 10, 3417–3421.

Ziv, N.E. and Spira, M.E. (1997). Localized and transient elevations of intracellular Ca²⁺ induce the dedifferentiation of axonal segments into growth cones. *J Neurosci* 17, 3568–3579.

Zuo, J., Ferguson, T.A., Hernandez, Y.J., Stetler-Stevenson, W.G. and Muir, D. (1998). Neuronal matrix metalloproteinase-2 degrades and inactivates a neurite-inhibiting chondroitin sulfate proteoglycan. *J Neurosci* 18, 5203–5211.

7. ABBREVIATIONS

AB	Antibody
ACTB	actin beta
AD	Alzheimer disease
Akt1	v-akt murine thymoma viral oncogene homolog 1
ALCAM	activated leukocyte cell adhesion molecule
ANOVA	Analysis of variance
AST	Anti scarring treatment
ATF3	activating transcription factor 3
BAG1	Bcl2-associated athanogene 1
BBB	Locomotionscale after Basso, Beattie and Bresnahan
BCI	Brain-computer interface
BCL2L1	BCL2-like 1
BCL2L13	BCL2-like 13
BDA	Biotinylated dextran amin
BDNF	brain derived neurotrophic factor
bFGF	basic fibroblast growth factor
Bid3	BH3 interacting domain
BM	Basal membran
BPY-DCA	2,2'-bipyridine-5,5'-dicarboxylic acid
BTBD14B	BTB (POZ) domain containing 14B
CAM	Cell adhesion molecules
cAMP	Cyclic adenosin monophosphat
CDK5	cyclin-dependent kinase 5
cGMP	cyclic guanosinemonophosphate
c-jun	v-jun sarcoma virus 17 oncogene homolog
CLDN11	claudin 11
Cnp1	cyclic nucleotide phosphodiesterase 1
CNS	Central nervous system
CNTF	ciliary neurotropic factor
CNTN2	contactin 2
Coll IV	Collagen IV
CPC	Cortical pyramidal cell
CRH	corticotropin releasing hormone
CSF2	colony stimulating factor 2
CSPG	Chondroitin sulfat proteoglykane
CST	Corticospinal tract
CTGF	connective tissue growth factor
DCC	deleted in colorectal cancer
Diablo	diablo homolog, Drosophila
DNA	Deoxyribonucleic acid
dpo	days post operation
DPY	2,2'-dipyridyl
DPYSL5	dihydropyrimidinase-like 5
DRG	Dorsal root ganglia
ECM	Extracellular matrix
EEG	Electroencephalogram
EGR2, Krox-20	early growth response 2
Elvax	Ethylen-Vinyl-Acetat Kopolymer
ENAH	enabled homolog
FAIM2	Fas apoptotic inhibitory molecule 2
FDA	Food and Drug Administration

FDR	False discovery rate
FES	Functional electrical stimulation
FEZ1	fasciculation and elongation protein zeta 1
FGF	fibroblast growth factor
Fig.	Figure
FWER	Family wide error rate
GAL1	galanin
GAP43	growth associated protein 43
GAPDH	Glyceraldehyde 3-phosphate dehydrogenase
GDNF	glial cell derived neurotrophic factor
GFAP	Glial fibrillary acidic protein
GO	Gene ontology
IL-4	interleukin 4
IL-6	interleukin 6
KALRN	kalirin
KEGG	Kyoto Encyclopedia of Genes and Genomes
Krox-20, EGR2	early growth response 2
LGALS1	galectin 1
Lmo4	LIM domain only 4
MAG	myelin associated glycoprotein
MAP2	microtubule associated protein 2
Mapk8ip	mitogen activated protein kinase 8 interacting protein
MAS	Microarray suite
MBEI	Model-based Expression Indexes
MBP	myelin basic protein
MM	Mismatch
MOBP	myelin-associated oligodendrocyte basic protein
MPZ	Myelin protein-zero
MS	Multiple sclerosis
MSB	Mean square between
MSE	Mean square error
NCAML1	neural cell adhesion molecule L1
NeuD4	neuronal d4 domain family member
NgR	Nogo receptor
NRP1	neuropilin-1
NT-3	neurotrophin-3
Oct-6, Scip	POU domain, class 3, transcription factor 1
ODC1	Ornithine decarboxylase 1
PCA	Principal component analysis
PH	pleckstrin homology
PirB	paired immunoglobulin-like receptor B
PKA	cAMP/protein kinase A
PKC	protein kinase C
PLC γ	phospholipase C γ
PLIER	Probe logarithmic intensity error (PLIER)
PM	Perfect match
PMP22	peripheral myelin protein 22
PN	peripheral nerve
PNS	Peripheral nervous system
PPARD	peroxisome proliferative activated receptor delta
PRDX2	peroxiredoxin 2
qPCR	Quantitative polymerase chain reaction
RGC	Retinal ganglion cells
RMA	Robust multiarray average

RNA	Ribonucleic acid
ROBO1	roundabout homolog 1
ROS	Reactive oxygen species
RST	rubrospinal tract
RTN4R	reticulon 4 receptor
RYK	receptor-like tyrosine kinase
S100B	S100 calcium binding protein beta
SCI	Spinal cord injury
Scip, Oct-6	POU domain, class 3, transcription factor 1
Sema6B	semaphorin 6B
SH3	Src-homology-3
SOD1	superoxide dismutase 1
SSEPs	Somatosensory evoked potentials
STAT5A	signal transducer and activator of transcription 5A
STNL	statin-like
STXBP1	syntaxin binding protein 1
Traf2	Tnf receptor-associated factor 2
TVA	Tierversuchsanlage
UNC5A	unc-5 homolog A
VBA	Visual basic for applications
VDR	vitamin D receptor

8. ACKNOWLEDGMENTS

I would like to give special thanks to my mentor, Prof. Dr. Hans Werner Müller, for giving me the opportunity to work on a very interesting project. It has been an unique experience that shaped my scientific outlook and furthermore will shape my professional life.

I would like to thank my “Zweitgutachter” Prof. Dr. Dieter Willbold.

I am especially grateful to Dr. Patrick Küry for his excellent supervision, technical support, encouragement and friendship.

I am indebted to Dr. Nicole Brazda and her colleagues in the TVA for the surgeries and the animal care as well as to Dr. Frank Bosse and Dr. Tineke Vogelaar for the fruitful discussions.

I want to thank the members of the Molecular Neurobiology Laboratory in Düsseldorf, for the friendly and motivating working atmosphere.

Last but not least, I would like to thank my family. This study is the result of their support, encouragement, help and love.

Hiermit erkläre ich, die vorliegende Arbeit selbstständig und unter ausschließlicher Verwendung der angegebenen Hilfsmittel und Quellen angefertigt zu haben. Alle Stellen, die aus veröffentlichten und nicht veröffentlichten Schriften entnommen sind, wurden als solche kenntlich gemacht. Diese Arbeit hat in gleicher oder ähnlicher Form noch keiner anderen Prüfungsbehörde vorgelegen.

Düsseldorf, den